A UNIQUE WAY TO FORM A VESICLE:
AMINOPEPTIDASE 1 AGGREGATION AND ITS BINDING TO RECEPTOR ATG19 FOR RECRUITMENT OF AUTOPHAGIC PROTEINS TO FORM A VESICLE IN THE CYTOPLASM-TO-VACUOLE-TARGETING PATHWAY IN YEAST

A Dissertation

presented to

the Faculty of the Graduate School

at the University of Missouri-Columbia

In Partial Fulfillment

of the Requirements for the Degree

Doctor of Philosophy

---

by

MARIANA MORALES QUIÑONES

Dr. Per E. Strømhaug, Dissertation Supervisor

DECEMBER 2011

DEDICATION

"Gratitude is happiness doubled by wonder".

I am forever indebted to my family for their love and support

my strong mother Maria Eugenia

my persevering father Javier

my loving sister Adriana

and my kind husband Jon

Thank you! ~ ***¡Gracias!***

ACKNOWLEDGEMENTS

Thanks to Per Strømhaug for his advice and unlimited patience. Thanks to all lab members who worked hard and in good spirits, and made important contributions to this research: Bandhana, Colleen, Jared, Katie, Katherine, Rebecca and Ty. Thanks to the graduate school at the University of Missouri and to the Keystone Symposium group for helping to fund my conference travels.

TABLE OF CONTENTS

LIST OF ILLUSTRATIONS

Figures **Page**

Tables **Page**

ABSTRACT

Misfolded protein aggregation causes disease and aging; autophagy counteracts this by eliminating damaged components, enabling cells to survive starvation. The Cytoplasm-to-vacuole-targeting (Cvt) pathway in yeast encompasses the aggregation of the premature form of Aminopeptidase 1 (prApe1) in cytosol, its targeting by its autophagic receptor Atg19, and its sequestration inside a vesicle formed by autophagic proteins for vacuolar transport. The goal of this research was to elucidate the mechanism of prApe1 aggregation and binding to its receptor Atg19, to better understand how selective autophagy takes place and to develop an *in vitro* assay of autophagy. This study shows that the propeptide of Ape1 is important for aggregation and vesicle formation, it is sufficient for binding to prApe1 and Atg19. Defective aggregation disrupts vacuolar transport, suggesting aggregate shape is important in vesicle formation, while Atg19 and Atg11 binding is not sufficient for vacuolar transport. Ape1 dodecamerization may cluster propeptides into trimeric structures, with sufficient affinity to form propeptide hexamers by binding to other dodecamers, causing aggregation. Furthermore, the N- and C-terminal domains of Atg19 are critical for its correct localization on the surface of aggregates. Atg19 with N- or C-terminal deletions localizes inside aggregates instead, which could interfere with its binding to cytosolic autophagic proteins and cargo for vesicle formation. Meanwhile, the coiled-coil of Atg19 is sufficient for binding to the helix-turn-helix propeptide of prApe1. This study also shows that the mechanism of Atg19 binding to Ape1 aggregates is modified after starvation by the Atg1-Atg13 complex, which plays a key role in autophagy induction and pre-autophagosomal structure (PAS) assembly. A novel *in vitro* assay was developed, in which prApe1 aggregates and binds Atg19 and Atg8. This could be used as a scaffold for an *in vitro* assay of autophagosome formation to elucidate the mechanisms of autophagy.

Chapter 1

Introduction

Autophagy

Autophagy is mainly known for its role during starvation, when cellular components are targeted for degradation so their building blocks can be reused, hence enabling cells to survive. Autophagy also plays a key role in the immune response, in cellular remodeling during development, and in the turnover of old and damaged components to prolong lifespan [1-6]. Autophagic proteins and regulators have highly conserved functions and domains, from yeast to plants and mammals [7]. Autophagy can be divided into several key steps: induction, vesicle nucleation, vesicle expansion and completion, protein retrieval from the maturing autophagosome, autophagosome docking and fusion with the lysosome or vacuole, and finally, autophagic body breakdown for release of cargo into the lysosome lumen. Vacuoles carry out hydrolysis and, therefore, are somewhat similar to lysosomes, but they have additional roles too, like storage and cell homeostasis, including maintaining pH and osmoregulation.

Autophagy in lifespan, development and apoptosis

Besides enabling cells to survive when starved of vital nutrients, autophagy enables cells to eliminate and recycle damaged components [8]. Autophagy helps

eliminate protein aggregates that interfere with cell function in yeast, plant and animal cells [9, 10]. Accumulation of aggregates may lead to ageing and neurodegenerative diseases [11, 12]. In animal models of Huntington's disease, Parkinson's disease and spinocerebellar ataxia, enhanced autophagy improved clearance of aggregated proteins and reduced the symptoms of neurodegeneration [13-15]. By clearing cellular damage, autophagy plays a key role in determining lifespan. Downregulation of TOR, a key negative regulator of autophagy, extends lifespan in *Drosophila*, although this could also be related to the impact TOR has on many other processes [16, 17]. Pertaining to other diseases, autophagy plays a part in modulation of the immune response, prevention of diabetes and obesity by helping pancreatic beta cell survival [18, 19]. By eliminating damaged organelles that release toxic oxygen radicals, it helps prevent cancer, while at the same enabling some cancerous cells to survive harsh conditions [20-22]. Consequently, cancer drugs that target autophagy are being tested.

Autophagy is also critical for development, specifically for remodeling cellular structures. For example, autophagy helps in the removal of mitochondria during red blood differentiation, while in nematodes autophagy is required for dauer development, the dormant life stage that enables *C. elegans* to hibernate and survive until conditions are favorable again [23, 24]. The importance of autophagy in cell development and homeostasis is illustrated by autophagy-deficient mice embryos. Oocytes lacking Atg5, which is involved in autophagic membrane development, fail to develop beyond the 8 cell stage and have lower rates of protein-synthesis because autophagy is required in the turnover of building blocks during cellular remodeling [25, 26]. Furthermore, Atg7

conditional-deficient mice with impaired autophagy in their CNS suffer neuronal death and accumulation of ubiquitin-containing inclusion bodies, because brain cells require a constant nutrient supply and must readily degrade defective protein aggregates [27, 28]. Atg7 is an E1-like enzyme essential for processing of Atg5 and Atg8 for autophagosome formation [29].

While autophagy is in essence a mechanism for survival, in multicellular organisms, it sometimes contributes to cellular destruction and may even be an inducer of apoptosis [30]. For example, in fruit flies autophagy may degrade the apoptosis inhibitor dBruce, hence triggering apoptosis [31]. Meanwhile, during DNA damage in human cells, upregulation of the Atg1 homologue Ulk1 by p53 leads to cell death [32].

Selective Autophagy

Although autophagy is universal and highly conserved, at the same time because the autophagic machinery is very adaptable, there are many different types of selective autophagy. These utilize the core autophagic machinery to package cargo into autophagosomes for transport or degradation, but target very specific components and their main role is in cell homeostasis and defense from pathogens. For example, selective autophagy can target a specific organelle like damaged mitochondria (mitophagy), a protein complex like ribosomes (ribophagy), an intracellular pathogen (xenophagy), or even defective protein aggregates (aggrephagy) (Fig. 1.1). Importantly, since the different modes of selective autophagy represent adaptations of the overall mechanism of macroautophagy, relying on many of the same proteins, any insight into a specific mode

of selective autophagy can be extrapolated to other pathways [33, 34]. Selective autophagy generally requires autophagic receptors and adaptors to target specific cargo. For example; in *Saccharomyces cerevisiae* the Atg19 receptor and its paralogue Atg34 specifically target vacuolar proteases; meanwhile in mammalian cells the Nix receptor is required for mitophagy, and the p62/SQSTM1 adaptor and NBR1 receptor target misfolded and aggregated ubiquitinated proteins to autophagosomes for degradation [35-39]. Viral and bacterial intracellular pathogens are targeted by selective autophagy during infection by autophagic receptors and adaptors including p62/SQSTM1, NDP52, and optineurin [40-48]. How autophagic receptors and adaptors interact with the membrane tethering protein Atg8, or its mammalian homologue LC3, is conserved. The receptors/adaptors Atg19, Atg34, p62, NBR11 and Nix all have WXXL motifs that form an intermolecular parallel beta-sheet for binding Atg8/LC3 [37-39, 49].

Selective autophagy plays an important role in the clearance of defective aggregates that cause neurodegenerative diseases; and also in cancer prevention by mitophagy's removal of damaged mitochondria that produce toxic reactive oxygen species [7, 9-12, 50]. The Cytoplasm-to-vacuole targeting pathway (Cvt) in *S. cerevisiae* is the best understood mode of selective autophagy. It has so far only been found in yeast, specifically in *S. cerevisiae* and *Pichia pastoris* [7, 51]. It utilizes the autophagic machinery during nutrient-rich conditions to transport hydrolyzing enzymes from cytosol to the vacuole [52-56]. Using a similar mechanism, both autophagy and the Cvt pathway assemble autophagic proteins for recruitment of lipid bilayers, shaping them into a double membrane autophagosome or Cvt vesicle that delivers its cargo to the vacuole.

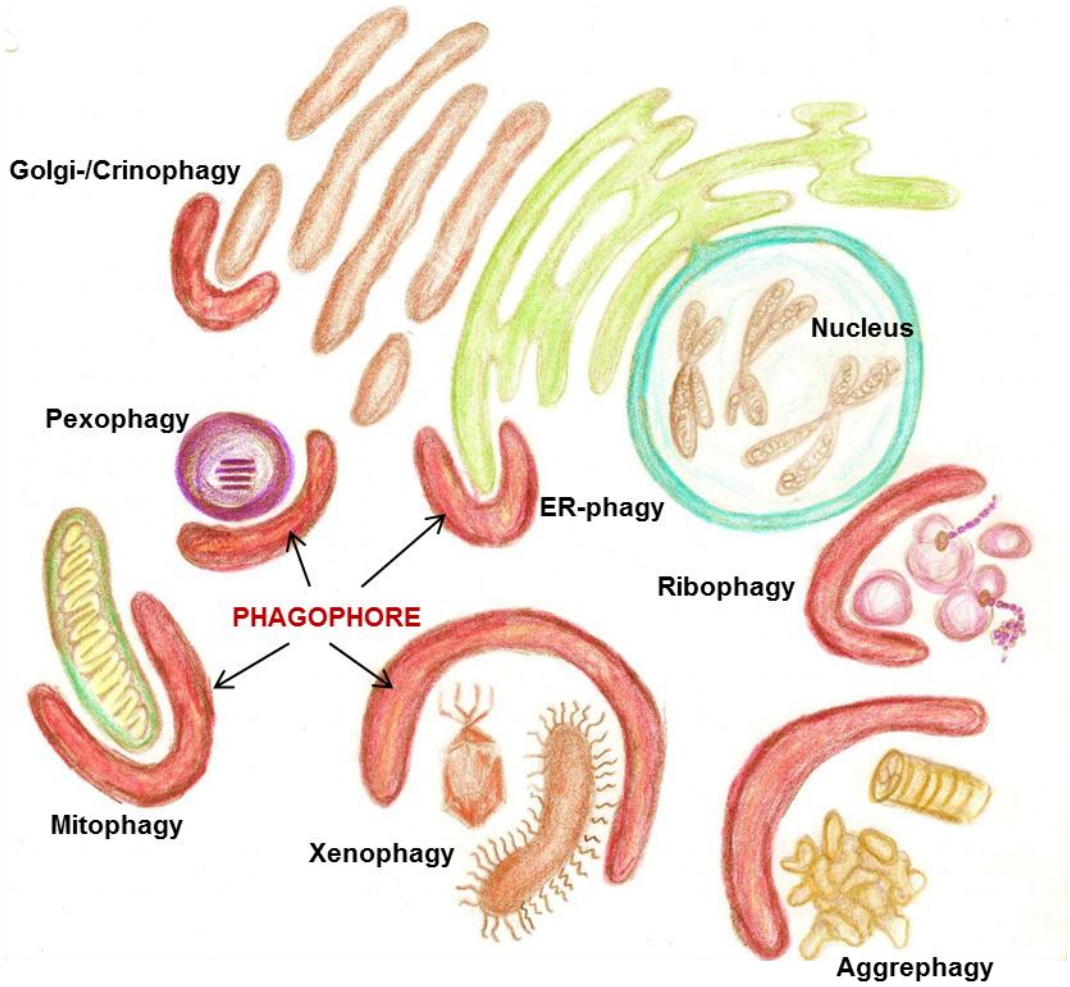

Figure 1.1. Different types of selective autophagy. Each different type of selective autophagy targets a distinct component. Phagophores are shown in red, which are double membrane structures that enclose cytoplasmic components, ultimately completely surrounding them and forming an autophagosome for delivery to the lysosome or vacuole. Autophagy can target many organelles: mitophagy targets mitochondria, ER-phagy targets the ER, pexophagy targets peroxisomes, and Golgi-phagy/Crinophagy targets Golgi. Xenophagy can target intracellular pathogens, virus and bacteria. Aggrephagy targets defective protein aggregates. Selective autophagy can also target specific protein complexes, for example ribophagy targets ribosomes. Selective autophagy plays a key role in cell homeostasis and disease prevention, even during nutrient-rich conditions. It eliminates damaged organelles, like mitochondria that leak toxic reactive oxygen species, and also gets rid of protein aggregates that are sometimes involved in neurodegeneration.

The Cvt pathway Explained (Fig. 1.2)

The Cvt pathway transports the hydrolyzing enzymes aminopeptidase 1 and 4 (Ape1 and Ape4), alpha mannosidase 1 (Ams1), and the cytosolic cysteine protease Lap3 [53, 54, 56, 57]. Interestingly, Ape1 forms dodecamers that aggregate [58]. Ape1 binds the autophagic receptor Atg19, which recruits autophagic proteins Atg8 and Atg11 for assembling more autophagic proteins for the formation of the vesicle [55, 59]. The domains on Atg19 for binding cargo and Atg8 and Atg11 have been elucidated (Fig. 1.3). Atg8 is conjugated to phosphatidylethanolamine (PE) for anchorage to membrane and consequently it plays a key role in tethering of membrane and vesicle completion [60, 61]. Atg11 also serves an important role, as an adaptor protein for recruiting autophagic proteins for vesicle formation, directly binding with Atg1, Atg17 and Atg20 [62]. Atg19 also binds two other cargo enzymes: Ape4 and Ams1 [53, 56]. Lap3 is also transported to the vacuole via the Cvt pathway, but in contrast to the other proteases, Lap3 is cytosolic, hence the purpose of its transport appears to be for its selective degradation [57]. For delivery of Ape1 to the lumen of the vacuole, the outer membrane of the vesicle fuses with the vacuole, where the inner lipid membrane is degraded by the lipase Atg15 to release the cargo.

Protein Aggregation in the Cvt pathway

The Cvt pathway in *S. cerevisiae* encompasses both protein aggregation and the autophagic machinery, making it different from other forms of vesicular traffic. Cytosolic Ape1 concentrates itself by forming an aggregate that recruits its receptor, Atg19, to

direct vesicle formation [63]. Protein aggregation begins with Ape1 synthesis in the cytosol, and its organization into tetrahedral dodecamers (four sided, pyramid-like structures made of twelve Ape1 proteins) [58, 64]. Increasing proton concentration causes dodecamers to disassemble in a step-wise manner, suggesting that during assembly, firstly monomers bind and form symmetrical dimers, these trimerize to form hexamers, then two hexamers bind to form the final dodecamer [65]. The *Borrelia burgdorferi* homologue also forms a dodecamer [47]. Mutants defective in dodecamerization are enzymatically inactive, thus dodecamerization is critical for functionality [66]. Ape1 dodecamers form an aggregate in cytosol that binds Atg19 for recruitment of a double membrane, for Cvt vesicle formation and vacuolar transport.

Ape1 is synthesized and exists in the cytosol as a precursor (prApe1) with an N-terminal propeptide of 45 amino acids [67, 68]. The propeptide directs transport to the vacuole via binding to Atg19, and (as will be shown below), is necessary for aggregation [69]. It is predicted to form a helix-turn-helix, of which the N-terminal helix is amphipathic [70]. Once in the vacuole, the propeptide is cleaved to generate the mature form, mApe1. Although many precursor proteins are inactive, prApe1 may be enzymatically active [66, 71]. Aggregation may facilitate vesicle formation and help inhibit prApe1 proteolytic activity. In comparison to the *B. burgdorferi* aminopeptidase, which does not form aggregates, prApe1 has additional amino acids that are predicted to be positioned on the dodecamer surface: 45 residues on its N-terminus that constitute the propeptide, and 10 residues on its C-terminus. Since the propeptide is cleaved by vacuolar proteinase B, it is accessible and hence, located on the surface of dodecamers.

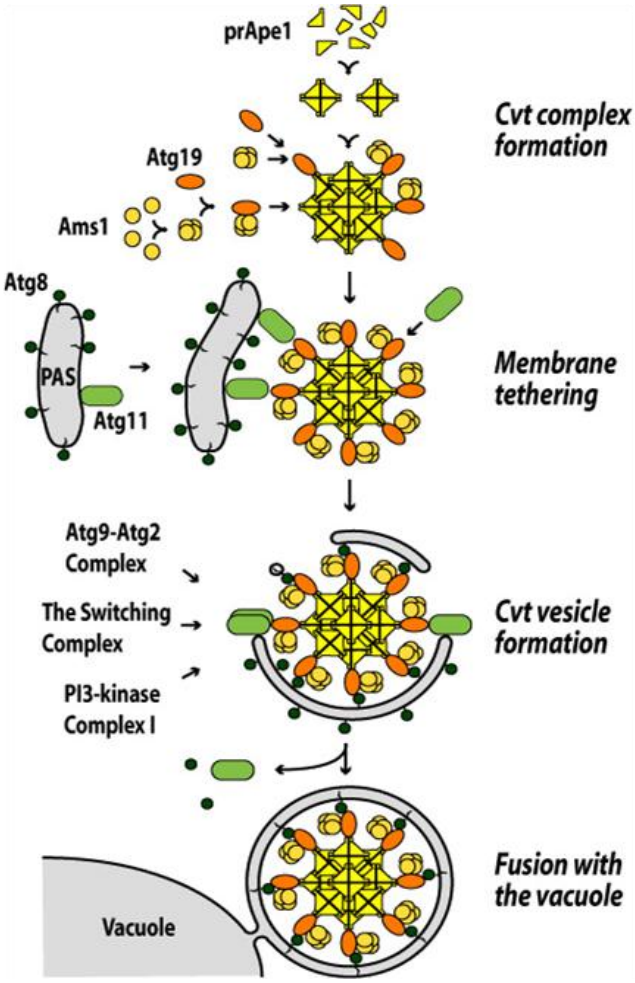

Figure 1.2. <u>Formation of the Cvt vesicle.</u> The Cvt pathway transports the hydrolyzing enzymes aminopeptidase 1 and 4 (Ape1 and Ape4), alpha mannosidase 1 (Ams1), and the cytosolic cysteine protease Lap4, taking them to the vacuole inside an autophagic vesicle. Both Ape1 and Ape4 form dodecamers, but only Ape1 is known to form aggregates in cytosol. Ape1 is synthesized as an inactive precursor, prApe1, which aggregates and binds the autophagic receptor Atg19. Atg19 in turn recruits autophagic proteins Atg8 and Atg11, for assembly of the autophagic machinery and membrane during Cvt vesicle formation. Autophagic membrane is recruited from the PAS, where several Atg proteins reside, including Atg8 and Atg11. The mechanism of Cvt vesicle formation remains to be elucidated. Atg11 dissociates from the Cvt complex before full maturation of the Cvt vesicle. Lap3 is also transported to the vacuole via the Cvt pathway, but in contrast to the other proteases, which are vacuolar, Lap3 is cytosolic. Hence, the purpose of its transport appears to be for its selective degradation. Since Lap3 has not been shown to bind to the receptor Atg19, it is unknown how it is targeted to the Cvt vesicle. The outer vesicle membrane docks and fuses with the vacuolar membrane, while the inner membrane is degraded by Atg15 to release the cargo.

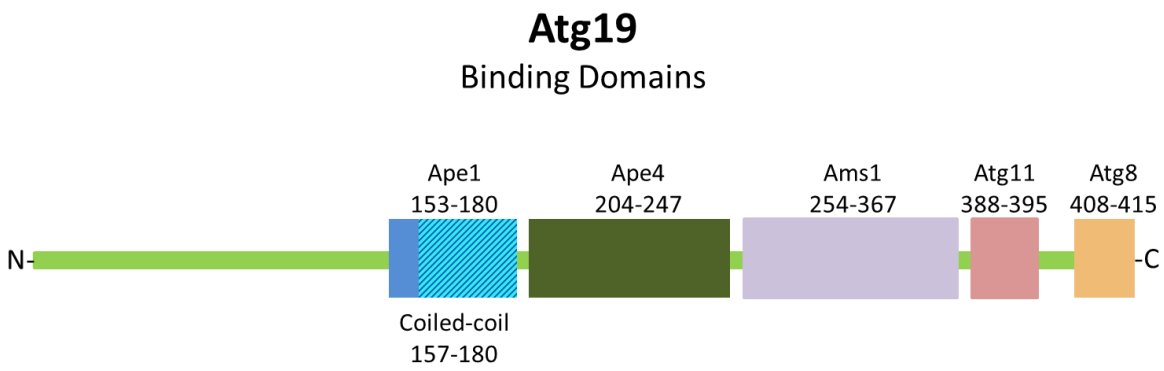

Figure 1.3. Schematic figure of the autophagic receptor Atg19. Atg19 binding domains that have been identified and their amino acid position. Atg19 binds vacuolar proteases that are synthesized in cytosol, and targets them for transport to the vacuole via the Cvt pathway. Ape1, Ape4 and Ams1 are all vacuolar proteases that bind to Atg19, their binding domains have been elucidated. Atg19 also binds two autophagic proteins, the adaptor protein Atg11, and the membrane tethering protein Atg8, which bind to its C-terminus. There is a putative coiled-coil region in the Ape1 binding site.

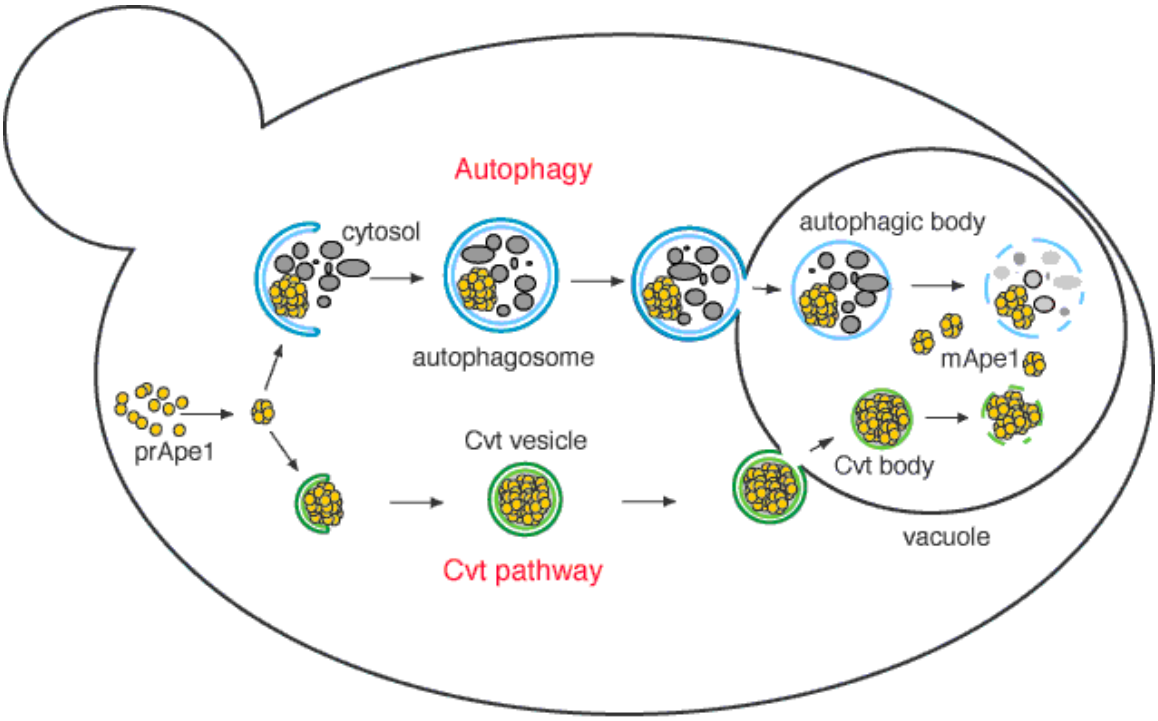

Klionsky, D.J. (2005). The molecular machinery of autophagy: unanswered questions, *J Cell Sci* **118**, 7-18.

Figure 1.4. <u>Ape1 transport via the Cvt pathway or autophagy</u>. Aminopeptidase 1 is synthesized in cytosol, as an inactive precursor that forms aggregates. These are then transported to the vacuole via the Cvt pathway during nutrient-rich conditions or by autophagy during starvation. During the Cvt pathway, prApe1 aggregates recruit autophagy proteins and membrane for formation of a double membrane Cvt vesicle, for subsequent transport to the vacuole. During autophagy, selected cellular components and prApe1 aggregates are surrounded by a double membrane to form an autophagosome. In *S. cerevisiae*, the membrane may be recruited from a specialized structure called the Pre-Autophagosomal Structure or Phagophore Assembly Site (PAS) where many Atg proteins accumulate. After vesicle or autophagosome formation, the outer vesicle membrane fuses with the vacuolar membrane, and the inner membrane is then hydrolyzed by vacuolar enzymes to release its cargo into the lumen, where they either serve as vacuolar proteases, or are degraded so their components can be reused for biosynthesis.

Atg1 helps regulate autophagy, assemble the PAS, and recruit Atg proteins

During starvation, the Cvt pathway cargo can be transported to the vacuole inside autophagosomes (Fig. 1.4) [52]. For Ams1 transport via autophagy, Ams1 binds Atg34, a paralogue of Atg19, which similarly interacts with Atg8 and Atg11, forming the Ams1 complex [72].

Induction of autophagy and selection of cargo must be tightly regulated to ensure the preservation of essential cellular components, while a rapid turnover of redundant components takes place. TOR, a phosphatidylinositol kinase homologue, is a key negative regulator of autophagy (Fig. 1.5) [73-75]. TOR and cAMP-dependent protein kinase (PKA) signaling independently target the Atg1-Atg13 complex during nutrient-rich conditions to prevent autophagy [76-79]. The Tor complex 1 (TORC1) and PKA directly phosphorylate Atg13, a modulator of Atg1 activity, albeit at different residues [78-80]. Upon starvation, inactivation of TORC1 enables dephosphorylation of Atg13, causing the Atg1-Atg13 complex to assemble the Atg17-Atg29-Atg31 complex, which in turn helps recruit autophagic proteins to the PAS to initiate autophagy [81-87]. During the Cvt pathway, Atg1 and Atg13 instead help recruit Atg11, Atg20 and Atg24 for vesicle formation [88]. Atg1 and Atg13 are also important for Atg9 and Atg23 retrieval transport. Atg9 is a transmembrane protein thought to act as a lipid carrier for vesicle expansion, while Atg23 is associated with it; Atg9 is involved in both autophagy and the Cvt pathway, while Atg23 only functions in the later [89]. Other proteins that the Atg1-Atg13 complex helps recruit to the PAS are Atg2, Atg8, Atg14, Atg16 and Atg18 [85, 90, 91].

Although Atg13 is involved in both autophagy and the Cvt pathway, in *atg13*Δ cells there is still some mApe1 present, suggesting prApe1 vacuolar transport via the Cvt pathway is diminished, but not completely abolished. Hence, Atg1 maintains some level of activity in the absence of Atg13 during nutrient-rich conditions [92].

Atg1 has a structural role, but it is also a serine/threonine kinase. Although its homologues in *Drosophila melanogaster, Caenorhabditis elegans* and mammals are all involved in autophagy and in neuronal development, there are also differences in their function [23, 93-104]. In yeast, Atg1 kinase activity is important in both the Cvt pathway and autophagy, for PAS disassembly and perhaps also for autophagosome expansion; however, only structural function is required for assembly of the PAS and of the Atg1-Atg13-Atg17 complex for the recruitment of additional autophagic proteins [85, 105].

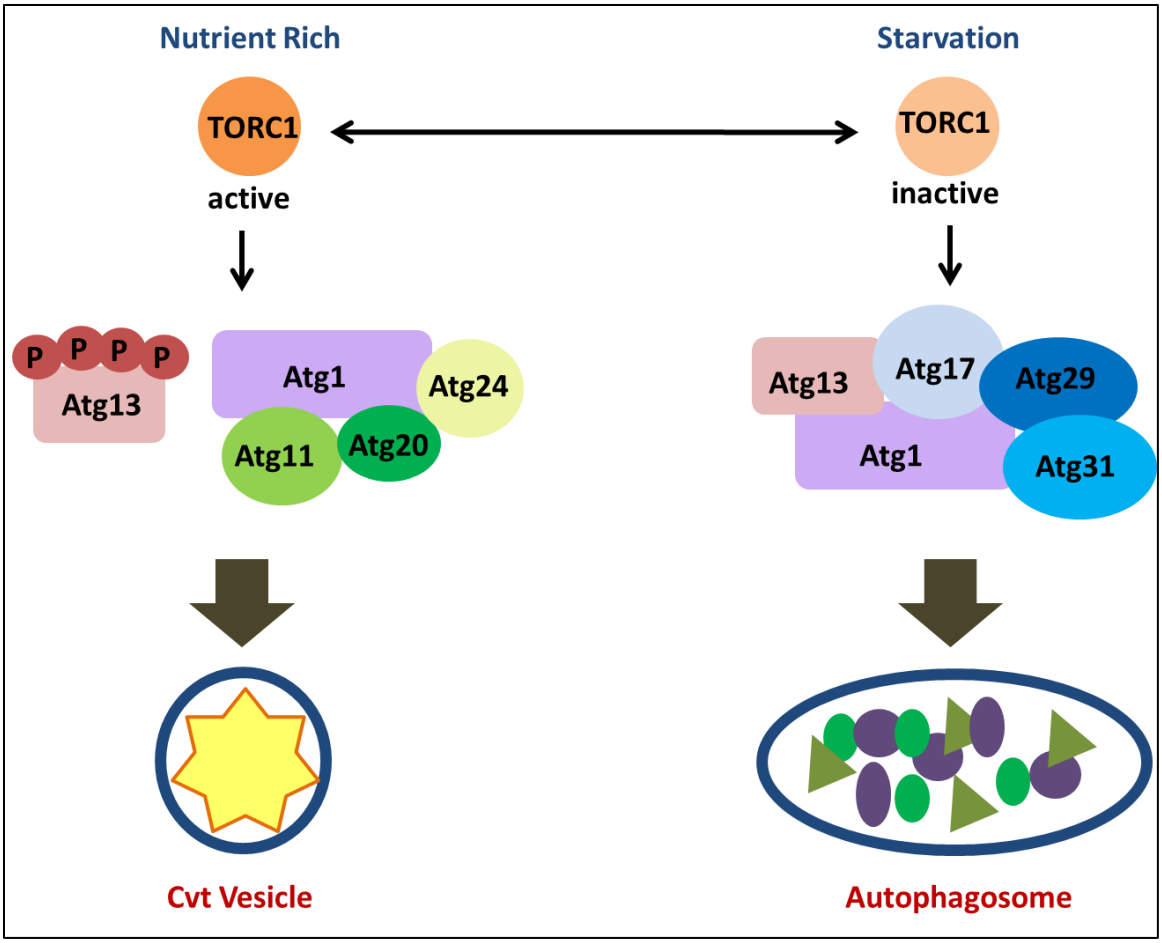

Figure 1.5. **Atg1 interacts with several autophagic proteins, and is required for both the Cvt pathway and autophagy**. Atg1 is a serine/threonine kinase essential for the initial building of the autophagosome and Cvt vesicle. It is directly controlled by TOR kinase, a nutrient sensor and key negative regulator of autophagy. Atg1 associates with Atg13, 17, 29, 31, 11, 20 and 24. Atg13, a modulator of Atg1 activity, participates both in autophagy and the Cvt pathway. Lack of Atg13 greatly diminishes Cvt transport while not completely abolishing it. Atg17, 29 and 31 only function in autophagy, while Atg11, 20 and 24 only function in the Cvt pathway. Atg1 is found to be in a complex with Atg13 and Atg17. The function of Atg1 is not well understood, but it seems to play a role in PAS assembly and disassembly, and in autophagosome maturation. In animals it is critical for neuronal development.

Protein Name	Summary
Aminopeptidase 1 (Ape1)	Vacuolar protease made in cytosol, transported to the vacuole via the Cvt pathway. Binds Atg19. Forms dodecamers that aggregate in cytosol. Synthesized as a precursor (prApe1) with a 45 amino acid N-terminal propeptide, that is cleaved in the vacuole to generate the mature protein (mApe1). Transport of other Cvt cargo is dependent on Ape1.
Aminopeptidase 4 (Ape4)	Vacuolar protease made in cytosol, transported to the vacuole via the Cvt pathway. Binds Atg19. Forms dodecamers but does not aggregate, and does not have a propeptide.
α-mannosidase 1 (Ams1)	Vacuolar protease made in cytosol, transported to the vacuole via the Cvt pathway. Binds Atg19. Forms oligomers but does not aggregate. Also binds the Atg19 paralogue Atg34, which targets Ams1 to the vacuole inside autophagosomes during autophagy.
Lap3	Cytosolic protease transported to the vacuole via the Cvt pathway. Does not bind Atg19. Is perhaps transported to the vacuole for degradation.
Atg1	Serine/threonine kinase. Key modulator of autophagy. Has a structural function, forming a complex with Atg13 and Atg17 during induction of autophagy. Recruits Atg11, Atg20 and Atg24 for Cvt vesicle formation; and Atg17, Atg29 and Atg31 for autophagosome formation. The function of Atg1 remains to be elucidated. It is required for both the Cvt pathway and autophagy.
Atg8	Anchored to membrane. Involved in membrane tethering and membrane expansion during autophagosome formation. Essential for the Cvt pathway and autophagy.
Atg11	Binds several proteins, including Atg1, Atg17, Atg19 and Atg20. Hence thought to serve as an adaptor protein for the Cvt pathway and autophagy. Required for the Cvt pathway.
Atg13	Atg1 modulator. Directly regulated by the nutrient sensor TORC1 complex. Required for autophagy, important for the Cvt pathway.
Atg19	Autophagic receptor, binds Cvt cargo vacuolar proteases to transport them to the vacuole, including Ape1, Ape4 and Ams1. Also binds autophagic proteins Atg11 and Atg8 for formation of a Cvt vesicle.
Atg34	Atg19 paralogue that binds Ams1, Atg8 and Atg11, and targets Ams1 to autophagosomes during starvation for vacuolar transport.

Table 1.1. Summary of the key Cvt pathway and autophagic proteins discussed in dissertation.

Origin of Autophagic Membrane: the Great Controversy

An essential part of autophagy is the recruitment and nucleation of the membrane, which forms a double membrane structure that has been termed the phagophore. The phagophore is assembled at the PAS. Ever since the earliest days of autophagy research, there has been great controversy over the origin of the membrane for phagophore formation, and evidence has pointed to the ER, Golgi, mitochondria and plasma membrane [106, 107]. One of the key limitations is that only one integral membrane protein that is also part of the core autophagic machinery has been identified: Atg9. Its function is not well understood, and its localization is perplexing, since in mammals it transits between the endosome and Golgi, while in yeast it cycles between the PAS and peripheral tubules and vesicle clusters, often adjacent to the mitochondria [108-110].

Presently, the strongest candidates for the origin of the phagophore are the ER and Golgi, since proteins mediating exit from the Golgi, including the Conserved Oligomeric Golgi (COG) subunits, Golgi ADP ribosylation factors (ARFs) and sec proteins, together with the TRAPPIII complex and the Rab GTPase Ypt1, are all important for recruitment of autophagic proteins to the PAS [111-114]. Rab Ypt1 is essential for ER-Golgi and Golgi traffic, and is activated by TRAPP complexes (I, II and III), which act as a guanine nucleotide exchange factor (GEF) and help in tethering vesicles to acceptor compartments. TRAPPIII is required for both autophagy and the Cvt pathway, and localizes to the PAS, and hence may play a role in directing ER or Golgi membrane for phagophore formation [115, 116]. This is consistent with electron microscopy tomography that has shown ER connected with phagophores, while Atg14 localization to

the ER is critical for autophagy; Atg14 also localizes to the phagophore and is essential for autophagosome formation by regulating PtdIns(3)P synthesis for Atg protein recruitment to the PAS [117-120].

Evidence pointing to the mitochondria or plasma membrane as origins of the phagophore, however, continues to be scrutinized. In mammalian cells, photobleaching has shown the mitochondrial and autophagosomal membrane to be connected, while mitochondrial disruption diminishes autophagy [121]. As for the plasma membrane, in mammalian cells Atg16L1, thought to be involved in vesicle expansion, interacts with the heavy chain of clathrin, and co-localized with plasma membrane associated cholera toxin peripheral vesicles. Furthermore, inhibition of endocytosis via clathrin-coated vesicles diminished autophagosome formation [122].

Vesicle Nucleation: In the beginning of vesicle formation (Fig. 1.6)

Vesicle nucleation is mediated by the phosphatidylinositol (PtdIns) 3-kinase complex I, which consists of Atg6, Atg14, Vps34 and Vps15 [123, 124]. Atg14 determines PAS localization of complex I, and its localization in turn depends on Atg17, Atg13 and Atg9 [90, 125]. The function of Atg6 is not well understood. Its homologue in mammalian cells, Beclin 1, has been implicated in balancing autophagy with apoptosis and cell growth, and it is a tumor suppressor; hence it is plausible that Atg6 orchestrates autophagy with other cellular functions [126-128]. Vps34 has inositol kinase activity. It is a PtdIns 3-kinase belonging to the class III kinases, phosphorylating PtdIns at the D-3 position of the inositol ring [129, 130]. Vps15 also has enzymatic activity; it is a

serine/threonine protein kinase that phosphorylates Vps34, which is required for Complex I formation [131]. Furthermore, Vps15 is anchored to membrane, partly because it is myristoylated at its N-terminus, which enables it to tether the complex to the membrane [132].

Vps34 phosphorylation of PtdIns to produce PtdIns(3)P is critical for autophagy. PtdIns(3)P localizes to the PAS, autophagosome, the late endosome, and the vacuolar membrane and lumen [133]. Specifically, the inner surface of the autophagosome is enriched with PtdIns(3)P, which serves as a landmark for assembly of autophagic proteins. Atg18, Atg20, Atg21 and Atg24 bind to PtdIns(3)P; Atg18 and Atg21 bind via their conserved PX domains, while Atg21 is mainly required for the Cvt pathway [88, 134-136]. Atg18 can also bind PtdIns(3,5)P2, but this is not required for autophagy, instead it is required for maintaining vacuolar morphology [137]. Atg18 binds Atg2 to form the Atg18-Atg2 complex, which has a role in membrane formation and during Atg9 retrieval [138]. PtdIns(3)P is also involved in Atg8 and Atg12-Atg5 recruitment to the PAS [90]. Atg8 is critical for membrane tethering and vesicle completion; while Atg12-Atg5 are involved in its conjugation to phosphatidylethanolamine (PE) to anchor it to the membrane [61, 139-142]. PtdIns(3)P is also thought to affect the size of autophagosomes, by determining the curvature of the membrane and the rate of recruitment of the autophagic machinery. Consistent with this, Atg14 truncations and lower levels of Atg8 generate smaller autophagosomes[125, 141].

Atg9 is a transmembrane protein that is also involved in nucleation. Besides localizing at the PAS, it is also found in small punctate structures throughout cytosol and

on the surface of mitochondria [108-110, 143]. In nutrient-rich conditions, Atg9 is critical in the Cvt pathway [144, 145]. For Cvt vesicle formation, Atg11 binding recruits Atg9 to the PAS, an interaction that is facilitated by actin [144, 146]. Upon induction of autophagy, Atg9 localization to the PAS is instead dependent on Atg17 binding [84]. Atg9 can form a multimeric complex under both nutrient-rich and starvation conditions, which is required for its trafficking to the PAS, and mutants that fail to multimerize lead to formation of abnormal autophagosomes [147, 148]. However, it is unclear how exactly Atg9 helps to deliver membrane for autophagosome formation. Meanwhile, Atg23 is a peripheral membrane protein that shows a similar localization, but is mainly required for the Cvt pathway [149-152]. Atg23 binds Atg9 and Atg27, forming a complex that is important for efficient cycling of Atg9 between the periphery and PAS.

Vesicle Expansion and Completion: A vesicle is born (Fig. 1.6)

After vesicle nucleation, the phagophore must expand and complete formation of the autophagosome, sealing the cargo inside. Vesicle expansion requires recruitment of additional membrane, mediated by ER and Golgi traffic constituents: TRAPIII, Ypt1, COG and Sec2/4. Another important step of vesicle expansion and completion is Atg8 conjugation to phosphatidylethanolamine (PE), which anchors soluble Atg8 to the membrane. Atg8 is an ubiquitin-like (Ubl) protein that plays a key role in membrane expansion by tethering membrane, and in vesicle completion and closure by mediating self-fusion. Hence, its absence causes aberrantly small autophagosomes while effectively blocking transport via autophagy or the Cvt pathway [61, 139, 141]. For Atg8

conjugation to PE, firstly its C-terminal arginine must be proteolytically cleaved by the protease Atg4 to reveal a glycine residue that can in turn be conjugated to PE [153, 154]. Another Ubl protein is Atg12, which is conjugated to Atg5 instead of PE, forming Atg12-Atg5 [142, 155]. Atg7 is an E1-like enzyme that activates both Atg8 and Atg12 for conjugation [156-158]. Afterwards, Atg3 and Atg10 are the E2-like enzymes that catalyze the conjugation itself: Atg3 conjugates Atg8 to PE, while Atg10 conjugates Atg12 to Atg5 [159-161]. After Atg12-Atg5 formation, an Atg16 multimer binds and forms a tetrameric complex, Atg12-Atg5·Atg16, whose function is not well understood except that it is important for Atg8 conjugation to PE [162, 163].

Retrieval: Getting back what you put in (Fig. 1.6)

After autophagosome or Cvt vesicle completion, only two autophagic proteins remain associated: Atg8-PE and Atg19. The latter mainly has a role in the Cvt pathway as a cargo receptor. All the other autophagic proteins dissociate and since they are soluble, they can remain in cytosol or be recruited to a nascent phagophore. The exceptions are Atg9, a transmembrane protein, and Atg23, a peripheral membrane protein. Their retrieval requires the Atg1-Atg13 complex. Atg9 retrieval, in addition, requires binding to Atg2 and Atg18, while Atg18 localization at the PAS is dependent on PtdIns(3)P [89, 109, 135, 145, 164, 165]. While the mechanism of retrieval is not well understood, inevitably it must involve the loss of some lipids from the autophagosome; hence, there must be a balance between vesicle expansion and retrieval.

Docking and Fusion: Your delivery is here

The autophagosome or Cvt vesicle outer membrane fuses with the vacuolar membrane in yeast, releasing the autophagic body into the vacuolar lumen. The autophagic body is constituted of the inner membrane and the cargo that is still inside it. Fusion must be regulated in some way, to ensure that autophagosome completion takes place prior to fusion, otherwise the cargo would remain in cytosol. The mechanism that controls fusion has yet to be elucidated and may involve removal of one or several components of the autophagic machinery. For example, Atg8-PE is removed from the outer surface of autophagosomes prior to fusion, by Atg4 cleavage of PE to free Atg8 from the membrane. Failure to do this causes defective traffic by both autophagy and the Cvt pathway. Furthermore, it is possible Atg8 can be recycled by re-conjugating to PE, for another round of autophagosome formation.

On the other hand, the machinery for docking and fusion of autophagosomes and Cvt vesicles has been identified, and is constituted by similar components as those required for vacuolar fusion with endosomes, with vesicles derived from endosomes or Golgi, and for homotypic fusion. The fusion machinery consists of a Rab protein and its corresponding guanine nucleotide exchange factor (GEF) for tethering, a soluble NSF attachment protein receptor (SNARE) and an N-ethylmaleimide-sensitive factor (NSF) for fusion and priming, and the class C Vps protein complex for modulation of SNARE pairing, also known as the homotypic fusion and vacuole protein sorting (HOPS) complex [134, 166]. The SNARE proteins include Vam3, Vam7, Vti1 and Ykt6 [167-169]. Ypt7 is the Rab required for tethering, while the Ccz1-Mon1 complex functions as

its GEF [170-173]. Also required are the NSF, SNAP and a GDP dissociation inhibitor (GDI) homologs Sec17, Sec18 and Sec19 [174].

Vesicle Breakdown and Permease Efflux: Recycling the trash (Fig. 1.6)

After fusion of the autophagosome or Cvt vesicle outer membrane with the vacuole, lipase Atg15 will then degrade the inner membrane that still surrounds the autophagic body, thus releasing its cargo [175-177]. Without Atg15, autophagic bodies accumulate inside the vacuole, and consequently there is a decrease in the protein turnover rate. Once cargo is released, it can be broken down so its subunits can be reused. Linking degradation with biosynthesis is Atg22, since it is a vacuolar integral membrane protein that transports amino acids out of the vacuole and into cytosol, where they can be used to make new proteins [178]. Consistent with this, Atg22 is critical for cell viability under starvation conditions.

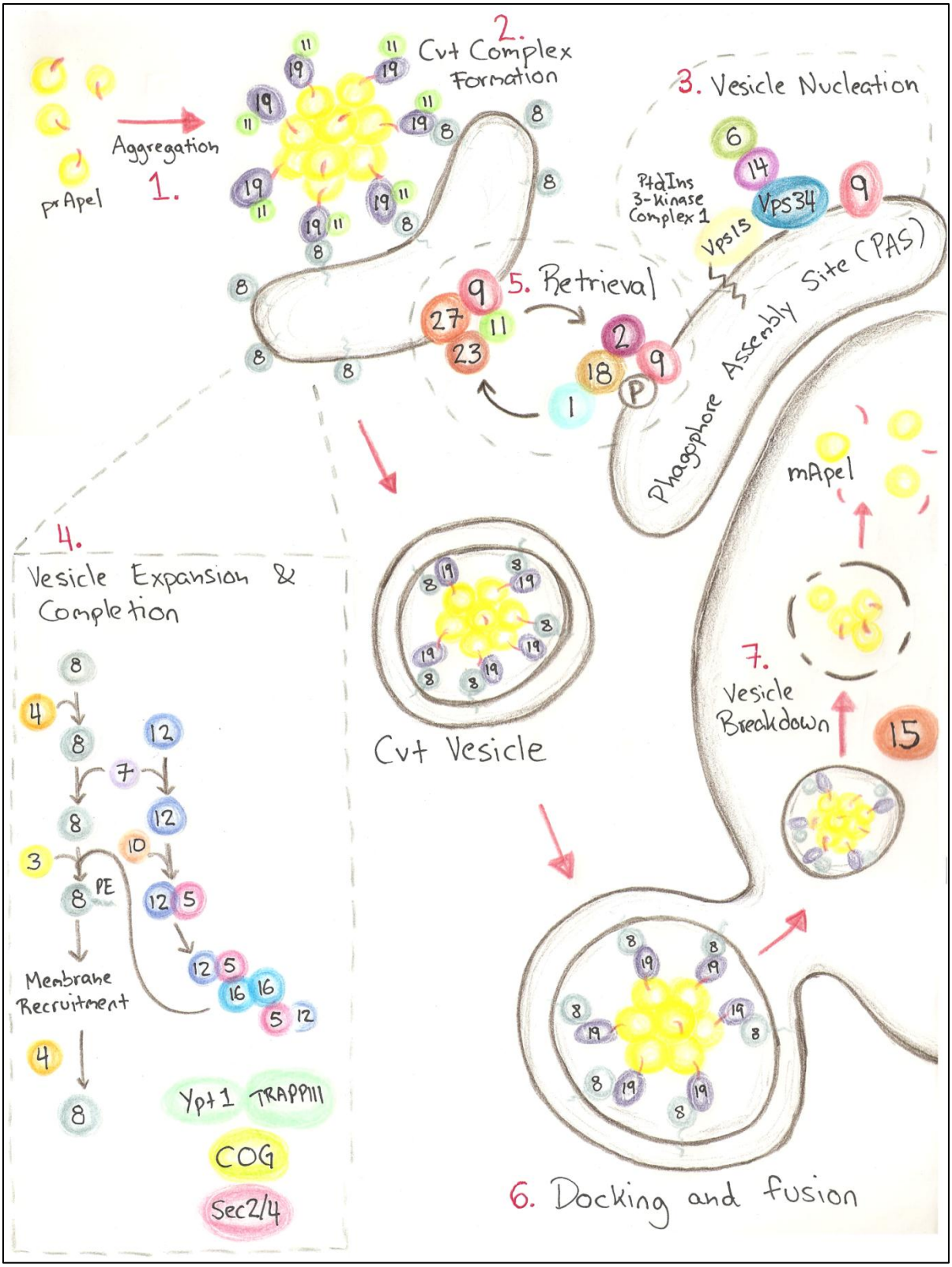
prApe1
Aggregation
1.
2.
Cvt Complex Formation
3. Vesicle Nucleation
PtdIns 3-kinase Complex 1
Vps15
Vps34
Phagophore Assembly Site (PAS)
5. Retrieval
mApe1
4.
Vesicle Expansion & Completion
Membrane Recruitment
PE
Cvt Vesicle
7.
Vesicle Breakdown
Ypt1
TRAPPIII
COG
Sec2/4
6. Docking and fusion

Figure 1.6. Summary of the Cvt pathway, and how it utilizes the autophagic machinery for vesicle formation. Numbers in black represent autophagic proteins, i.e. '19' means 'Atg19'. (1) Aggregation: Ape1 is synthesized in cytosol as a precursor (prApe1), with a 45 amino acid N-terminal propeptide, and forms aggregates. (2) Cvt complex formation: prApe1 binds to the autophagic receptor Atg19. Atg19 binds Atg11, an adaptor protein, and Atg8, a lipidated protein for tethering membrane. The Cvt complex recruits the autophagic machinery for vesicle formation, which involves several processes that are similar to those used in autophagosome formation: (3) vesicle nucleation, (4) vesicle expansion and completion, and (5) retrieval of integral membrane proteins that will not be part of the completed vesicle. A double membrane Cvt vesicle is formed. (6) Its outer membrane docks and fuses with the vacuole. (7) Finally, degradation of the inner membrane by the lipase Atg15 releases the cargo into the vacuole. The propeptide of prApe1 is cleaved off, to produce its mature form mApe1, which no longer forms aggregates.

Cvt Pathway	Selective Autophagy	Core Machinery	Nonselective Autophagy
Atg11	Atg11	Atg1	Atg17
Atg19	Atg19	Atg2	Atg29
Atg20	Atg20	Atg3	Atg31
Atg21	Atg21	Atg4	
Atg23	Atg23	Atg5	
Atg24	Atg24	Atg6	
Atg27	Atg25	Atg7	
	Atg26	Atg8	
	Atg27	Atg9	
	Atg28	Atg10	
	Atg30	Atg12	
Cvt Cargo	Atg32	Atg13	
Ape1	Atg33	Atg14	
Ape4	Atg34	Atg15	
Ams1	Atg35	Atg16	
Lap3		Atg18	
		Atg22	

Table 1.2. Summarizing the pathways autophagic proteins are involved in. List of Atg yeast proteins involved in the Cvt pathway, selective autophagy (Cvt, pexophagy and mitophagy), nonselective autophagy, and those involved in all processes because they constitute the core machinery for vesicle formation. Also includes a list of cargo proteases transported via the Cvt pathway.

Studying Autophagy Today: The New Frontier

The study of autophagy has greatly expanded over the past few decades, completely transforming our previous view of autophagy. Instead of being a simple form of bulk transport that is only used during some forms of starvation, autophagy is prevalent throughout the lifetime of all eukaryotic cells, coming to their rescue every time their existence is challenged, whether it is depletion of nitrogen, carbon or fatty acids, an attack from pathogens, mechanical or temperature stress, accumulation of misfolded proteins or reactive oxygen species (ROS), or some other form of cellular dysfunction [179]. To be able to respond to all different types of cellular emergencies, the core machinery of autophagy has been adapted, generating many different types of autophagy that can target specific compartments or cargo, and that are tightly regulated, these include: selective autophagy of the ER (ER-phagy), selective autophagy of the Golgi (Golgi-phagy), selective autophagy of peroxisomes (pexophagy), gigantic macroautophagy (utilized in programed nucleus death during gamete formation in *Tetrahymena thermophila*), chaperone-mediated autophagy (CMA), mammalian endosomal microautophagy (e-MI), mitophagy, and the Cvt pathway [180-186]. Bacteria and viruses can also be targeted to autophagosomes, including gastrointestinal and respiratory parasites such as *Salmonella typhimurium*, norovirus and coronavirus [44, 187, 188].

There has been a great effort to identify autophagy during multiple cellular processes in model organisms, including yeast, fruit flies, *C. elegans*, mammals and plants, mainly by using Atg8 and its homologue LC3 as markers. Meanwhile, we

continue to dissect the signaling pathways that induce and regulate autophagy. Scientists interested in the mechanism of autophagy are working on identifying autophagic receptors and their cargo, determining the origin and mode of recruitment of autophagic membrane, establishing the hierarchy and function of autophagic proteins, and unraveling the mechanism of autophagosome maturation and completion.

S. cerevisiae has played a key role, since several of the proteins involved in autophagosome formation have been identified through the generation of yeast mutants that are deficient in autophagy [134, 189-191]. Consequently, we have been using this system to elucidate the mechanism of Cvt vesicle formation. We focused on the mode of prApe1 aggregation and recruitment of the autophagic receptor Atg19, how Atg19 in turn recruits the autophagic machinery for vesicle formation, and how this is regulated under nutrient-rich and starvation conditions. Since *in vitro* assays have proven useful in understanding cellular trafficking, we worked on generating an *in vitro* assay of autophagy by using the Cvt complex as a scaffold for recruiting autophagic proteins and membrane.

Chapter 2

Materials and Experimental Procedures

Strains and Media

Standard methods were used for growth and manipulation of cell strains. Cells were incubated at 30°C with shaking at 250 RPM. For growth of yeast under nutrient-rich conditions, cells were grown to exponential phase in liquid broth constituted of synthetic minimal medium plus dextrose (0.17% yeast nitrogen base without ammonium sulfate and without amino acids, 0.5% ammonium sulfate, 2% glucose, and supplemented with the required amino acids). However, for growth in starvation conditions, cells were grown in a similar media but without ammonium sulfate and without amino acids (0.17% yeast nitrogen base without ammonium sulfate and without amino acids, and 2% glucose). Cells were starved for 3-4 hours.

Rosetta Escherichia coli cells were grown in liquid broth (1% Bacto-Tryptone, 0.5% yeast extract, 0.5% NaCl); incubated at 37°C with shaking at 250 RPM. The *LacZ* promoter was induced with a final concentration of 1 mM IPTG for 2 hours.

Yeast strain	Genotype	Reference
BY4742	*(MATa/α his3Δ1/his3Δ1 leu2Δ0/leu2Δ0 LYS2/lys2Δ0 met15Δ0/MET15 ura3Δ0/ura3Δ0)*	ResGen
*atg1*Δ	BY4742; *atg1*Δ*::Kan*	ResGen
*atg8*Δ	BY4742; *atg8*Δ*::Kan*	ResGen
*atg11*Δ	BY4742; *atg11*Δ*::Kan*	ResGen
*atg13*Δ	BY4742; *atg13*Δ*::Kan*	ResGen
*atg17*Δ	BY4742; *atg17*Δ*::Kan*	ResGen
*atg18*Δ	BY4742; *atg18*Δ*::Kan*	ResGen
*atg19*Δ	BY4742; *atg19*Δ*::Kan*	ResGen
*atg20*Δ	BY4742; *atg20*Δ*::Kan*	ResGen
*atg24*Δ	BY4742; *atg24*Δ*::Kan*	ResGen
*atg29*Δ	BY4742; *atg29*Δ*::Kan*	ResGen
*atg31*Δ	BY4742; *atg31*Δ*::Kan*	ResGen
*ape1*Δ	BY4742; *ape1*Δ*::Kan*	ResGen
*ams1*Δ	BY4742; *ams1*Δ*::Kan*	ResGen
*atg8*Δ *atg11*Δ	BY4742; *atg11*Δ*::Kan atg8*Δ*::HIS3*	Morales Quinones, M. and Stromhaug, P.E. (2012)
*ams1*Δ *atg8*Δ *atg11*Δ	BY4742; *ams1*Δ*::Kan atg11*Δ*::LEU2 atg8*Δ*::HIS3*	This study
*atg19*Δ *ape1*Δ	BY4742; *atg19*Δ*::Kan ape1*Δ*::LEU2*	Morales Quinones, M. and Stromhaug, P.E. (2012)
PJ69-4A *atg19*Δ *ape1*Δ	*(MAT**a** trp1-901 leu2-3, 112 ura3-52 his3-200 gal4Δ gal80Δ LYS::GAL1-HIS3 GAL2-ADE2. GAL2 met2::GAL7-lacZ); atg19*Δ*::Kan ape1*Δ*::TRP1*	Morales Quinones, M. and Stromhaug, P.E. (2012)

Table 2.1. Yeast strains

Plasmids and Primers

Standard methods were used for cloning procedures. PCR was performed using PCR R-Taq 2x Master Mix (MidScience), ligation with T4 DNA ligase (NEB), following the manufacturer's instructions.

Plasmid	**Reference**
RFP-ape1 pRS306	Stromhaug, P.E., et al.(2004)
RFP-ape1 atg19-GFP pRS306	Morales Quinones, M. and Stromhaug, P.E. (2012)
ape1 pRS307	Morales Quinones, M. and Stromhaug, P.E. (2012)
ape1 pRS425	Morales Quinones, M. and Stromhaug, P.E. (2012)
ape1 pRS426	Morales Quinones, M. and Stromhaug, P.E. (2012)
pCu ape1-GFP pRS416	Labbe, S. and D.J. Thiele, (1999)
GFP-atg19 pRS416	Leber, R., et al., (2001)
atg8ΔR pRS416	Ho, K.H. and W.P. Huang (2009)
atg11ΔN pRS416	Yorimitsu, T. and D. J. Klionsky (2005)
pGAD-atg19	Chang, C.Y. and W.P. Huang (2007)
pGBDU-ape1	James, P., J. Halladay, and E.A. Craig (1996)
pGBDU-propeptide	Morales Quinones, M. and Stromhaug, P.E. (2012)
pGAD-C2	James, P., J. Halladay, and E.A. Craig (1996)
pGBDU-C2	James, P., J. Halladay, and E.A. Craig (1996)
propetide-6xHis-pET29	Morales Quinones, M. and Stromhaug, P.E. (2012)

Table 2.2. Plasmids

Construct	Template	Primer sequence 5' – 3'
ape1Δ2	Genomic	ATCATATAGAAGTCATCGACTAGTCATATGG AACAACGTGAAATACTGGAACAATTGAAG
ape1Δ2-3	Genomic	ATCATATAGAAGTCATCGACTAGTCATATGC AACGTGAAATACTGGAACAATTGAAGAAA
ape1Δ2-4	Genomic	AATATCATATAGAAGTCATCGACTAGTCATA TGCGTGAAATACTGGAACAATTGAAGAAA
ape1Δ2-5	Genomic	AATATCATATAGAAGTCATCGACTAGTCATA TGGAAATACTGGAACAATTGAAGAAAACT
ape1Δ2-7	Genomic	AATATCATATAGAAGTCATCGACTAGTCATA TGCTGGAACAATTGAAGAAAACTCTGCAG
ape1Δ2-11	Genomic	AATATCATATAGAAGTCATCGACTAGTCATA TGAAGAAAACTCTGCAGATGCTAACTGTA
ape1Δ2-45	Genomic	GGATCCAAGCTTAGATCTATGGAGCACAATT ATGAGGATATTGCACAGGAATTCATTGAT
atg19	pFA6a-GFP-HIS3	GGTGACGACAATGAAAAAGCCCTGACTTGG GAAGAACTC
atg19Δ395-415	pFA6a-GFP-HIS3	ACGTTACCAGAACTGGATGACTCTAGTATCA TCA GTACA
atg19Δ300-415	pFA6a-GFP-HIS3	AACTGCAAACTGAAGTTTACTGACGCTGGCG ATAAGCCA
atg19Δ180-415	pFA6a-GFP-HIS3	CAAAAGGTCACAAATAAAGAACCTAACCAC AGAATAAGC
atg19Δ212-415	Genomic	TGAAGTGAACTTGCGGGGTTTTTCAGTATCT ACGATTCATAGACTGTATTCAACTCTGT
atg19Δ2-138	Genomic	TGAAGTGAACTTGCGGGGTTTTTCAGTATCT ACGATTCATAGCTGGTTCCGAAGAAGAG
atg19Δ2-155	Genomic	TGAAGTGAACTTGCGGGGTTTTTCAGTATCT ACGATTCATATCAAGAGAATGCTTGGAT
atg19Δ2-168	Genomic	TGAAGTGAACTTGCGGGGTTTTTCAGTATCT ACGATTCATAAAGTTGGAAGAATCGTTA
atg19Δ168-415	Genomic	TGAAGTGAACTTGCGGGGTTTTTCAGTATCT ACGATTCATATTCCAACTAAAGGAGTTG
atg19Δ190-415	Genomic	TGAAGTGAACTTGCGGGGTTTTTCAGTATCT ACGATTCATAGCTTATTCAGTGGTTAGG

Table 2.3. Primers

Yeast Two-Hybrid Assay

This assay tests the interaction between two proteins [192]. When the proteins bind, they form a transcription factor that expresses a reporter. One protein is N-terminally fused to a DNA binding domain (BD) and the other protein is N-terminally fused to a transcription activation domain (AD). If the proteins do not interact, then the two domains will be kept separate, and the reporter gene will not be expressed. Even if the BD attaches to DNA, without the AD no transcription will occur. The auxotrophic markers HIS3 and ADE2 were used as reporters, which when expressed enable the yeast cells (PJ69-4A) to grow in media lacking adenine or histidine, since HIS3 and ADE2 encode enzymes involved in the biosynthesis of histidine and adenine, respectively. If there is a strong interaction, enough adenine will be made to enable the cells to grow in its absence. If there is a weak interaction, then cells will require adenine, while making enough histidine to grow in media that lacks histidine. Hence growth in media without adenine indicates a strong interaction, while growth only in media without histidine indicates a poor interaction. No growth in either suggests the proteins do not interact with each other.

Yeast Cell Lysis

Cells were collected by centrifugation, and resuspended in lysis buffer (2, 200 or 250 mM potassium phosphate, pH 7; or Tris-HCl with 0 or 500 mM sodium chloride, pH 7.0). The protease inhibitor PMSF was added before lysis, to a final concentration of 1

mM, to prevent protein degradation. Cells were broken with 0.4 mm glass beads (Sigma-Aldrich) by vigorous vortexing for 1 minute at 4°C and incubated for 1 minute on ice. This procedure was repeated for 10 cycles. Lysates were pre-cleared (whole cells removed) by centrifugation at 1,500 RCF for 1 minute. Soluble prApe1 and aggregates were separated by centrifugation at 6,000 RCF for 1 minute.

SDS-PAGE and Western Blot

An equal optical density of cells was used to make protein samples, which was measured using a spectrophotometer. The lysates were incubated in sample buffer (50 mM sodium phosphate, 25 mM MES, 1% SDS, 3 M urea, 0.05% bromophenol blue, 10 mM β-mercaptoethanol) for 2 minutes at 100°C and were fractionated by electrophoresis using vertical 6, 8, 10 or 13% Tris-glycine SDS-polyacrylamide gels. Proteins were transferred to a polyvinylidene fluoride membrane (Immobilon-P; Millipore) and were analyzed by Western blotting. Antibodies against Ape1 or Atg19 were generous gifts from Daniel J. Klionsky, University of Michigan, and were detected by chemiluminescence (SuperSignal West Pico: Thermo Scientific).

Density Glycerol Gradient

For gradient analysis, 200 µl of cell extracts were loaded on a 5.5 ml 20–50% glycerol step-gradient (20, 30, 40 and 50%; each layer had a 1.3 ml volume) prepared in 20 mM K-PIPES, pH 6.8, 1 mM PMSF [64]. The gradients were spun in an

ultracentrifuge (Optima LE-80K; Beckman) for 5 hrs at 55,000 RPM, at 4°C, using a SW55Ti rotor (Beckman). Thirteen fractions were collected from the top of the gradient and precipitated using trichloroacetic acid to a final 20% concentration, 10 minutes in ice, followed by 2 acetone washes and the pellet was resuspended in protein buffer (see "SDS-PAGE and Western Blot" above for recipe). Albumin (66.4 kDa), ferritin (481.2 kDa) and thyroglobulin (670 kDa) were used as markers. Fractions were resolved by SDS-PAGE and analyzed by Western blot using antibody against Ape1.

Immunoprecipitation

Immunoprecipitation was carried out following the manufacturer's specifications, using an Ni-NTA Kit for purification of 6xHis-tagged proteins (QIAGEN). *propeptide-6xHis* was constructed for expression using the pET29 plasmid, for immunoprecipitation and prApe1 aggregate disassembly. *Rosetta* cells expressing the propeptide-6xHis construct were grown in LB until exponential phase, shaken at 250 RPM at 37°C. Cells were collected by centrifugation and lysed using 1mg/ml of lysozyme in lysis buffer (50 mM sodium phosphate, 300 mM sodium chloride, 3 mM imidazole, pH 8), and incubated at 4°C for 30 min. Lysates were pre-cleared (intact cells removed) by centrifuging at 15,000xg for 30 min, at 4°C. Lysates were incubated with Ni-NTA agarose beads (QIAGEN) overnight at 4°C. Beads were washed 3x with lysis buffer. Yeast lysates were incubated with propeptide-6xHis agarose beads for 2hrs at 4°C. Beads were washed 3x with yeast lysis buffer. Samples were resolved by SDS-PAGE and analyzed by Western blot using an antibody against Ape1 or Atg19.

DSP Cross-linking

Dithiobis (succinimidyl propionate) (DSP) was used to cross-link proteins, following the manufacturer's specifications (Pierce). DSP was dissolved in DMSO at a 25 mM final concentration, and immediately added to the cell lysate to a final 2 mM concentration, and incubated for 2 hours in ice. The reaction was stopped by adding Tris-HCl, pH 7.5, to a final 20 mM concentration.

Proteinase K Treatment

Proteinase K (PrtK) was added to cell lysates to a final 5 µg/ml or 50 µg/mL concentration, and incubated for 30 minutes at 4°C, unless a different time interval is stated. The reaction was stopped using PMSF to a final 1 mM concentration, pellet fractions were washed twice to remove residual PrtK. Alternatively, when samples were analyzed by SDS-PAGE and Western blot, the reaction was stopped by adding protein buffer and incubating at 100°C for 2 minutes.

Microscopy and Image Editing

The Leica DM5000 automated upright microscope system was used for fluorescence and differential interference contrast (DIC) microscopy. Images were taken with the Leica DFC350 low light monochrome digital camera.

When comparing *in vivo* or *in vitro* localization of GFP or RFP tagged Atg8, Atg11 or Atg19, the same exposure time was maintained between different images. When taking *in vivo* or *in vitro* images of large prApe1 aggregates (about 0.5-5µm in diameter).

where prApe1 was tagged with RFP or GFP, the exposure time had to be modified to prevent saturation. Large prApe1 aggregates are made of more RFP or GFP-tagged prApe1, so they have a stronger level of fluorescence, and hence exposure time would have to be decreased to avoid saturation. In contrast, small aggregates, which have less RFP or GFP-tagged prApe1 protein, have a lower level of fluorescence, hence exposure time would have to be increased to ensure the aggregates were visible. Also, aggregates of a similar size were imaged when possible, so as to maintain similar exposure times.

Exposure times were maintained at minimum in all cases, to minimize photo bleaching the samples, and to minimize saturation in the images. Because of this the fluorescence is often very faint when images are printed on paper. To visualize the images better, Adobe Photoshop was used to edit the images. Different images that are compared within the same figure where edited in a similar way, specifically, their brightness and contrast is increased at similar levels.

Chapter 3

Elucidating the mechanism of prApe1 aggregation

prApe1 aggregates *in vitro* in buffers that potentiate hydrophobic interactions

AIM: To identify under what chemical conditions prApe1 forms aggregates *in vitro*, as part of developing an *in vitro* assay of Cvt vesicle formation and to elucidate the mechanism of aggregation.

prApe1 forms aggregates *in vitro*

In *atg19Δ* cells RFP-prApe1 aggregates were visible as a single large red punctum in cytosol (Fig. 3.1.A). However, when cells were lysed in a 10 mM Tris HCl pH 7 buffer, aggregates disassembled *in vitro*. To identify a buffer in which aggregates would be stable *in vitro*, *atg19Δ RFP-Ape1* cells were lysed in buffers with different NaCl concentrations. RFP-prApe1 aggregates were stable *in vitro* in a 0.5 M sodium chloride buffer (Fig. 3.1.A).

We then investigated whether soluble prApe1 can form aggregates *in vitro*. *atg19Δ Ape1-GFP* and *atg19Δ RFP-Ape1* were lysed separately using a 2 mM potassium phosphate buffer, pH 7. After lysates were mixed, no aggregates were visible, suggesting prApe1 was soluble. To cause aggregation, potassium phosphate was added to a final concentration of 0.2 M. We verified the formation of red and green large (about 2 μm)

spherical aggregates constituted by prApe1-GFP and RFP-prApe1, showing that soluble prApe1 formed aggregates *in vitro* (Fig. 3.1.B).

Buffers that potentiate hydrophobicity stabilize aggregates

Protein aggregation is often caused by hydrophobicity. The Hofmeister series classifies ions by their ability to change the arrangement of water molecules and influence the solubility of non-polar molecules [193-196]. Early members of the series decrease the solubility of non-polar molecules (salting out). These effects have been studied in protein folding, protein-protein interactions, and in enzymatic activity [195, 197-199]. We found that salts expected to increase hydrophobic interactions (ammonium sulfate, potassium phosphate, sodium phosphate and sodium fluoride) stabilized prApe1 aggregates, while salts predicted to decrease hydrophobic interactions (potassium iodide, sodium chlorate and calcium chloride) caused prApe1 aggregates to disassemble (a 0.2 M salt concentration was used) (Fig. 3.2.A). Thus hydrophobicity appears to be involved in prApe1 aggregation. To identify the best buffers for stabilizing prApe1 aggregates *in vitro*, the stability of prApe1 aggregates was tested using different concentrations of four of the buffers that stabilize aggregates (Fig. 3.2.B). 0.2 M potassium phosphate and 0.5 M sodium chloride buffers effectively stabilize prApe1 aggregates. A 0.2 M potassium phosphate buffer was generally used because intracellular concentrations of sodium and chloride are typically very low for osmoregulation in cells [200].

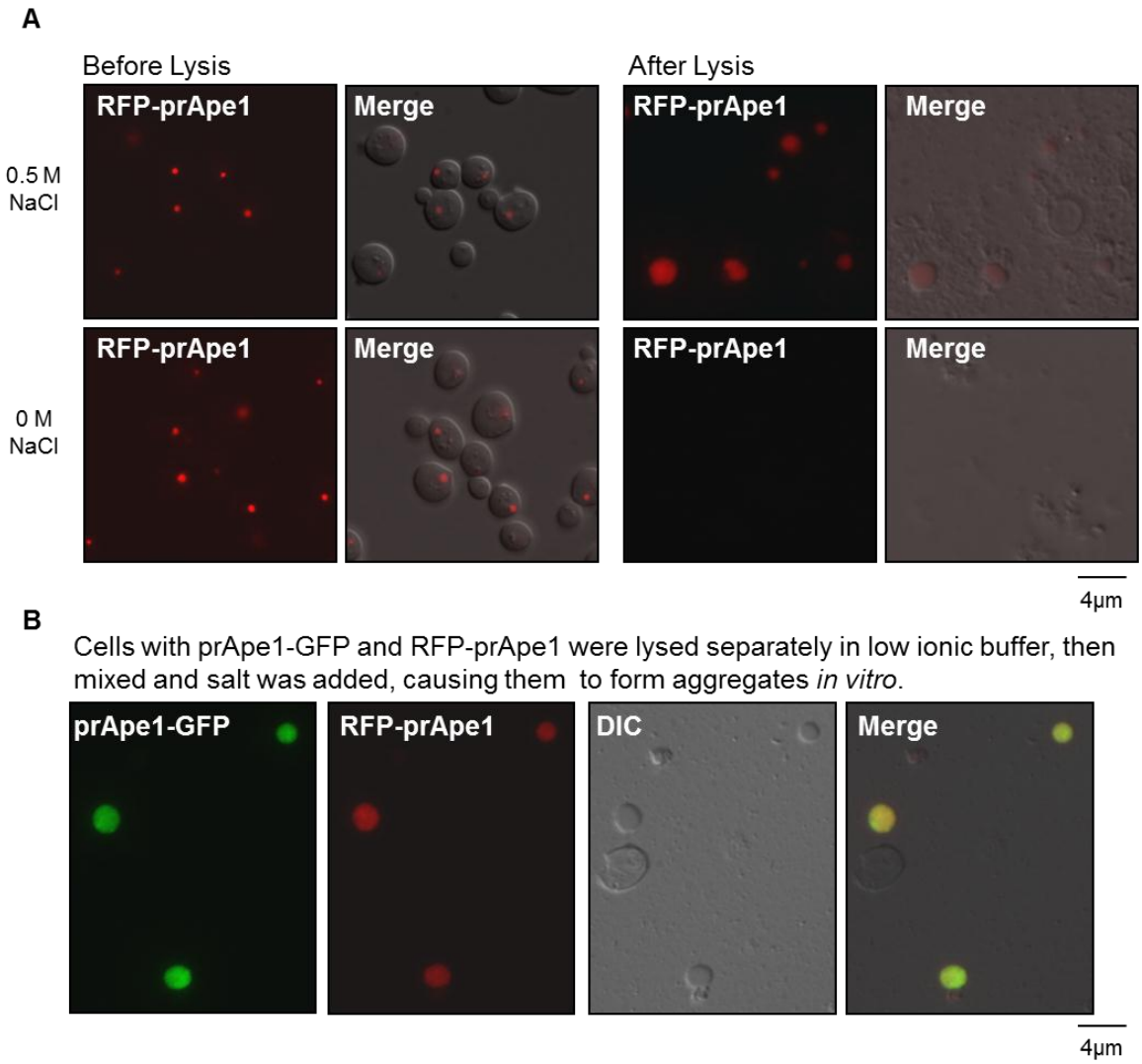

Figure 3.1. <u>prApe1 forms aggregates *in vitro*</u>. A) Aggregates are stable in 0.5 M sodium chloride. *atg19Δ* cells with RFP-prApe1 on left panels, showing red prApe1 aggregates forming puncta *in vivo*. Cell lysates of the same cells on the right panels, showing large prApe1 spherical aggregates of about a 2µm diameter, in a high ionic strength buffer (0.5 M NaCl), but no aggregates are present in the low ionic strength buffer (no NaCl). Cells were lysed in 0 or 0.5 M sodium chloride buffer, Tris-HCl, pH 7. Panels labeled "Merge" indicate that the DIC and RFP images were merged. **B) prApe1-GFP and RFP-prApe1 form aggregates *in vitro***. *atg19Δ* cells with prApe1-GFP or RFP-prApe1 were lysed separately in a 2 mM potassium phosphate buffer. Lysates were then mixed and potassium phosphate added to a final concentration of 200 mM. RFP-prApe1 and prApe1-GFP formed large spherical aggregates (about 2µm in diameter).

Our methodology and choice of a 0.2-0.25 M potassium phosphate buffer is physiologically relevant in respect to the ionic strength of the cell extract. Previous studies using *S. cerevisiae* have measured the cytosolic concentration of potassium and free phosphate to be between 290-340 mM for potassium, and 10-75 mM for free phosphate [201-207]. Similar studies show that the concentration of additional free ions is very low: 5 mM for sulfate, 0.05-0.5 mM for calcium, 0.1-1 mM for magnesium, about 20 mM for sodium and about 0.1 mM for chloride [201-204, 208-213]. It must also be noted that for removal of whole cells that failed to lyse, a very low centrifugal speed was used, 1500 RCF for 1 minute, to ensure aggregates were not lost in the pellet fractions. Consequently most of the cytosolic components would still be present during the *in vitro* studies. In addition, since a high density of cells was used during lysis (whole lysates consist of about 1/3 of cells and 2/3 of buffer), cytosolic components would only be diluted by about a 1:3 ratio. Lastly, our results from studies using sodium chloride are valid, since aggregate stability in 0.5 M sodium chloride was similar as when using 0.2 M potassium phosphate.

The effects of amino acids, sugars and detergents on aggregate stability

Sugars stabilized aggregates, possibly by increasing viscosity and by changing the water structure through their hydroxyl groups (Fig. 3.2.C). We also tested a non-polar (alanine), polar (serine), and a basic (arginine) amino acid. Only arginine stabilized aggregates *in vitro*. If hydrophobicity is involved in prApe1 aggregation, non-polar amino acids may interfere with aggregation by blocking hydrophobic regions on the

protein. Basic or acidic amino acids may act as salts and potentiate hydrophobic interactions. In agreement with the foregoing argument, the basic amino acid arginine stabilized prApe1 aggregates. Detergents help solubilize membranes and reduce non-specific interactions, so we also tested whether detergents disrupt aggregate stability (Fig. 3.2.C). *atg19Δ* cells were lysed in a 0.25 M potassium phosphate buffer, and different detergents were added up to 1% concentration. Tween-20 did not disrupt prApe1 aggregation.

A

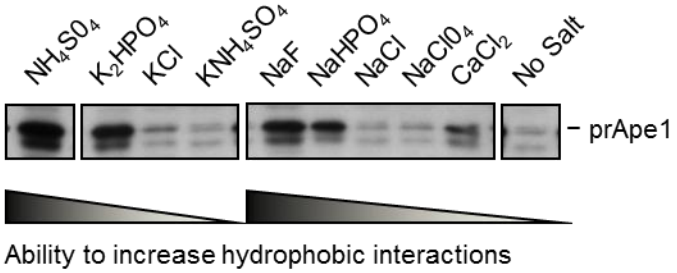
NH_4S0_4
K_2HPO_4
KCl
KNH_4SO_4
NaF
$NaHPO_4$
NaCl
$NaCl0_4$
$CaCl_2$
No Salt
prApe1
Ability to increase hydrophobic interactions

B

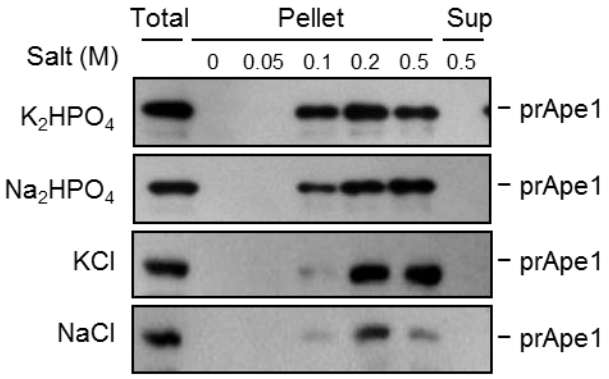
Total
Pellet
Sup
Salt (M)
0
0.05
0.1
0.2
0.5
0.5
K_2HPO_4
Na_2HPO_4
KCl
NaCl
prApe1

C

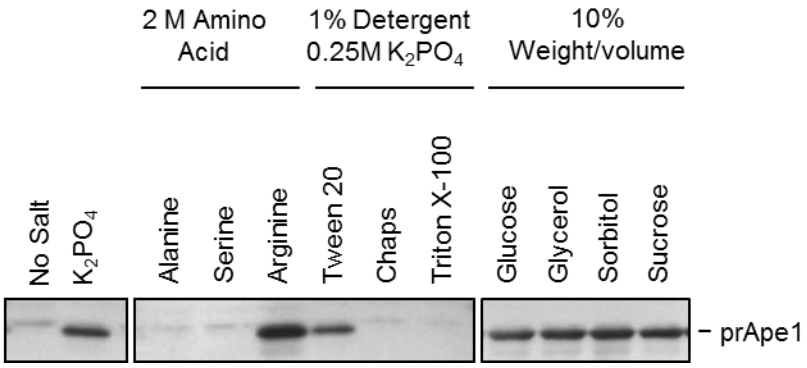
2 M Amino Acid
1% Detergent 0.25M K_2PO_4
10% Weight/volume
No Salt
K_2PO_4
Alanine
Serine
Arginine
Tween 20
Chaps
Triton X-100
Glucose
Glycerol
Sorbitol
Sucrose
prApe1

Figure 3.2. <u>Buffers that potentiate hydrophobicity stabilize aggregates.</u> A) Salts that potentiate hydrophobic interactions stabilize aggregates. *atg19Δ* cells were lysed in Tris HCl buffers of different salt compositions, salts were at a final 0.2 M concentration. Salts predicted to potentiate hydrophobic interactions increased aggregate stability, while those that decrease hydrophobic interactions caused aggregate disassembly. **B) 0.2 M potassium phosphate and 0.5 M sodium chloride buffers stabilize aggregates.** *atg19Δ* cells were lysed in buffers of different salts and concentrations to find out the optimum salt concentration for aggregate stability. Aggregates were stable at 0.1 M concentration of potassium phosphate or sodium phosphate, and at 0.2 M when using potassium chloride or sodium chloride. Figure A shows that potassium phosphate and sodium phosphate potentiate hydrophobicity better than potassium chloride and sodium chloride, and that a lower concentration of the former was required for aggregate stability. **C) Aggregates in 0.2 M potassium phosphate buffer remain stable in 1% Tween-20 detergent, and are stable in buffers with high concentrations of arginine and sugars.** *atg19Δ* cells were lysed in buffers with different amino acids, detergents and sugars. The basic amino acid arginine stabilized aggregates, while the hydrophobic alanine and the polar uncharged serine did not. This is consistent with the role of hydrophobicity in aggregation, which predicts that basic or acidic amino acids may act similarly to salts that potentiate hydrophobicity. Since aggregates are stable in Tween-20 detergent and in sugars, buffers containing these can be used when studying Ape1 aggregates. **A, B and C)** To determine whether prApe1 formed aggregates, soluble prApe1 was separated from aggregated prApe1 by centrifugation (6000 RCF for 1 minute). Soluble prApe1 localizes in the supernatant fraction, while aggregates localize in the pellet. Fractions were resolved by Western Blot with an antibody against Ape1. **A and C**) Only the pellet fractions containing prApe1 aggregates, are shown, and not the supernatant fraction containing only soluble prApe1.

The propeptide mediates prApe1 aggregation

AIM: To determine the role of the Ape1 propeptide in the formation and disassembly of Ape1 aggregates, by investigating whether the Ape1 propeptide is necessary for dodecamerization and aggregation.

The Ape1 propeptide is required for aggregation

Hydrophobicity is important for prApe1 aggregation; hence if the propeptide forms an amphipathic structure, its hydrophobic region could contribute to aggregation. The propeptide is cleaved by the vacuolar enzyme proteinase B to form mApe1, which does not aggregate in the vacuole, which suggests the propeptide may be required for aggregation [71, 214, 215]. To investigate whether the 45 residue propeptide plays a role in aggregation, a GFP tagged construct of Ape1 that lacked the propeptide (*Δ2-45-GFP*) was made. The cellular localization of prApe1Δ2-45-GFP in *ape1Δ* cells was compared to that of full length, GFP tagged Ape1 (prApe1-GFP). *ape1Δ Ape1-GFP* cells showed small punctate structures and green vacuoles, suggesting prApe1-GFP aggregates and goes to the vacuole (Fig. 3.3.). *ape1Δ Ape1Δ2-45-GFP* cells instead show a diffuse green cytosolic signal, and no vacuolar localization. The lack of prApe1Δ2-45-GFP aggregates suggests that the propeptide is required for aggregation *in vivo*.

The four N-terminal amino acids are required for aggregation

To identify which regions of the Ape1 propeptide are required for aggregation, prApe1 lacking the 2nd N-terminal residue, or N-terminal residues 2-3, 2-4, 2-5, 2-7 or 2-11, and tagged with GFP, were expressed in *ape1Δ* cells (Fig. 3.3. and Table 3.1). Their localization was compared to that of prApe1-GFP and prApe1Δ2-45-GFP. We looked for wild-type aggregation (formation of a single, punctate cytosolic aggregate) and for defective aggregation (multiple, irregular shaped punctate aggregates) in cytosol, and for green vacuoles, which would suggest that prApe1 was transported to the vacuole and so that the Cvt pathway is not blocked. prApe1Δ2-GFP forms a single punctate aggregate in cytosol similar to prApe1-GFP and is transported to the vacuole, which appeared green. prApe1Δ2-3-GFP has a block in vacuolar transport (no green vacuoles) but still forms single punctate aggregate. prApe1Δ2-4-GFP, prApe1Δ2-5-GFP and prApe1Δ2-7-GFP form multiple small punctate aggregates suggesting aggregation was defective. prApe1Δ2-11-GFP was similar to prApe1Δ2-45-GFP, showing a diffuse cytosolic GFP signal that suggests a complete block in aggregation.

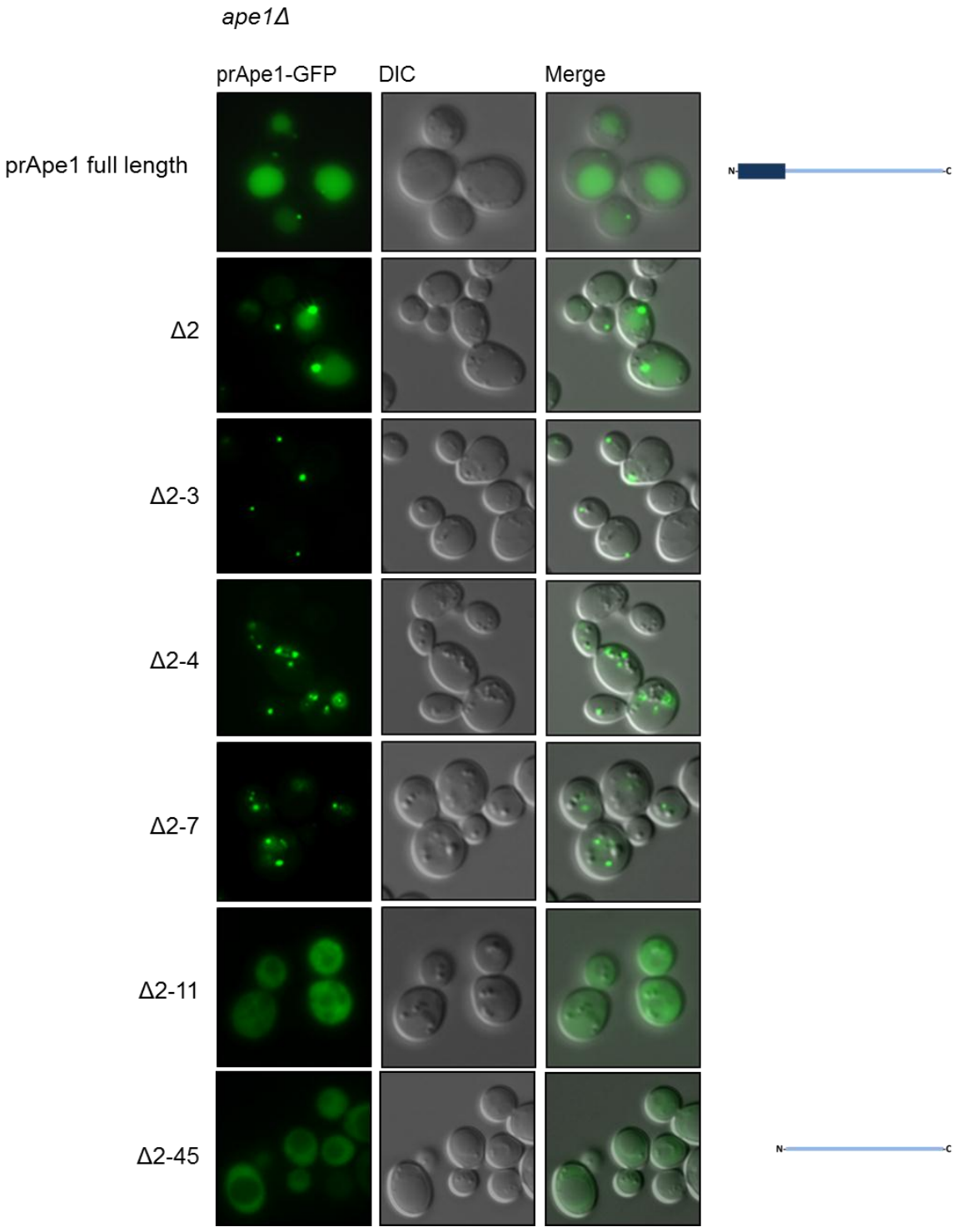
ape1Δ
prApe1-GFP
DIC
Merge
prApe1 full length
Δ2
Δ2-3
Δ2-4
Δ2-7
Δ2-11
Δ2-45
N
C
N
C

Figure 3.3. <u>The propeptide is required for aggregation and vacuolar transport</u>. *ape1Δ* cells with prApe1-GFP that have N-terminal deletions (number of residues deleted is indicated on the left). Punctate structures are aggregates. Multiple, small puncta or a diffuse cytosolic GFP signal indicate aggregation is defective. Full length prApe1-GFP and prApe1Δ2-GFP (missing only the 2nd N-terminal residue) formed a single large aggregate per cell, while being effectively transported to the vacuole, where GFP was visible. The three N-terminal amino acids are important for vacuolar transport, since GFP is not visible in the vacuole. The four N-terminal amino acids in the propeptide are required for proper aggregation, since instead of a single aggregate per cell there were multiple small ones. Deletion of the eleven N-terminal amino acids appears to completely disrupt aggregation, since GFP was diffuse throughout cytosol, similar to when the entire propeptide, the 45 N-terminal amino acids, was removed.

prApe1	MEEQREILEQ LKKTLQMLTV EPSKNNQIAN EEKEKKENEN SWCILEHNYE
Ape1Δ2	MEQREILEQ LKKTLQMLTV EPSKNNQIAN EEKEKKENEN SWCILEHNYE
Ape1Δ2-3	MQREILEQ LKKTLQMLTV EPSKNNQIAN EEKEKKENEN SWCILEHNYE
Ape1Δ2-4	MREILEQ LKKTLQMLTV EPSKNNQIAN EEKEKKENEN SWCILEHNYE
Ape1Δ2-5	MEILEQ LKKTLQMLTV EPSKNNQIAN EEKEKKENEN SWCILEHNYE
Ape1Δ2-7	MLEQ LKKTLQMLTV EPSKNNQIAN EEKEKKENEN SWCILEHNYE
Ape1Δ2-9	MQ LKKTLQMLTV EPSKNNQIAN EEKEKKENEN SWCILEHNYE
Ape1Δ2-11	MKKTLQMLTV EPSKNNQIAN EEKEKKENEN SWCILEHNYE
Ape1Δ2-45	MEHNYE
mApe1	EHNYE

Table 3.1. Ape1 N-terminal deletions, in comparison with prApe1 and mApe1. For prApe1, the 50 N-terminal amino acids are shown. For mApe1, only amino acid recidues from 46-50 are shown, because the 45 N-terminal acids, constituted of the entire propeptide, are cleaved by proteinase B in the vacuole to generate the mature form of Ape1.

The propeptide is required for aggregation *in vitro*

We investigated whether *in vitro* aggregation was also directed by the propeptide. *atg19Δ* with RFP-prApe1 cell lysate was mixed with either *atg19Δ ape1Δ* with prApe1-GFP or with *atg19Δ ape1Δ* with prApe1Δ2-45-GFP (no propeptide) cell lysate, in a 0.2 M potassium phosphate buffer, pH 7, in which aggregates are stable. The green prApe1-GFP punctate aggregates bound to the surface of the larger (about 2µm in diameter) prApe1/RFP-prApe1 aggregates, forming large red spherical aggregates with green rings on the surface (Fig. 3.4.A). However, when prApe1Δ2-45-GFP was present instead, no green rings formed on the surface of aggregates, suggesting the propeptide is required for aggregation *in vitro*, and that pre-assembly of aggregates is not sufficient for prApe1 binding. Since prApe1 forms aggregates of a similar spherical shape both *in vivo* and *in vitro*, aggregation perhaps occurs by a similar mechanism and not due to non-specific binding.

To further verify that the propeptide is required for aggregation, differential centrifugation of cell lysates was used to separate aggregates from soluble protein (Fig. 3.4.B). Wild-type, *atg19Δ* or *atg19Δ Ape1Δ2-45* cells were lysed in a 0 or 0.5 M sodium chloride buffer. Only prApe1 in 0.5 M sodium chloride was found in the pellet fraction, suggesting buffers that potentiate hydrophobic interactions are required for aggregate stability. Meanwhile, mApe1 was in the supernatant, showing it does not aggregate because the propeptide is required.

Propeptide cleavage disassembles aggregates

While cytosolic prApe1 forms aggregates, vacuolar mApe1 does not. This suggests that vacuolar proteolytic cleavage of the propeptide causes aggregates to disassemble. To test this, the stability of aggregates after propeptide cleavage by proteinase K (PrtK) was studied. Previous studies show that prApe1 is cleaved by PrtK to generate a fragment the same size as mApe1, while mApe1 is very resistant to PrtK activity, perhaps because the dodecameric form is very stable and minimizes the surface area that is exposed to proteolysis, protecting residues that are sensitive to PrtK activity inside [134]. PrtK was added for different time periods, to a final 50 µg/mL concentration, to *atg19Δ* cell lysates. Differential centrifugation separated aggregates from soluble protein (Fig. 3.4.C). Between 2-5 minutes after addition of PrtK, most of the propeptides had been cleaved, and most Ape1 was disassembled and present in the supernatant fraction. Cleavage of the propeptide by PrtK leads to disassembly of aggregates *in vitro*, suggesting that vacuolar removal of the propeptide by proteinase B disassembles aggregates *in vivo*.

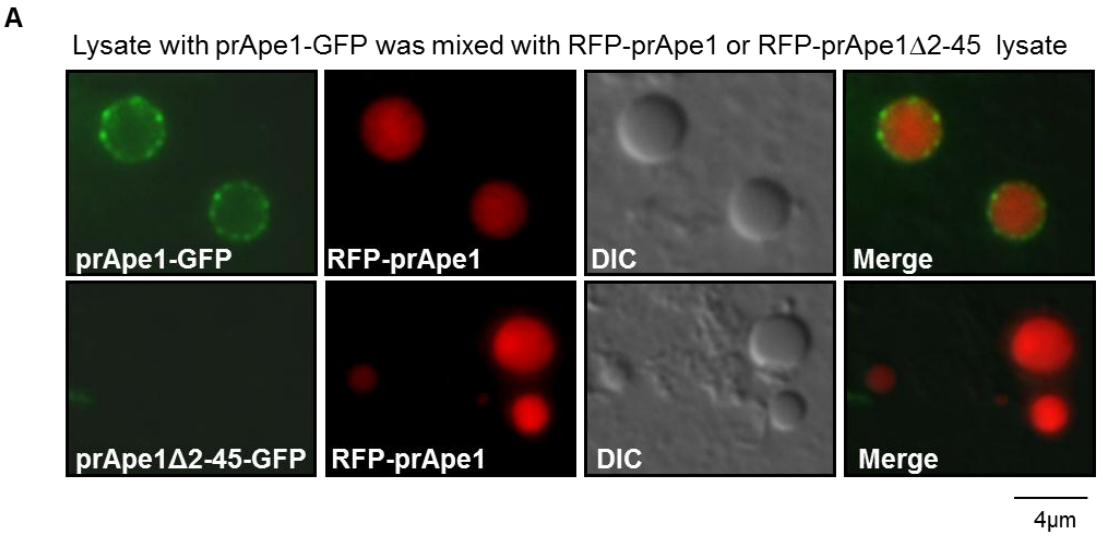
A
Lysate with prApe1-GFP was mixed with RFP-prApe1 or RFP-prApe1Δ2-45 lysate
prApe1-GFP
RFP-prApe1
DIC
Merge
prApe1Δ2-45-GFP
RFP-prApe1
DIC
Merge
4μm

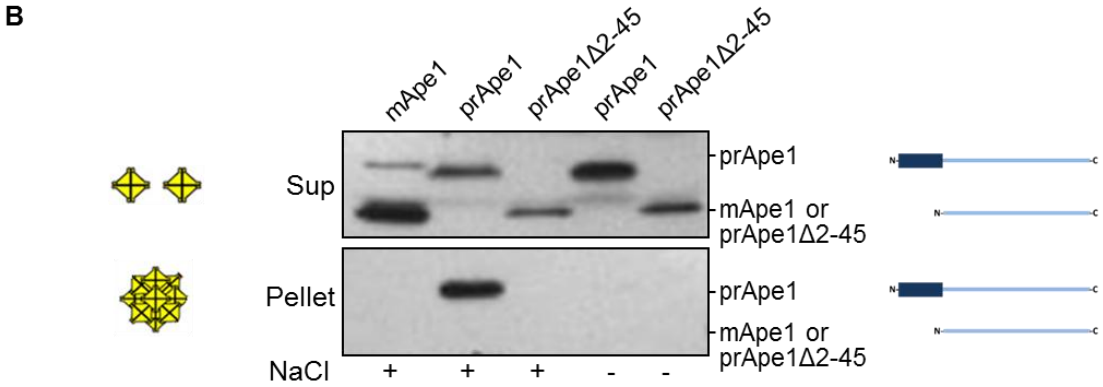
B
mApe1
prApe1
prApe1Δ2-45
prApe1
prApe1Δ2-45
Sup
Pellet
NaCl
+ + + - -
prApe1
mApe1 or
prApe1Δ2-45
prApe1
mApe1 or
prApe1Δ2-45

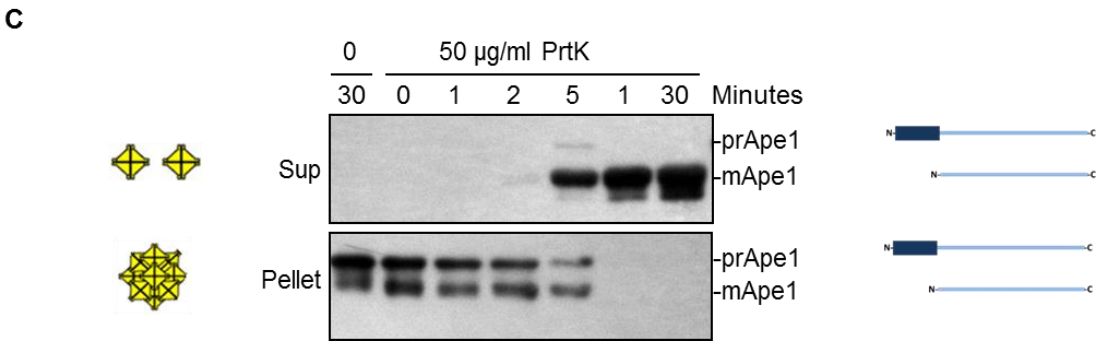
C
0
50 μg/ml PrtK
30 0 1 2 5 1 30 Minutes
Sup
Pellet
prApe1
mApe1
prApe1
mApe1

Figure 3.4. <u>The propeptide is required for aggregation *in vitro*.</u> A) prApe1Δ2-45-GFP does not bind RFP-prApe1/prApe1 aggregates. *atg19Δ* cell lysate with RFP-prApe1 and prApe1 overexpressed, was mixed with *atg19Δ* cell lysate with either prApe1-GFP or prApe1Δ2-45-GFP (no propeptide) in a 0.2 M potassium phosphate buffer, pH 7. prApe1 was overexpressed to form large aggregates for better visualization. prApe1-GFP bound the surface of the large (1-4μm diameter) RFP-prApe1/prApe1 aggregates, appearing as a green ring around the red aggregates. Ape1Δ2-45-GFP does not localize to the surface of aggregates, suggesting the propeptide is required for aggregation, while aggregate pre-assembly is not sufficient for recruitment of more prApe1. Because cells were lysed in the high ionic buffer (0.2 M potassium phosphate), prApe1-GFP formed aggregates in the form of green puncta before lysates were mixed. prApe1-GFP remained as green puncta when bound to the surface of the large spherical shaped RFP-prApe1/prApe1 aggregates **B) mApe1 and prApe1Δ2-45 do not form aggregates.** Wild type, *atg19Δ* or *atg19Δ ape1Δ2-45* cells were lysed in a 0 or 0.5 M sodium chloride buffer. Only prApe1 in 0.5 M sodium chloride forms stable aggregates *in vitro* and was in the pellet fraction, mApe1 and prApe1-Δ2-45 were in the supernatant. **C) Cleavage of propeptides disassembles aggregates.** *atg19Δ* cells were lysed in a 0.5 M sodium chloride buffer. 50 μg/mL of PrtK was added for different time intervals, mApe1 was mostly in the supernatant fraction, showing cleavage of the propeptide causes aggregates to disassemble. Some mApe1 is in the pellet fraction, perhaps dodecamers with some, but not all propeptides cleaved off can still form aggregates. Cleavage of the propeptide by vacuolar proteases to produce mApe1 is likely the cause of aggregate disassembly in the vacuole. Although no mApe1 is shown for comparison, other studies show prApe1 gets cleaved by PrtK to generate a fragment the same size as mApe1, and that mApe1 is much more resistant to PrtK than prApe1. **B and C)** Centrifugation separated aggregates from soluble protein. Fractions were resolved by SDS-PAGE and Western Blot with an antibody against Ape1.

The propeptide is not required for dodecamerization

Although wild-type cells with both full length prApe1 and prApe1Δ2-45-GFP showed a diffuse cytosolic localization of GFP due to the defective aggregation of prApe1Δ2-45-GFP, there were also green punctate structures and green vacuoles, suggesting prApe1Δ2-45-GFP can be incorporated into prApe1 aggregates and transported to the vacuole (Fig. 3.5.A). This behavior contrasts with *ape1*Δ cells that only express prApe1Δ2-45-GFP, which does not form aggregates and does not go to the vacuole (Fig. 3.3.). mApe1 is similar to prApe1Δ2-45 in that it lacks the propeptide, because its 45 N-terminal residues are cleaved by the vacuolar protease proteinase B. mApe1 forms dodecamers but does not form aggregates in the vacuole, suggesting the propeptide is not required for dodecamerization, only for aggregation [216]. To investigate whether prApe1Δ2-45 forms dodecamers we used *ape1Δ*, wild type, *atg19Δ* and *atg19Δ ape1Δ ape1Δ2-45* cell lysates and estimated the molecular weight of prApe1, mApe1 and prApe1Δ2-45 using a glycerol density gradient (Fig. 3.5.B). prApe1, mApe1 and prApe1Δ2-45 were present in similar fractions as thyroglobulin, of a molecular weight of 670 kDa, suggesting they form a dodecamer: the molecular weight of an individual prApe1 is 61 kDa, while that of Ape1 and mApe1 is 56 kDa. Hence the propeptide is not required for dodecamerization.

The propeptide is sufficient for binding to prApe1, and does not bind mApe1

Comparison of the *S. cerevisiae* Ape1 dodecamer with its *B. burgdorferi* homologue suggests that the propeptide may protrude from the surface of the dodecamer, consistent

with its role in aggregation and the fact that it is readily cleaved by proteinase B and PrtK [217]. Propeptides protruding from the dodecamer surface could readily bind to other dodecamers to form aggregates. To investigate whether the propeptide can bind prApe1 independently, binding of the propeptide to prApe1 and mApe1 was tested *in vitro*. We made a construct of the propeptide consisting of the 45 N-terminal amino acids of Ape1, with a 6xHi*s* tag (propeptide-6xHis), and expressed it in *E. coli* cells. Cells were lysed and the propeptides bound to Ni^{+} coated agarose beads. Binding of the propeptide to prApe1 and mApe1 from wild type yeast lysate was then tested (Fig. 3.6.A). The propeptide binds prApe1 but not mApe1, suggesting that during aggregation propeptides from separate dodecamers interact with each other, dimerizing. Binding only occurred in a 0.5 M sodium chloride buffer, suggesting hydrophobicity directs propeptide binding to prApe1. The propeptide is hypothesized to have an N-terminal amphipathic helix, thus the hydrophobic region of the amphipathic helix may direct aggregation [70].

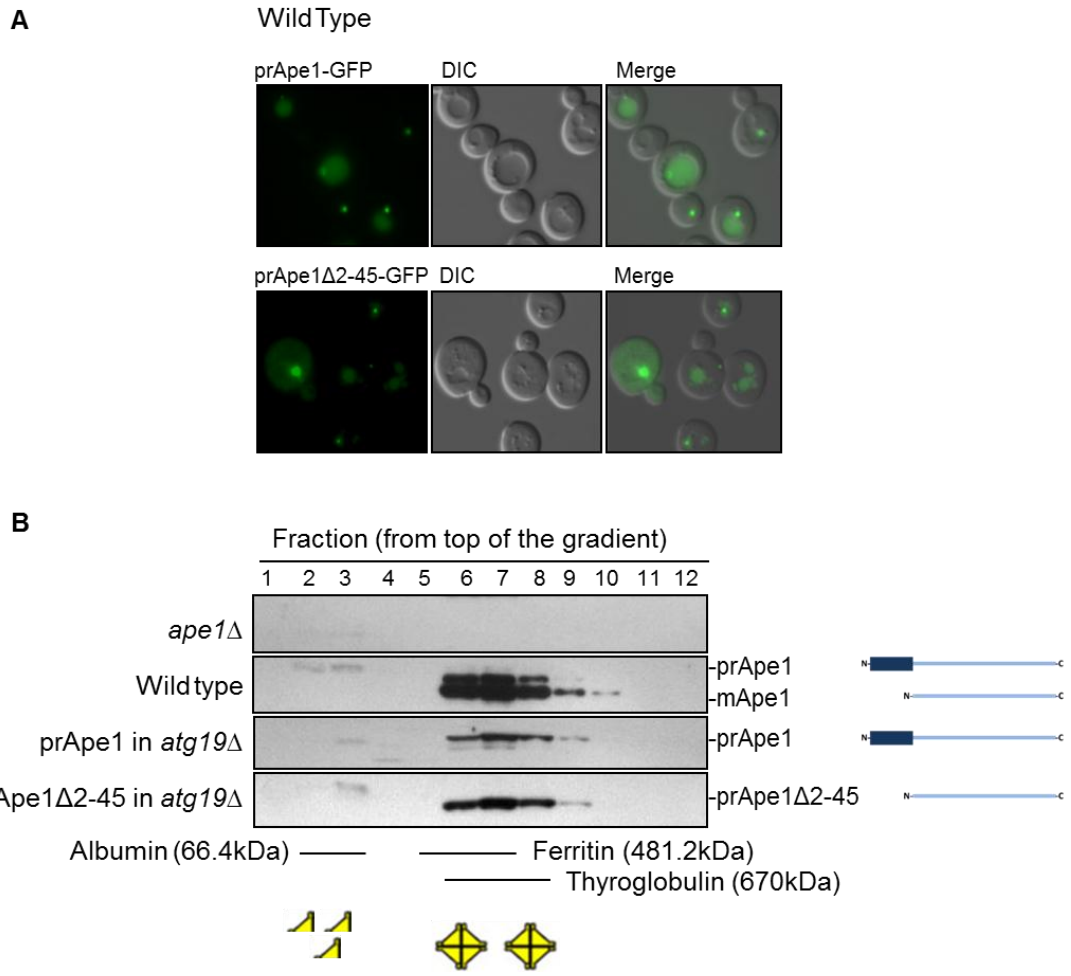

Figure 3.5. <u>The propeptide is not required for dodecamerization</u>. A) prApe1Δ2-45-GFP, lacking the propeptide, was incorporated into prApe1 aggregates and transported to the vacuole. Wild-type cells with full length prApe1, and either prApe1-GFP or prApe1Δ2-45-GFP (without the propeptide). Both full length prApe1-GFP and prApe1Δ2-45-GFP without the propeptide were incorporated into punctate aggregates, and transported to the vacuole, which appears green, suggesting that they dodecamerize, since prApe1Δ2-45 does not aggregate. **B) The propeptide is not required for dodecamerization**. *ape1Δ,* Wild type, *atg19Δ* or *atg19Δ ape1Δ2-45* cells were lysed and loaded onto a step glycerol gradient. Albumin, ferritin and thyroglobulin were used as markers. prApe1, mApe1 and prApe1Δ2-45 were all present in similar fractions as thyroglobulin. Fractions were analyzed by Western Blot using an antibody against Ape1. prApe1 dodecamers would have a 732 kDa molecular weight, while mApe1 and prApe1Δ2-45 dodecamers would weigh 672 kDa. Since thyroglobulin has a very similar molecular weight of 670 kDa, their presence in exactly the same fractions indicates that all Ape1 constructs were forming dodecamers. prApe1 was also present in the next heavier fraction, fraction 10, consistent with its slightly higher molecular mass.

High propeptide concentrations disassemble aggregates

To further verify that the propeptide can independently bind to prApe1, we tested whether binding of the propeptide to prApe1 would physically interfere with aggregation. *atg19Δ* cells were lysed in 0.25 M potassium phosphate buffer, and different concentrations of propeptide-6xHis were added. Differential centrifugation was used to differentiate aggregates from soluble protein. The greater the concentration of propeptide, the less prApe1 found in the pellet fraction, suggesting the propeptide binds prApe1 and physically interferes with aggregation (Fig. 3.6.B). The high concentration (2 mg/ml) of propeptide-6xHis required to disassemble aggregates suggests propeptide binding to prApe1 is weak. For aggregation, the local concentration of prApe1 propeptides is naturally higher on dodecamers compared to that in free solution. Propeptides may even be positioned in clusters by the way prApe1 proteins are assembled into a dodecamer, which would facilitate binding between propeptides from separate dodecamers, causing aggregation.

The four N-terminal amino acids are required for propeptide binding to prApe1

To verify that the mechanism of propeptide binding to prApe1 is similar to prApe1 aggregation, we verified whether the same N-terminal deletions that disrupt aggregation also interfere with propeptide binding. *atg19Δ ape1Δ* cells expressing prApe1 with deletion of the 2nd N-terminal residue, or of N-terminal residues 2-3, 2-4, 2-5 and 2-11, were lysed in a 0.2 M potassium phosphate buffer (Fig. 3.6.C). Lysates were mixed with agarose beads coated with Ni^{+} and propeptide-6xHis. Consistent with studies showing

that prApe1Δ2-GFP and prApe1Δ2-3-GFP formed a similar aggregate in cytosol as in full length prApe1-GFP, prApe1Δ2 and prApe1Δ2-3 bound propeptide-6xHis (Fig. 3.6.C). Even more, while prApe1Δ2-4-GFP, prApe1Δ2-5-GFP and prApe1Δ2-11-GFP aggregate defectively or not at all, prApe1Δ2-4, prApe1Δ2-5 and prApe1Δ2-11 do not bind propeptide-6xHis. This suggests propeptide-6xHis binding to prApe1 uses a similar mechanism as prApe1 aggregation, requiring the four N-terminal amino acids.

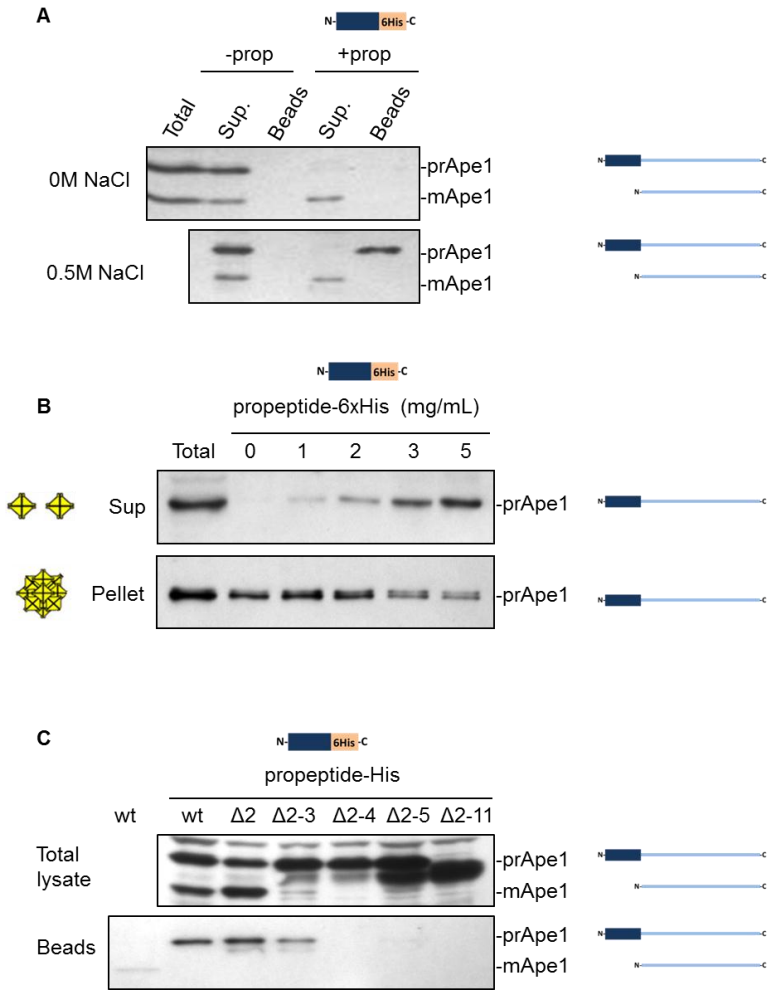

Figure 3.6. <u>The propeptide is sufficient for binding to prApe1, and does not bind mApe1</u>. **A) The propeptide binds prApe1.** Wild-type yeast lysate with 0 or 0.5 M sodium chloride, was mixed with propeptide-6xHis coated agarose beads. As a control Ni^{+} coated agarose beads without propeptide-6xHis bound were used. prApe1 bound propeptide-6xHis in the 0.5 M but not in the 0 sodium chloride buffer, mApe1 did not bind in either. **B) High propeptide concentration disassembles aggregates.** *atg19Δ* lysed in a 0.25 M potassium phosphate buffer with different concentrations of the propeptide-6xHis (0-5mg/mL). A high concentration of the propeptide disassembles prApe1 aggregates. Centrifugation separated aggregates from soluble protein. **C) The four N-terminal amino acids of prApe1 are required for binding to the propeptide.** Wild type, *ape1Δ2*, *ape1Δ2-3*, *ape1Δ2-4*, *ape1Δ2-5*, *ape1Δ2-11* cell lysate was added to Ni^{+} coated agarose beads coated with propeptide-6xHis. Only prApe1, Ape1Δ2 and Ape1Δ2-3 bound to propeptide-6xHis. This is consistent with the formation of defective aggregates *in vivo* in cells with prApe1Δ2-4-GFP. **A, B and C**) Fractions were analyzed by SDS-PAGE followed by Western blot with antibody against Ape1.

Putting the propeptide on prApe1 homologues is not sufficient for aggregation

Ape1 has several homologues that similarly form dodecamers. Its cytosolic paralogue in *S. cerevisiae*, Ape4, is an aspartyl aminopeptidase that is also transported to the vacuole via the Cvt pathway by binding to Atg19. Ape4 has no propeptide and does not aggregate. Its homologue PpApe1, is from *Pichia pastoris*. It too is a vacuolar protease transported via the Cvt pathway to the vacuole. Although PpApe1 has a propeptide and aggregates, its propeptide is structurally different from that of *S. cerevisiae*. To investigate whether the *S. cerevisiae* Ape1 propeptide would be sufficient for Ape4 and PpApe1 to aggregate, we made constructs which fused the *S. cerevisiae* Ape1 propeptide to the N-terminus of Ape4 and PpApe1, and tagged them with GFP on their C-terminus to visualize their localization (pr-Ape4-GFP and pr-PpApe1-GFP) (Fig. 3.7.A). In the case of PpApe1, its propeptide was replaced with the *S. cerevisiae* propeptide. Neither homologue construct formed aggregates; instead their localization was diffuse throughout cytosol. We then tested if addition of the propeptide was sufficient for binding to propeptide-6xHis anchored to Ni+ coated agarose beads (Fig. 3.7.B). Samples were analyzed by SDS-PAGE and Western blot using an antibody against GFP. prApe1-GFP bound to the propeptide as expected, but pr-Ape4-GFP and pr-PpApe1-GFP did not, similar to prApe1Δ2-45-GFP. This suggests that the positioning of the propeptide is critical for aggregation and for binding to other propeptides. Also, while the dodecamer shape and surface polarity of prApe1 enable it to aggregate, in contrast the specific dodecamer structure of Ape4 interferes with its aggregation.

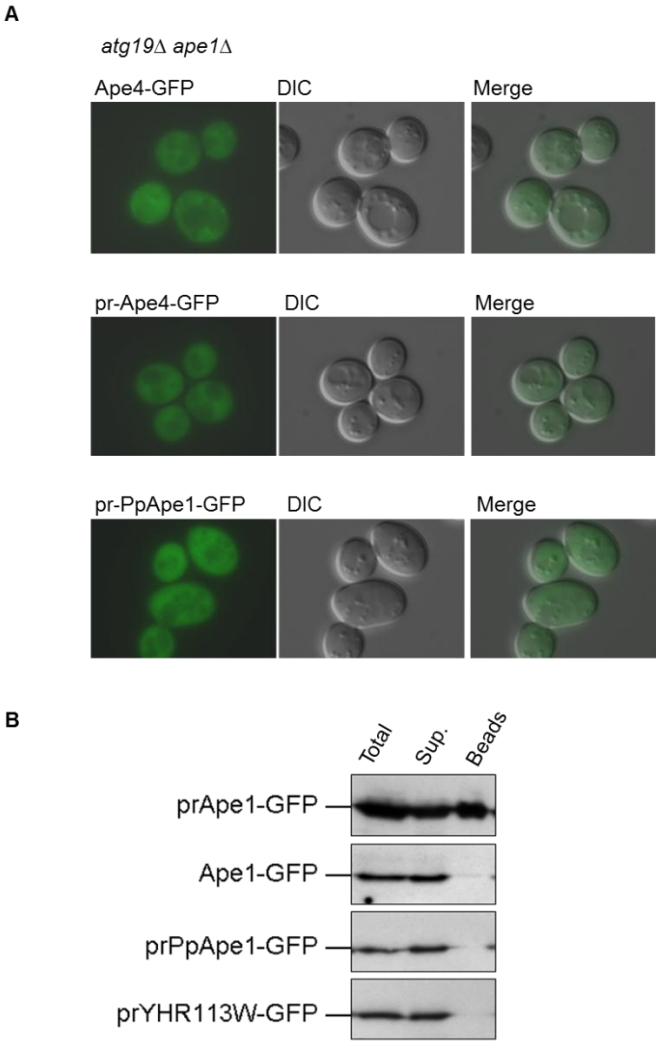

Figure 3.7. <u>Correct dodecamer shape and propeptide positioning are critical for aggregation.</u> A) N-terminal fusion of the propeptide to Ape4 or PpApe1 is not sufficient for aggregation. The *S. cerevisiae* Ape1 propeptide was placed on the N-terminus of its dodecameric paralogue Ape4 and its homologue *P. pastoris* Ape1, which were also C-terminally tagged with GFP (pr-Ape4-GFP and pr-PpApe1-GFP). Their localization was visualized in *atg19*Δ*/ape1*Δ cells. There were no punctate aggregates; instead GFP was diffuse throughout the cytosol, indicating fusion of the propeptide was not sufficient for aggregation. **B) N-terminal fusion with the propeptide is not sufficient for propeptide dimerization**. *atg19*Δ*/ape1*Δ cells expressing prApe1-GFP, prApe1Δ2-45-GFP, pr-Ape4-GFP or pr-PpApe1-GFP were lysed in a 0.25 M potassium phosphate buffer, and mixed with Ni+ coated agarose beads covered with propeptide-6xHis. Samples were analyzed by SDS-PAGE and Western blot analysis using an antibody against GFP. Only prApe1-GFP bound to the propeptide, indicating fusion of the propeptide is not sufficient for propeptide dimerization.

Chapter 4

Elucidating the mechanism of Atg19 binding to prApe1 aggregates

The propeptide mediates Ape1 binding to Atg19, even during defective aggregation

AIM: To better understand how Ape1 and Atg19 interact, by determining whether the Ape1 propeptide is sufficient for binding to Atg19. Also, to investigate whether Atg19 binding to prApe1, and Atg19 recruitment of adaptor protein Atg11, are sufficient for vacuolar transport via the Cvt pathway.

The Ape1 propeptide is required for Atg19 binding

To study the role of the Ape1 propeptide in Atg19 binding, we looked at Atg19 co-localization with full length and deletion prApe1 proteins. In *ape1Δ* with GFP-Atg19 cells with N-terminal deletions in RFP-prApe1 and prApe1, RFP-prApe1Δ2-4 co-localized with GFP-Atg19, suggesting they still bound; however, RFP-prApe1Δ2-5 does not effectively co-localize with GFP-Atg19, suggesting their binding was defective (Fig. 4.1.A).

Furthermore, a two-hybrid assay was used to verify the importance of the Ape1 propeptide in Atg19 binding, using PJ69-4A *ape1Δ atg19Δ* cells transformed with fusion plasmids expressing AD-Atg19, and BD-prApe1 with N-terminal deletions (Fig. 4.1.B).

BD-prApe1Δ2 and BD-prApe1Δ2-4 bind AD-Atg19 similarly to full length BD-prApe1. When more than five N-terminal amino acids were deleted from prApe1, Atg19 binding is blocked, suggesting that the five N-terminal residues are required for Atg19 binding.

Atg19 binding to aggregates is not sufficient for vacuolar transport

Interestingly, prApe1Δ2-4-GFP was not effectively transported to the vacuole (Fig. 3.3), even though the two hybrid assay and GFP-Atg19 co-localization with RFP-prApe1Δ2-5 suggest Atg19 binds prApe1Δ2-4 (Fig. 4.1). This is consistent with the lack of mApe1 in *ape1Δ2-4* cells (to generate mApe1, prApe1 must be transported to the vacuole, where proteinase B cleaves the propeptide to generate mApe1) (Fig. 3.6.C). In contrast, wild type, *ape1Δ2* and *ape1Δ2-3* cells have mApe1 (Fig. 3.6.C). Since prApe1Δ2-4-GFP binds Atg19, perhaps the impaired vacuolar transport results from defective aggregation, since there were multiple punctate, irregular shaped aggregates in the cytosol instead of the single punctate aggregate formed by full length prApe1-GFP (Fig. 3.3). Therefore, aggregate shape might be important for Cvt vesicle formation, either for recruitment of autophagic proteins or membrane.

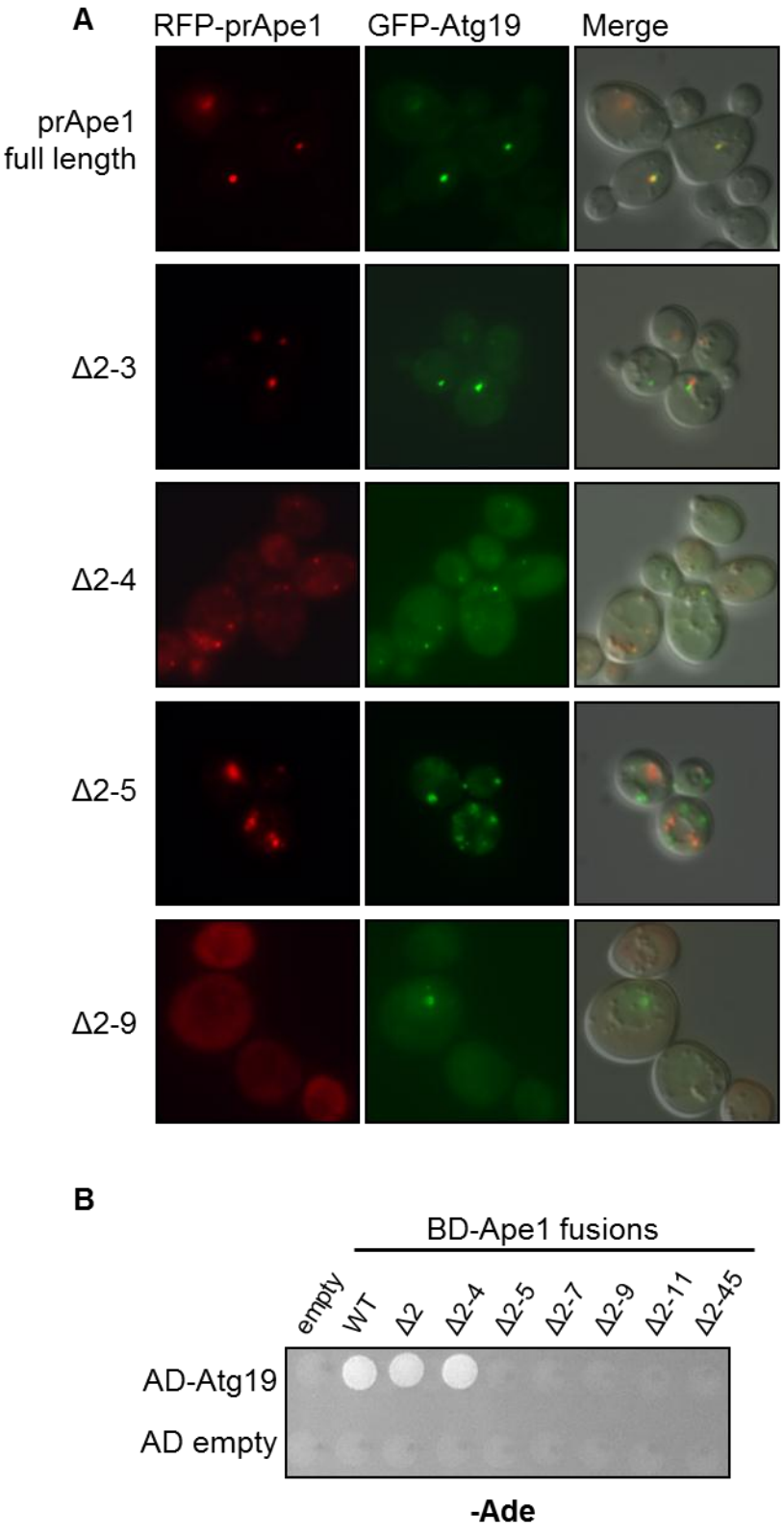
A
RFP-prApe1
GFP-Atg19
Merge
prApe1
full length
Δ2-3
Δ2-4
Δ2-5
Δ2-9
B
BD-Ape1 fusions
empty
WT
Δ2
Δ2-4
Δ2-5
Δ2-7
Δ2-9
Δ2-11
Δ2-45
AD-Atg19
AD empty
-Ade

Figure 4.1. <u>The Ape1 propeptide is required for Atg19 binding.</u> A) RFP-prApe1Δ2-5 does not localize with GFP-Atg19. Cells with GFP-Atg19, and prApe1-RFP with N-terminal deletions. GFP-Atg19 co-localizes with RFP-prApe1Δ2-4 defective aggregates at about a 50% frequency, but GFP-Atg19 does not co-localize with RFP-prApe1Δ2-5 defective aggregates, thus the five N-terminal residues are required for Atg19 binding. Left hand labels indicate which Ape1 N-terminal residues were deleted. **B) Two-hybrid showing that the five N-terminal amino acids of Ape1 are required for Atg19 binding.** PJ69-4A *ape1Δ atg19Δ* cells where used to test the interaction of AD-Atg19, and BD-prApe1 with N-terminal deletions. BD-prApe1Δ2-5 does not interact with AD-Atg19, while Atg19 full length, Δ2 and Δ2-4 do. Two-hybrid results were consistent with the co-localization assay in figure A.

Aggregation is not sufficient for Atg19 binding

Without the propeptide, prApe1 does not aggregate. To investigate whether it is aggregation or the propeptide itself that is required for Atg19 binding, we tested Atg19 binding to aggregates that have had their propeptides cleaved off by PrtK (Fig. 4.2.B). For this assay *atg19Δ* with RFP-Ape1 lysate was treated with the cross-linker dithiobis (succinimidyl propionate) (DSP), or with DSP plus PrtK, and then mixed with *ape1Δ atg8Δ* with GFP-Atg19 lysate in a 0.2 M potassium phosphate buffer. Lysates were cross-linked with DSP so that aggregates do not disassemble when PrtK cleaves the propeptide from their surface; we are assuming that DSP cross-linked aggregates remain the same as those that are not cross-linked. To prevent PrtK from cleaving GFP-Atg19, PMSF to a final 1 mM concentration was added to inhibit PrtK activity, and aggregates were washed two times in a 0.2 M potassium phosphate buffer to remove PrtK. These results show that GFP-Atg19 bound to the surface of aggregates from untreated and DSP-treated lysate. However, GFP-Atg19 did not bind aggregates treated with both DSP plus PrtK, suggesting the propeptide is required for Atg19 binding to the aggregate surface. Also, while prApe1-GFP and RFP-prApe1 form homogenous red and green aggregates *in vitro*, GFP-Atg19 instead localizes only to the surface of the RFP-prApe1/prApe1 aggregate *in vitro* and *in vivo* (Fig 3.1.B, and 4.2.A and B). Thus the mechanism of Atg19 and prApe1 binding is different from aggregation.

The propeptide is sufficient for binding Atg19

The Ape1 propeptide is required for binding to Atg19 and may be sufficient for targeting GFP to the vacuole [70, 218]. This suggests the propeptide may bind Atg19 independently. To test this we developed a two-hybrid assay, using PJ69-4A *ape1Δ/atg19Δ* cells, in which BD-propeptide bound to AD-Atg19, thus showing the propeptide binds to Atg19 *in vivo* (Fig. 4.3.A). Furthermore, we tested binding of propeptide-6xHis to Atg19 from *ape1Δ* cell lysate *in vitro*, using Ni^{+} and propeptide-6xHis coated agarose beads (Fig. 4.3.B). In addition, to test whether hydrophobicity also directed Atg19 binding to the propeptide we used a 0 or a 0.5 M sodium chloride buffer. Atg19 bound propeptide-6xHis, but in contrast to prApe1, Atg19 bound in either a 0 and 0.5 M sodium chloride buffer, suggesting that Atg19 binding does not solely rely on hydrophobicity, but requires electrostatic interactions. Interestingly, Atg19 bound to the propeptide migrates a little slower than Atg19 remaining in the supernatant, suggesting Atg19 may be modified covalently in some way, and that this modification may play a role in its binding to the propeptide of Ape1.

Atg19 can recruit Atg11 to defective aggregates

Even though Atg19 binds prApe1Δ2-4, vacuolar transport was defective, suggesting defective aggregation may interfere with recruitment of autophagic proteins or membrane during vesicle formation. Atg19 recruits the adaptor Atg11, which has a key role in recruiting the autophagic machinery. To test whether Atg11 could still bind to defective aggregates, its localization was verified in wild-type cells expressing GFP N-terminally

tagged Atg11Δ2-950; and also prApe1 and RFP-prApe1, both with N-terminal deletions: Δ2, Δ2-3, Δ2-4 and Δ2-9 (Fig. 4.4). Atg11Δ2-950 was used instead of full length Atg11 because, when fused with GFP, it shows better localization than the full length, perhaps because the size of GFP interferes with protein-protein interactions [62]. GFP-Atg11Δ2-950 bound aggregates even when they were defective when using prApe1Δ2-4. This suggests that while proper aggregation is critical for vesicle completion, it is not required for the receptor Atg19 to recruit Atg11.

A

Atg11Δ GFP-Atg19 RFP-Ape1 cells with prApe1 overexpressed

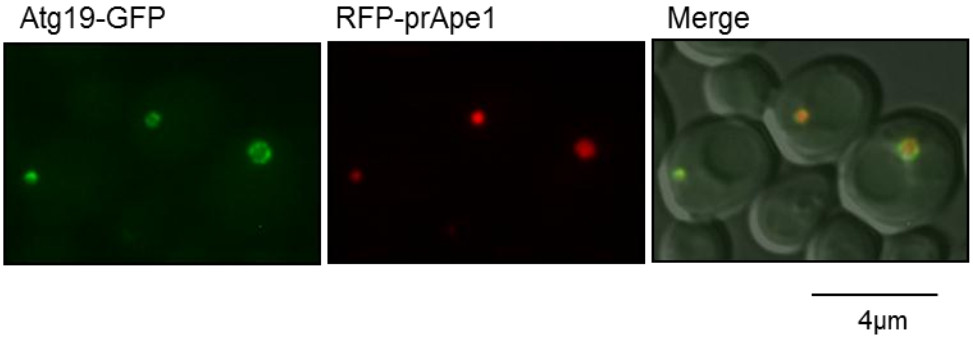

B

GFP-Atg19 and *RFP-prApe1* cell lysate mixture

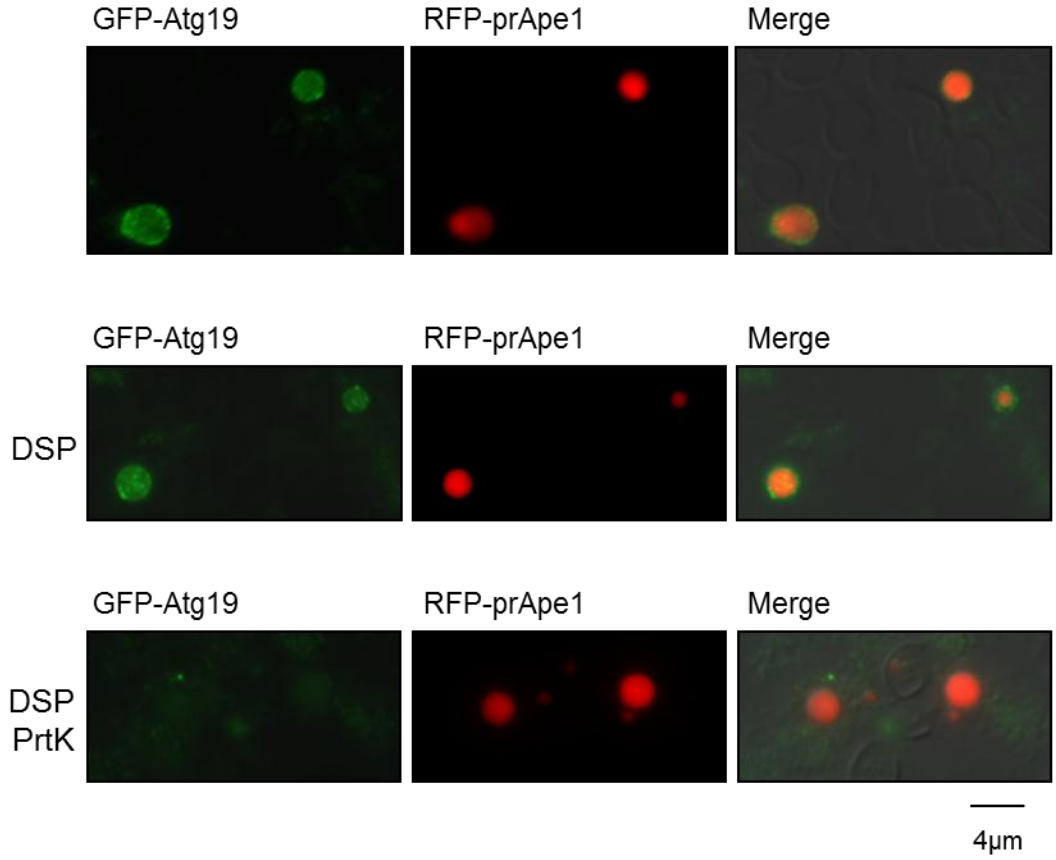

Figure 4.2. <u>Aggregation is not sufficient for Atg19 binding, the propeptide is required</u>. A) Atg19 binds to the aggregate surface. In *atg11Δ* cells with GFP-Atg19 and RFP-Ape1, RFP-prApe1 formed a single aggregate and GFP-Atg19 localized to the surface, forming red aggregate spheres of about a 0.2 μm diameter with a green ring around. prApe1 was overexpressed to obtain larger aggregates that are more easily visualized. **B) The propeptide is required for Atg19 binding to the aggregate surface.** *atg19Δ* with RFP-Ape1 cell lysate was treated with DSP, or DSP and PrtK, then mixed with *ape1Δ atg8Δ* with GFP-Atg19 lysate. DSP cross-links aggregates, PrtK cleaves propeptides. After PrtK-treatment, PrtK activity was inhibited by adding PMSF to a final concentration of 1mM, then RFP-prApe1 aggregates were washed twice to remove PrtK and ensure it did not cleave GFP-Atg19. GFP-Atg19 bound to the surface of aggregates from untreated and DSP treated lysate, but not to those that lacked surface propeptides after treatment with both DSP and PrtK. Thus the propeptide is required for Atg19 binding, while formation of aggregates is not sufficient for Atg19 binding.

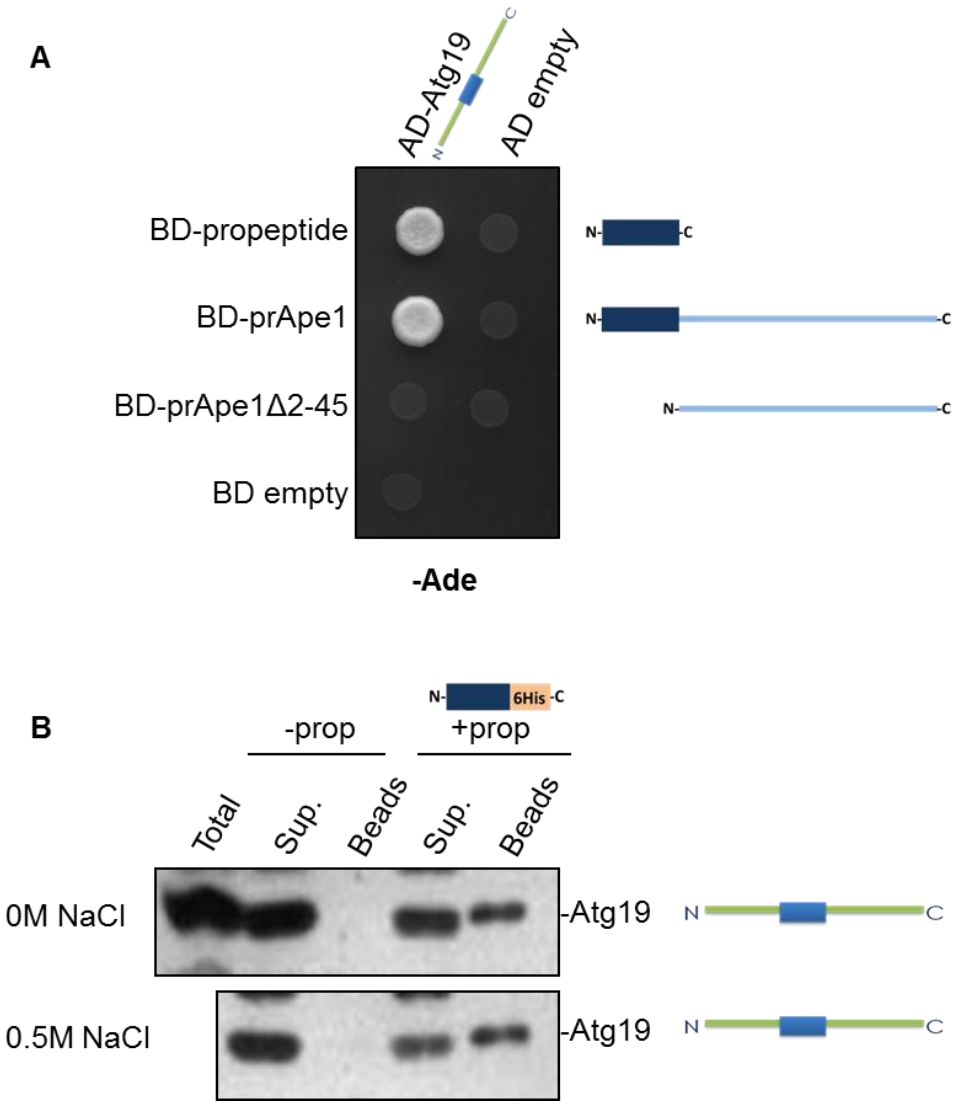

Figure 4.3. <u>The propeptide is sufficient for Atg19 binding</u>. A) The propeptide binds Atg19 *in vivo*. Two-hybrid assay with PJ69-4A *ape1Δ atg19Δ* cells. AD-Atg19 interacts with BD-propeptide similarly to BD-prApe1, but not with BD-Ape1Δ2-45. Thus the propeptide is sufficient for an interaction with Atg19. **B) The propeptide binds Atg19 *in vitro*.** *ape1Δ ams1Δ* yeast lysate with 0 or 0.5 M sodium chloride, was mixed with propeptide-6xHis coated agarose beads (+prop). *ams1Δ* was used in case Ams1 binding to Atg19 interferes with prApe1 binding, since both are cargo of the Cvt pathway that bind Atg19. As a control Ni^{+} coated agarose beads without propeptide-6xHis bound were used (-prop). Atg19 bound to propeptide-6xHis both in 0 and 0.5 M sodium chloride buffer. Unlike prApe1 binding to propeptide, which requires a high concentration of salts that potentiate hydrophobicity, Atg19 bound in the absence of sodium chloride, suggesting electrostatic interactions are involved while hydrophobicity plays a lesser role.

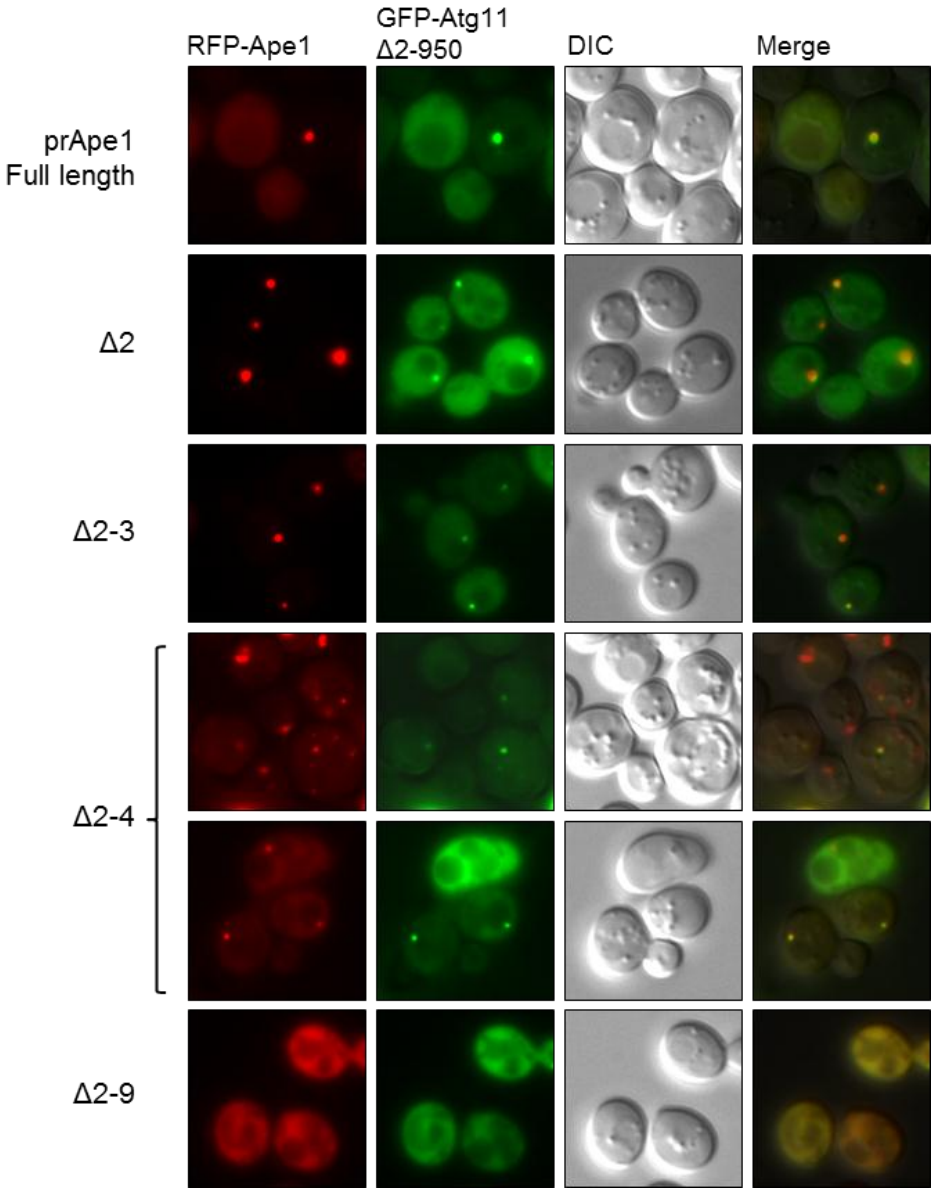

Figure 4.4. <u>Atg19 recruits Atg11 to defective aggregates</u>. Wild-type cells expressing RFP-prApe1 and prApe1, both with N-terminal deletions, and GFP-Atg11Δ2-950. GFP-Atg11Δ2-950 co-localizes with RFP-prApe1Δ2-4 aggregates, even though aggregation was defective. This is consistent with Atg19 binding defective aggregates, also constituted by RFP-prApe1Δ2-4. Atg11 is an adaptor protein that helps recruit the autophagic machinery for vesicle formation. Despite Atg19 and Atg11 binding, there was no transport of prApe1 to the vacuole during defective aggregation, suggesting the aggregate shape may play a role in vesicle formation, possibly by helping bend membrane around the complex. GFP-Atg11Δ2-950 and RFP-prApe1Δ2-4 co-localization frequency is of about 50%.

The coiled-coil of Atg19 binds the propeptide of Ape1

AIM: To investigate whether the Ape1 propeptide, a helix-turn-helix, and the Atg19 coiled-coil interact directly with each other, causing protein binding.

To investigate what domains of Atg19 may be involved in regulating its binding to Ape1, we used a two-hybrid assay, with AD N-terminally fused to Atg19 constructs (AD-Atg19) and BD N-terminally fused to full length prApe1 (BD-prApe1) or to just its propeptide, the 45 N-terminal amino acids of prApe1 (BD-propeptide) (Fig. 4.5). We focused our attention on the putative coiled-coil region of Atg19 (amino acid residues 157-180), since coiled-coils are often involved in protein interactions, while a previous study suggests that the coiled-coil is required for Atg19 binding [219].

The coiled-coil domain and a small region flanking it are both sufficient and necessary for binding to prApe1. However, while cells with full length AD-Atg19 and BD-prApe1 grew on adenine selection, cells with AD-Atg19Δ2-138/212-415 only grew on histidine selection, suggesting the interaction is weaker when only the coiled-coil is present. Furthermore, results were similar between cells with full length prApe1, as those with just its propeptide, suggesting the Atg19 coiled-coil interacts directly with the propeptide. Interestingly, in cells with AD-Atg19Δ2-155 there was a weak interaction with the propeptide (cell growth on histidine selection), but no interaction with prApe1; meanwhile with AD-Atg19Δ2-138 there was a strong interaction with both the prApe1 and the propeptide, similar to that seen with full length Atg19. Since the only difference

between these constructs are amino acids 138-155, these may interact with full length prApe1 at a region distinct from the propeptide, and this may contribute to a stronger interaction.

To verify binding we looked at co-localization by tagging the Atg19 constructs with GFP on their N- or C-terminus, while using RFP-prApe1 (Fig. 4.6). We verified that the internal, coiled-coil domain of Atg19 is sufficient for binding to prApe1 aggregates, since the construct consisting of little more than the internal Atg19 coiled-coil (GFP-Atg19Δ2-138/212-415) co-localized with RFP-prApe1, consistent with the two-hybrid assay, as well as with previous studies that show that the coiled-coil is required for Atg19 binding to prApe1 [219, 220]. Also, all constructs with N- or C-terminal deletions that showed an interaction with full length prApe1 in the two-hybrid assay co-localized with aggregates. Meanwhile, GFP-Atg19Δ2-155 did not co-localize with RFP-prApe1 aggregates and was diffuse throughout cytosol, consistent with the results in the two-hybrid assay, in which Atg19Δ2-155 only had a weak interaction with the propeptide, while not binding to full length prApe1.

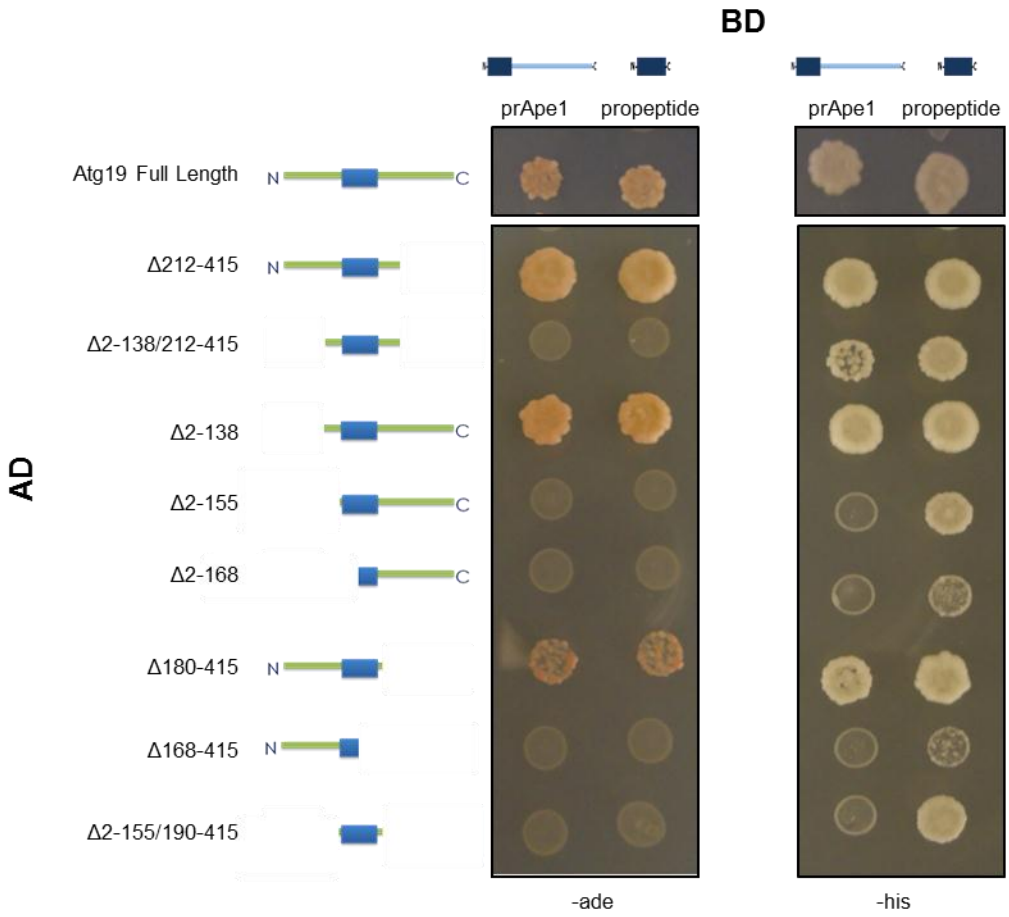

Figure 4.5. **The coiled-coil interacts directly with the propeptide of Ape1**. Two-hybrid assay testing Atg19 binding with full length prApe1 or with its 45 amino acid N-terminal propeptide. Proteins were fused to the AD or BD domain at their N-terminus: Atg19 with AD, prApe1 and its propeptide with BD (AD-Atg19, BD-prApe1 and BD-propeptide). PJ69-4A cells were grown on adenine or histidine selection. Cells growing in adenine selection suggest a strong interaction is taking place, cells only growing in histidine selection suggest the interaction is weak. The coiled-coil is necessary for binding to prApe1: AD-Atg19Δ2-138/212-415 interacted with BD-prApe1 and BD-propeptide, while partial removal of the coiled-coil in AD-Atg19Δ2-138 and AD-Atg19Δ168-415 blocked binding to both BD-prApe1 and BD-propeptide. While AD-Atg19Δ2-138 interacted strongly with both BD-prApe1 and BD-propeptide, AD-Atg19Δ2-155 only interacted with BD-propeptide, suggesting the Atg19 amino acid region 138-155 is necessary for a strong interaction with full length prApe1 at a region outside the propeptide.

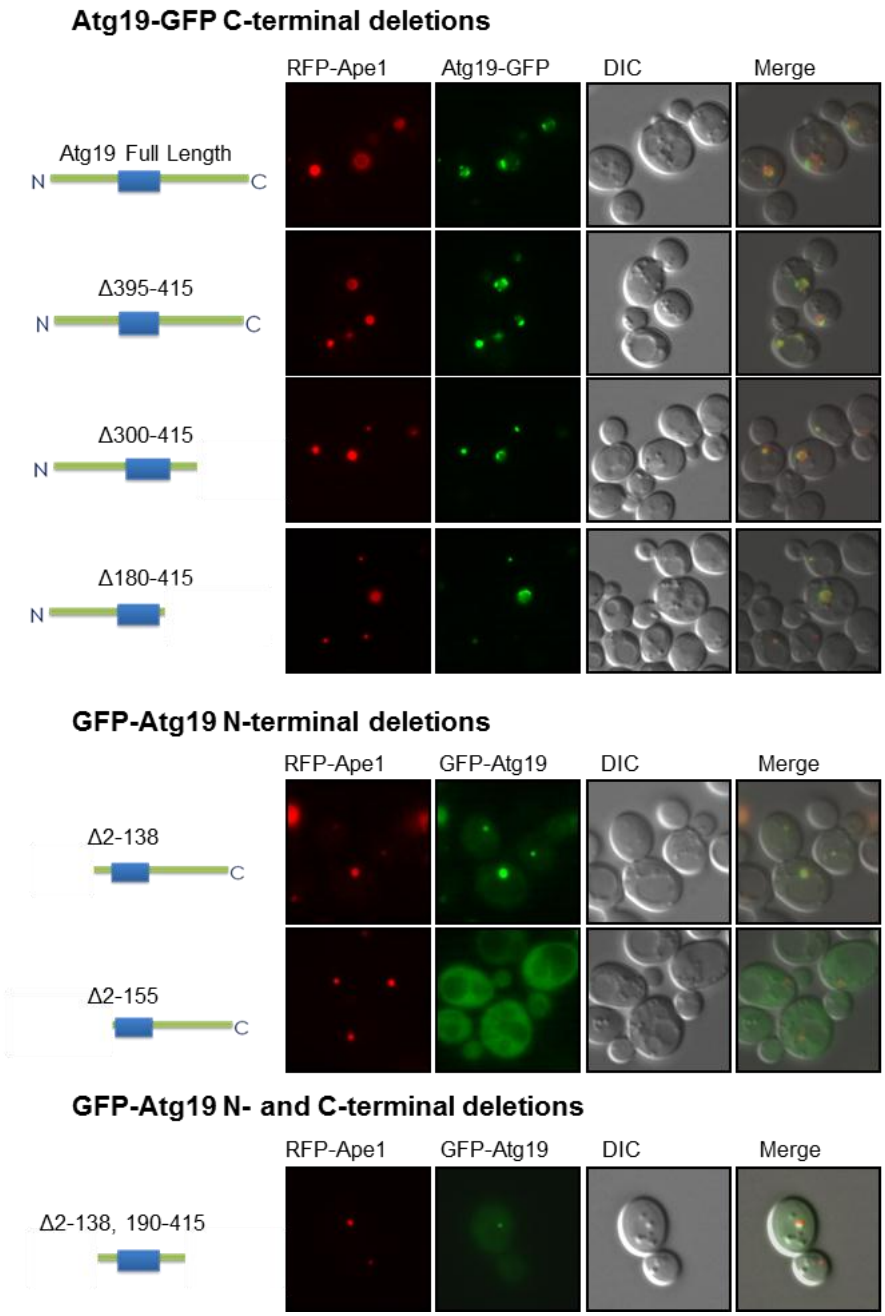

Figure 4.6. <u>The coiled-coil of Atg19 is necessary for binding to prApe1 aggregates</u>. Atg19 constructs with N- and C-terminal deletions were tagged with GFP at their N- or C- terminus, in *atg19*Δ cells expressing RFP-prApe1. GFP-Atg19Δ2-138/212-415, consisting of little more than the coiled-coil of Atg19, co-localized with RFP-prApe1 aggregates. Consistent with the two-hybrid study, where AD-Atg19Δ2-155 interacted only with the propeptide, and not with full length prApe1, GFP-Atg19Δ2-155 did not localize with aggregates.

Atg19 localizes to the surface of prApe1 aggregates

AIM: To investigate how Atg19 localizes only to the surface of aggregates, instead of inside them, by determining whether this is caused by Atg19 binding to the autophagic proteins Atg8 and Atg11, or by its binding to additional cargo Ams1 and Ape4. Alternatively, Atg19 may intrinsically localize to the aggregate surface.

C- and N-terminal Atg19 deletions enable it to localize throughout Ape1 aggregates

Normally, Atg19 only binds to the surface of prApe1 aggregates; hence Atg8 and Atg11, and most likely also the remaining autophagic machinery, localize only to the prApe1 aggregate surface (Fig. 4.8) [55, 59]. Consistent with this, Atg19-GFP, Atg19Δ395-415-GFP and Atg19Δ300-415-GFP localized to the surface of aggregates *in vitro*, when wild-type cells expressing RFP-prApe1 and overexpressing prApe1 (for larger aggregates to better visualize Atg19 localization) were lysed in a 50 mM potassium phosphate buffer (Fig. 4.7.A). Because prApe1 was overexpressed, its concentration is much higher than in cells with only endogenous expression of prApe1 (such as those used in Fig. 3.2), which facilitates aggregation and so this salt concentration is enough for formation of aggregates *in vitro*. However, when large portions of the Atg19 N- or C-terminus were removed, Atg19 localized inside aggregates. Deletion of the 138 N-terminal amino acids enabled Atg19 to localize inside aggregates, although GFP-Atg19Δ2-138 was only faintly seen inside aggregates. When the C-terminal amino acids 212-415 were removed, Atg19

can also localize inside aggregates: GFP-Atg19Δ212-415, GFP-Atg19Δ180-415 and Atg19Δ180-415-GFP are inside aggregates. Furthermore, consistent with the *in vivo* studies, the coiled-coil is sufficient for binding *in vitro*: GFP-Atg19Δ2-138/190-415 was faintly seen inside aggregates. Alternatively, the diminished localization of Atg19 in some constructs could be due to a decrease in its levels rather than due to weaker binding with prApe1.

Atg19 inside aggregates is less accessible to PrtK

Atg19 localizes to the surface of aggregates, where it is easily accessible to cytosolic proteins. To investigate whether Atg19 inside aggregates may interfere with its interactions with cargo and Atg proteins, we tested whether it was degraded by PrtK *in vitro* (Fig. 4.7.B). Wild-type cells with RFP-prApe1, and either Atg19-GFP or Atg19Δ180-415-GFP, and overexpressing prApe1 (for larger aggregates), were lysed in a 50 mM potassium phosphate buffer, pH 7 (due to the higher concentration of prApe1, this salt concentration is sufficient for aggregation *in vitro*). PrtK was added to a final concentration of 50 µg/ml, and lysate was incubated in ice for 30 minutes. The reaction was stopped by adding PMSF to a final concentration of 1 mM. While full length Atg19-GFP, which localizes only to the surface of aggregates, was readily cut by PrtK *in vitro*, in contrast Atg19Δ180-415-GFP was not, and was visible inside RFP-prApe1 aggregates. An alternative explanation is that PrtK only cleaved the GFP tag of full length Atg19 due to the presence of a PrtK sensitive site that is missing from the deletion construct.

Untagged Atg19 localizes to the surface of aggregates

To verify that Atg19 localization to the surface of aggregates was not an artifact caused by the GFP tags, which could cause conformational changes or physically interfere with Atg19 entry into the aggregate, we checked at what rate untagged Atg19 was lysed by PrtK when aggregates were present or absent (Fig. 4.7.C). For formation of large aggregates that would by degraded gradually by PrtK, prApe1 was overexpressed. Untagged Atg19 inside aggregates would be physically inaccessible to PrtK, and hence would be degraded gradually. Similarly, when prApe1 was soluble and not aggregating (low salt buffer, 2 mM potassium phosphate), instead of in aggregate form (high salt buffer, 50 mM potassium phosphate), PrtK readily cleaved it *in vitro*. However, when prApe1 aggregated, it was cut gradually, since only prApe1 on the surface of aggregates was exposed to PrtK. We are assuming that, since PrtK has high enzymatic activity in a wide range of salts (according to its manufacturer), that its activity is similar in the 2 mM and 50 mM potassium phosphate buffer. Untagged, full length Atg19 was readily cut by PrtK *in vitro*, in the presence or absence of aggregates, in *atg11*Δ or *ape1*Δ cell lysates, respectively, when using a 50 mM potassium phosphate buffer. *atg11*Δ cell lysates were used to block prApe1 and Atg19 transport to the vacuole, since without the adaptor protein Atg11 the Cvt pathway is effectively blocked. The similar rate of cleavage of Atg19 by PrtK independently of whether there were aggregates present or not, suggests that Atg19 localized on the surface of aggregates instead of inside.

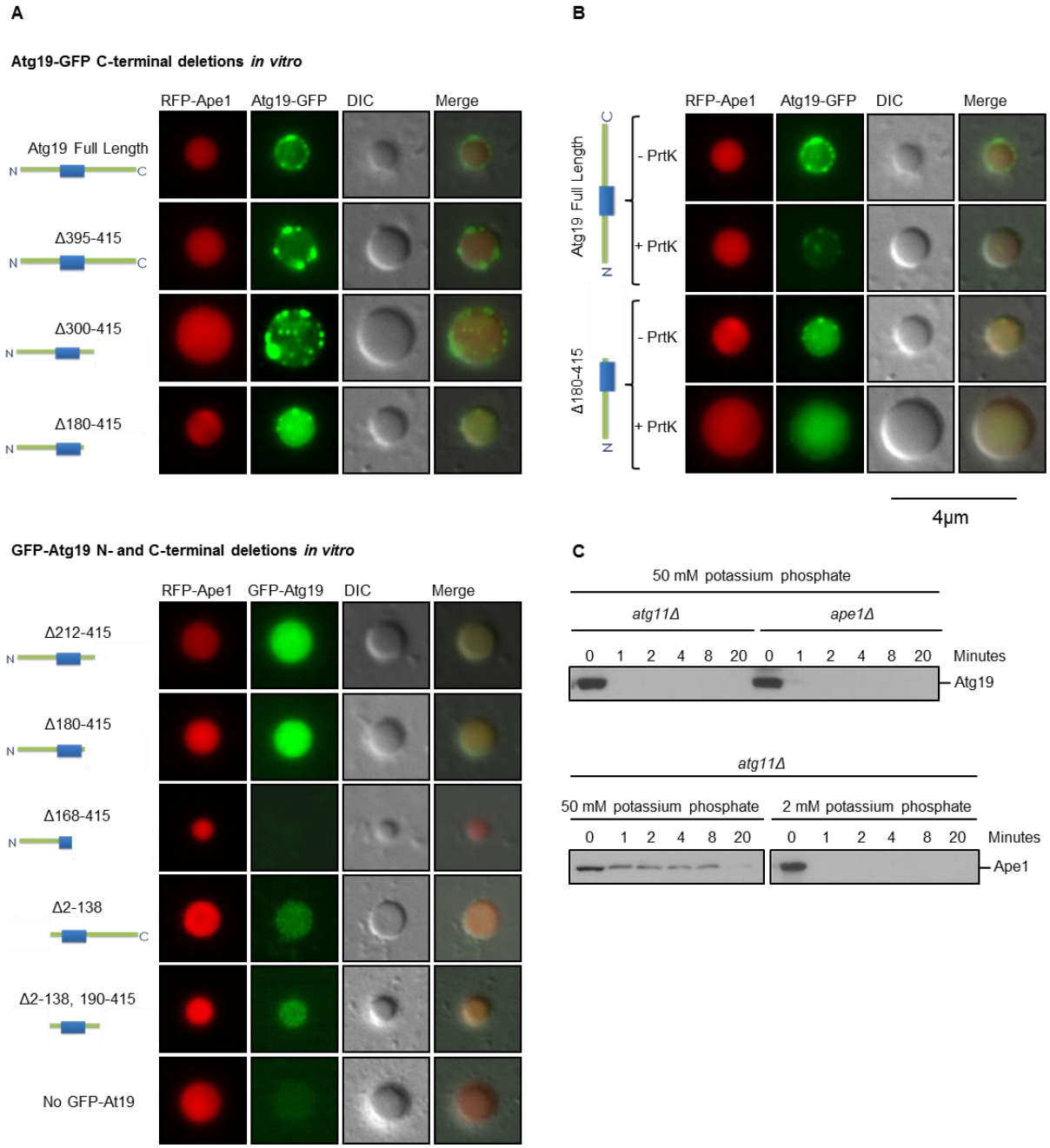
A
Atg19-GFP C-terminal deletions in vitro
RFP-Ape1
Atg19-GFP
DIC
Merge
Atg19 Full Length
Δ395-415
Δ300-415
Δ180-415
B
RFP-Ape1
Atg19-GFP
DIC
Merge
Atg19 Full Length
- PrtK
+ PrtK
Δ180-415
- PrtK
+ PrtK
4μm
GFP-Atg19 N- and C-terminal deletions in vitro
RFP-Ape1
GFP-Atg19
DIC
Merge
Δ212-415
Δ180-415
Δ168-415
Δ2-138
Δ2-138, 190-415
No GFP-At19
C
50 mM potassium phosphate
atg11Δ
ape1Δ
0 1 2 4 8 20 0 1 2 4 8 20 Minutes
Atg19
atg11Δ
50 mM potassium phosphate
2 mM potassium phosphate
0 1 2 4 8 20 0 1 2 4 8 20 Minutes
Ape1

Figure 4.7 <u>The Atg19 N- and C-terminus are required for localization on the aggregate surface, instead of inside it.</u> A) Atg19 with N- or C-terminal regions deleted can bind inside prApe1 aggregates *in vitro*. Lysate from wild-type cells with RFP-prApe1, and Atg19 C- or N-terminally tagged with GFP and with N- or/and C-terminal deletions. It is possible to differentiate between localization of Atg19 on the surface versus inside prApe1 aggregates. While using the microscope, the stage can be moved up and down to see different prApe1 aggregate cross-sections. If Atg19 is inside aggregates, aggregates will appear completely green throughout the different cross-sections. If Atg19 is on the surface, rings are visible when looking at the cross-section in the mid-section of the aggregate. Furthermore, when spherical aggregates role along the glass slide, Atg19 puncta on the surface move accordingly. Full length Atg19-GFP localized to the surface of aggregates. For binding to prApe1 the coiled-coil is required since GFP-Atg19Δ168-415 missing part of the coiled-coil does not localize to aggregates. Meanwhile, GFP-Atg19Δ2-138/190-415, consisting of little more besides the coiled-coil, localizes to aggregates, although the GFP signal was faint, suggesting a lower affinity for prApe1. Atg19 with amino acids 2-138 or 212-415 deleted can localize inside aggregates. Within a cell lysate, over 90% of Cvt complexes looked similar to those shown in this figure **B) Atg19Δ180-415-GFP inside aggregates is protected from degradation by PrtK.** Lysates from wild-type cells with RFP-prApe1 and either Atg19-GFP or Atg19Δ180-415-GFP were treated with PrtK and incubated for 30 minutes in ice. Atg19-GFP on the surface of aggregates was readily degraded by PrtK and hence was much less visible. In contrast, RFP-prApe1 and Atg19Δ180-415-GFP were still visible after PrtK treatment; perhaps they were degraded gradually because they were protected inside aggregates**. C) Untagged Atg19 is readily lysed by PrtK, suggesting it only localizes to the surface of aggregates, not inside.** prApe1 aggregates from *atg11*Δ cells were gradually lysed by PrtK (50 mM potassium phosphate buffer), while soluble prApe1 was readily lysed (2 mM of potassium phosphate buffer). Similarly, Atg19 was readily lysed by PrtK, both in the presence and absence of prApe1 aggregates, in lysate from *atg11*Δ and *ape1*Δ cells. The reaction was stopped by addition of protein sample buffer and incubating at 100°C for 2 minutes. **A, B and C)** Cells were mechanically lysed using glass beads in a 50mM potassium phosphate buffer, pH 7, unless a 2mM potassium phosphate is stated. **B and C)** After cell lysis, PrtK was added to a final 5µg/ml concentration, and incubated in ice.

Ams1, Atg11 and Atg8 also localize to the surface of prApe1 aggregates

Ams1 is another cargo protein for Atg19, while Atg8 and Atg11 bind Atg19 for recruitment of the autophagic machinery for Cvt vesicle formation [53, 55, 59]. To verify whether all these proteins localize solely to the surface of aggregates, similarly to Atg19, they were tagged with fluorescent proteins and their localization was verified *in vivo* (Fig. 4.8.B). During Atg8 processing, the C-terminal arginine is cleaved by Atg4. Hence, to ensure proper processing of Atg8 when different autophagic deficient strains were screened, Atg8ΔR was used. Atg11Δ2-950 was used instead of full length Atg11 because when fused with GFP, it shows better binding than the full length, perhaps because the large size of GFP interferes with protein-protein interactions [62]. prApe1 was over-expressed to make larger aggregates to better observe the Cvt complex. Atg19-CFP co-localized with Ams1-YFP on the surface of aggregates, and both appear as ring-like structures. Similarly, GFP-Atg11ΔN and GFP-Atg8ΔR localized to the surface of RFP-prApe1 aggregates, also forming ring-like structures (Fig. 4.8.B).

Atg19 surface localization is not due to binding to Atg8, Atg11 or Ams1

Atg19 without its C-terminus, Atg19Δ180-415, localizes inside aggregates (Fig. 4.7). Since the C-terminus of Atg19 has the binding domains for Atg8, Atg11 and Ams1, we investigated whether their binding was responsible for Atg19 localizing solely on the surface of aggregates (Fig. 4.8.C) [53, 55, 59]. Atg19 localized to the surface of aggregates in *ams1*Δ*/atg8*Δ*/atg11*Δ cell lysate. This suggests that Atg19 localization on the surface rather than inside of aggregates is independent of its interactions with Ams1,

Atg8 or Atg11, and that its C-terminus has a direct role in its correct surface localization, perhaps by physically interfering with its binding inside aggregates due to its shape or size. Surface localization would ensure that autophagic proteins and membrane surround aggregates, using them as a scaffold for bending membranes to form spherical Cvt vesicles. Alternatively, recently it was found that the C-terminus also binds Ape4, so we cannot discard the possibility that Ape4 binding to Atg19 causes it to localize to the aggregate surface. This is less likely since two-hybrid studies suggest that the Ape4 interaction with Atg19 is very weak [56].

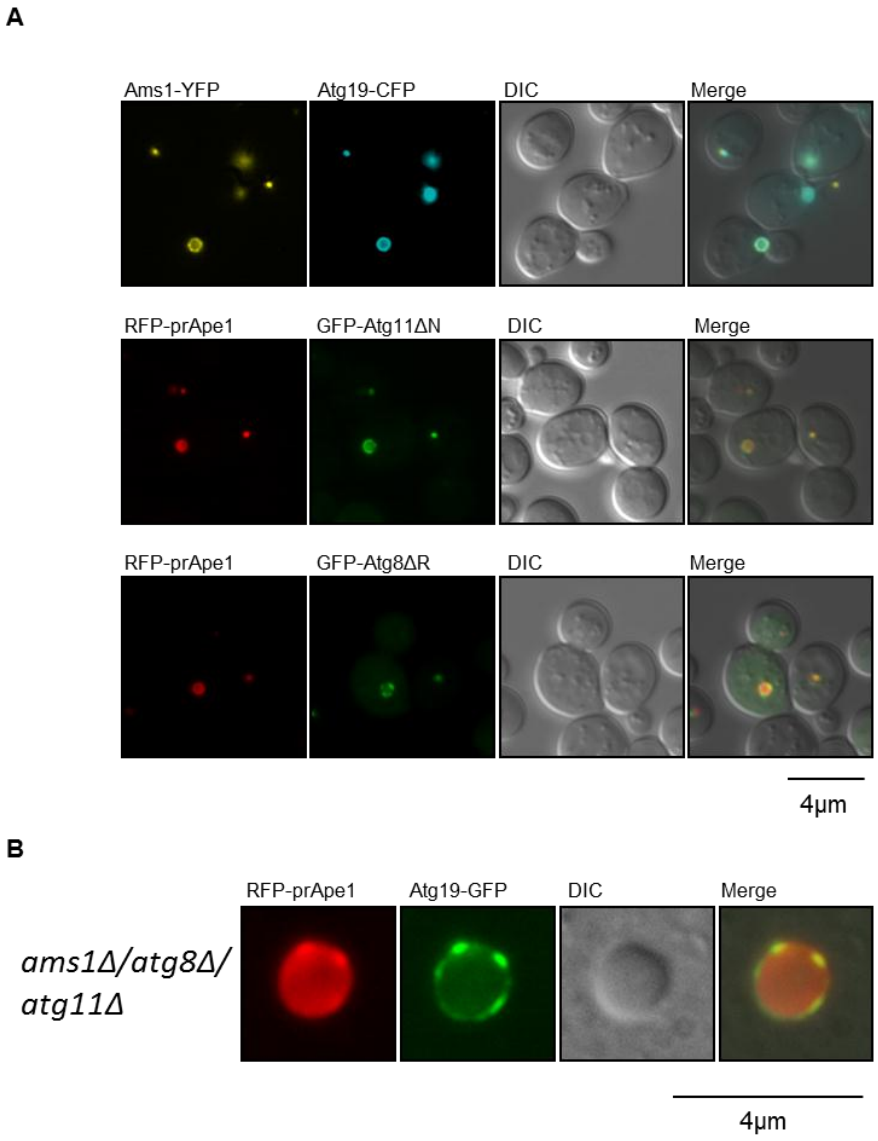

Figure 4.8. <u>While Ams1, Atg11 and Atg8 also localize to the surface of aggregates, their binding is not responsible for Atg19 surface localization</u>. A) Atg19 and Ams1 co-localize on the aggregate surface, while Atg8 and Atg11 also localize on the aggregate surface. For better visualization, prApe1 was over-expressed using a high-copy vector, to generate larger aggregates. *atg18*Δ cells expressing Atg19-CFP and Ams1-YFP, which co-localize on the surface of aggregates. *atg11*Δ cells expressing GFP-Atg11Δ2-950 and RFP-prApe1, and *atg1*Δ cells expressing GFP-Atg8ΔR and RFP-prApe1. GFP-Atg11Δ2-950 and GFP-Atg8ΔR localize on the surface of RFP-prApe1 aggregates. **B) Atg19 localizes to the surface of aggregates independently of Ams1, Atg11 and Atg8.** *ams1*Δ *atg8*Δ *atg11*Δ cell lysate, with Atg19-GFP and RFP-prApe1. Atg19-GFP localizes to the surface of aggregates *in vitro*.

Chapter 5

The Atg1-Atg13 Complex Regulates Atg19 Localization to prApe1 Aggregates

AIM: To investigate whether Atg19 localization to Ape1 aggregates changes between nutrient-rich and starvation conditions, and to identify autophagic proteins that regulate Atg19 localization to aggregates.

Starvation blocks Atg19 localization to aggregates *in vitro*

For transport of prApe1 to the vacuole via the Cvt pathway, receptor Atg19 binds and recruits the autophagic proteins Atg11 and Atg8, to initiate vesicle formation [55, 59]. Atg11 functions as an adaptor protein, while Atg8 helps in membrane tethering and fusion during vesicle expansion and completion. To see whether Atg19 localization was affected by Atg8 or Atg11, we looked at its localization *in vitro*. prApe1 was tagged at its N-terminus with RFP, while Atg19 was tagged at its C-terminus with GFP (RFP-prApe1 and Atg19-GFP, respectively). Untagged prApe1 was overexpressed using a high copy vector, in order to get larger aggregates and more readily see whether Atg19 localizes to their surface. Under nutrient-rich conditions, Atg19-GFP localized to the surface of RFP-prApe1 aggregates *in vitro*. However, after starvation, in lysates from the isogenic strains wild-type (BY4742), *atg8*Δ, *atg11*Δ or *atg8*Δ *atg11*Δ, Atg19 co-localized poorly with prApe1 *in vitro* after starvation (Fig. 5.1.A).

To investigate whether this was simply due to a decrease in the quantity of Atg19 after the induction of autophagy by starvation, we checked the amount of Atg19 before and after starvation, using SDS-PAGE and Western blot with an antibody against Atg19 (Fig. 5.1.B). To ensure that an equal amount of cells was used when preparing protein samples for Western blot analysis, a spectrophotometer was used to take optical density measurements of cell cultures. Although protein content was not measured, for the purpose of detecting significant changes in the amount of Atg19 before and after starvation, the optical density measurement should provide sufficient accuracy. The amounts of Atg19 before and after starvation remained similar in *atg8*Δ, *atg11*Δ and *atg8*Δ *atg11*Δ cells. Although there was a decrease in the amount of Atg19 in wild-type cells after starvation, perhaps due to its rapid transport to the vacuole by autophagy, this would only explain the lack of *in vitro* co-localization in wild-type cells. Interestingly, Atg19 migrates a little more slowly after starvation, suggesting it may have been covalently modified in some way. Furthermore, to determine whether the poor co-localization of Atg19 with aggregates *in vitro* was due to a complete block in its interaction with prApe1, or if instead it represents a lower affinity for prApe1, we tested co-localization *in vivo* (Fig. 5.1.C). Atg19 continues co-localizing with aggregates *in vivo* after starvation, suggesting the diminished co-localization *in vitro* may represent a weaker interaction between Atg19 and prApe1, rather than a complete loss of binding.

The Atg1-Atg13 Complex Regulates Atg19 co-localization to prApe1 aggregates

After starvation, Atg19 co-localization *in vitro* was diminished in the absence of Atg11 and Atg8, which are the only autophagic proteins known to bind to it. To try to determine what is changing Atg19 localization after starvation, we tested *in vitro* localization in cell extracts lacking proteins that are important for the induction of autophagy and/or the Cvt pathway. We tested Atg1, a key regulator that is critical for both autophagy and the Cvt pathway, and also tested Atg13, which modulates Atg1 activity and forms a complex with it [85, 105]. While Atg13 is critical for autophagy, the low levels of mApe1 in *atg13*Δ cells suggest that Atg13 greatly enhances Atg1 function during nutrient-rich conditions, but in its absence, Atg1 can still present some level of activity. We tested other proteins that interact with Atg1-Atg13, including Atg17, Atg29 and Atg31, which form a complex that is important for assembly of the PAS for autophagy; and Atg20 and Atg24, which form a complex that is critical for Cvt vesicle formation and that also includes Atg11 (Fig. 5.2.A). We also tested co-localization in *atg18*Δ cells, because Atg18 is a potential substrate of Atg1 kinase activity, according to a large-screen for phosphorylation substrates in yeast; and it is essential for both autophagy and the Cvt pathway, by playing a role in retrieval of Atg9 from autophagosomes and Cvt vesicles before their completion [221]. Furthermore, we determined the quantity of Atg19 in these cells using SDS-PAGE and Western blot analysis, with an antibody against Atg19 (Fig. 5.2.B). In all cells Atg19-GFP effectively co-localizes with RFP-prApe1 aggregates *in vitro* when cells were grown in nutrient-rich conditions (data not shown). In stark contrast, only in *atg1Δ* and *atg13*Δ cells did Atg19

continue co-localizing *in vitro* after starvation, suggesting the localization change is dependent on the Atg1-Atg13 complex, but not on the downstream complexes associated with it. However, it must be noted that in *atg29*Δ and *atg31*Δ cells the quantity of Atg19 after starvation was low, as was shown by SDS-PAGE and Western blot analysis, so in these cells we cannot rule out that rare co-localization simply represents low levels of Atg19. Nevertheless, the quantity of Atg19 remained stable in *atg17*Δ, *atg18*Δ, *atg20*Δ and *atg24*Δ cells, in which case lack of Atg19 binding *in vitro* cannot be simply explained by degradation.

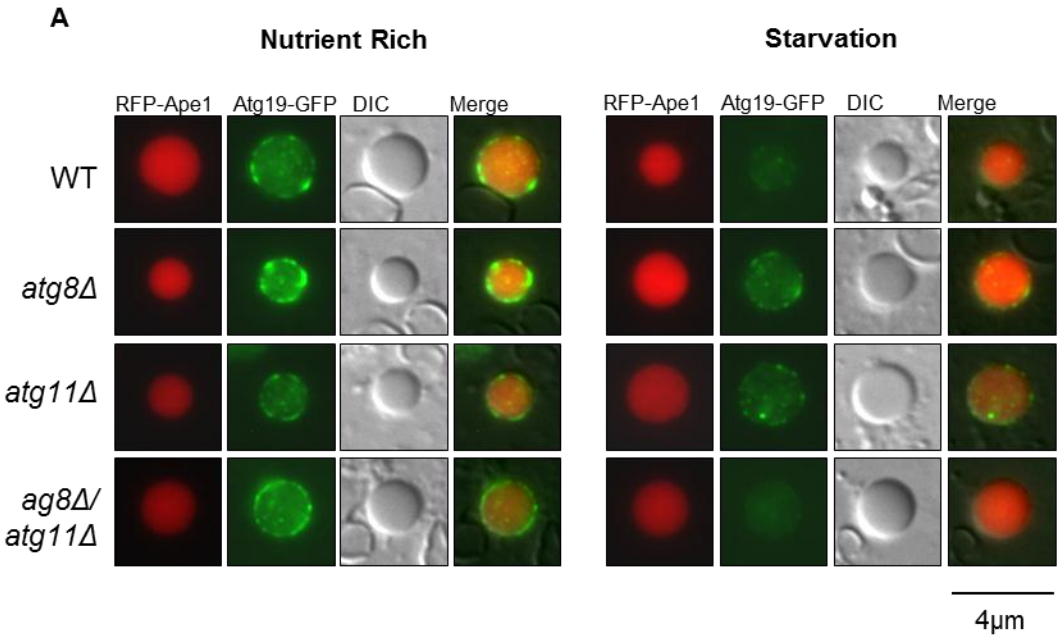
A
Nutrient Rich
Starvation
RFP-Ape1
Atg19-GFP
DIC
Merge
WT
atg8Δ
atg11Δ
ag8Δ/
atg11Δ
4μm

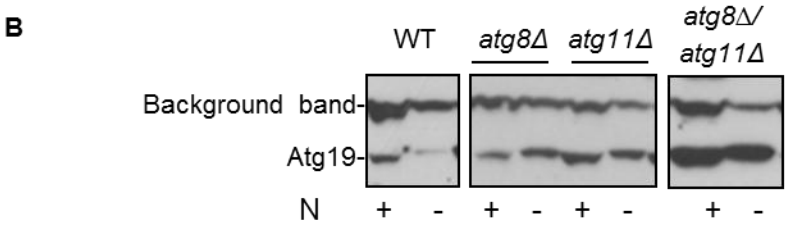
B
WT
atg8Δ
atg11Δ
atg8Δ/
atg11Δ
Background band-
Atg19-
N + - + - + - + -

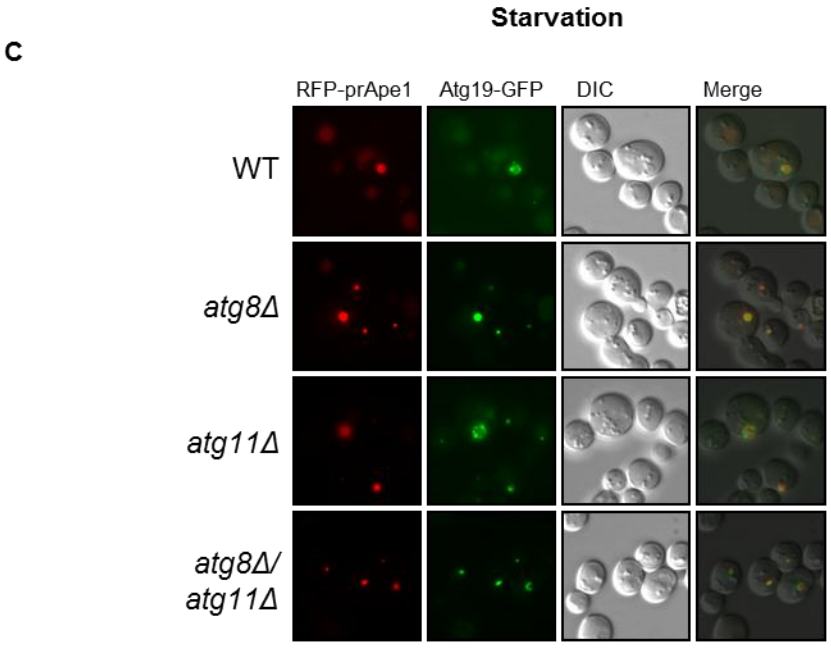
C
Starvation
RFP-prApe1
Atg19-GFP
DIC
Merge
WT
atg8Δ
atg11Δ
atg8Δ/
atg11Δ

Figure 5.1. <u>Starvation blocks Atg19 localization to aggregates *in vitro*.</u> A) Atg19 co-localized with prApe1 aggregates *in vitro* when cells were grown in nutrient-rich conditions, but not after cells were starved. Lysates from cells with Atg19 binding partners Atg8 and/or Atg11 knocked out, and with RFP-prApe1 and Atg19-GFP. Cells were either grown in nutrient-rich conditions or starved for 4 hours. Hundreds of Ape1 aggregates were examined under the microscope. Aggregate size varies from about 0.5-4 μm. While Atg19-GFP frequently localizes to aggregates *in vitro* before starvation (about 75% of aggregates had green rings around them, similar to those shown in the figure on the left hand panels), after starvation localization was diminished (about 60% of aggregates had almost no Atg19-GFP visible on their surface and are similar to those shown in the figure on the right hand panel, about 20% had a little more Atg19-GFP localizing, although generally not as much as before starvation, and about 20% showing no Atg19-GFP localizing). Cells were mechanically lysed using glass beads, in a 50mM potassium phosphate buffer, pH 7. **B) The quantity of Atg19 remains similar before and after starvation, except in wild-type cells, where there is less Atg19 after starvation.** Equal amounts of cells were used for preparing protein samples, for accurate measurement of Atg19 cellular levels. Cell quantity was estimated by measuring absorbance using a spectrophotometer. Protein samples were analyzed through SDS-PAGE and Western blot using an antibody against Atg19**. C) Atg19 binds prApe1 aggregates *in vivo*, even after starvation.** Starved cells with RFP-prApe1 and Atg19-GFP, and overexpressing prApe1 using a high copy vector for larger, more visible aggregates. Atg19-GFP continues to co-localize with aggregates *in vivo* after starvation, suggesting the diminished co-localization *in vitro* in figure A represents a change in the mechanism rather than a complete block in Atg19 binding.

Atg1 kinase activity blocks Atg19 co-localization with aggregates *in vitro*

To determine whether Atg1 kinase activity or/and its protein-protein interactions determined the mechanism of Atg19 localization we examined Atg19 co-localization *in vitro* when Atg1 lacked its 20 C-terminal amino acids, Atg1Δ20C, and using a kinase deficient mutant protein, Atg1ΔK54A M102A, which can still bind to its known interaction partners [85]. *atg1Δ20C* cells display defects in PAS assembly, in recruitment of autophagic proteins, and diminished (albeit not abolished) binding to Atg13 [85]. *atg1ΔK54A M102A* cells show higher levels of autophagic proteins at the PAS, suggesting they have defective PAS disassembly [85]. Atg19 from *atg1Δ20C* cells localizes poorly to prApe1 aggregates after starvation, indicating Atg1 diminished binding to Atg13 and loss of binding to the Atg17-Atg29-Atg31 complex, which is required for autophagy, was not sufficient to allow Atg19 localization (Fig. 5.2.C). However, Atg19 from *atg1ΔK54A M102A* cells co-localizes *in vitro* after starvation, suggesting Atg1 kinase activity is required to regulate the localization mechanism of Atg19.

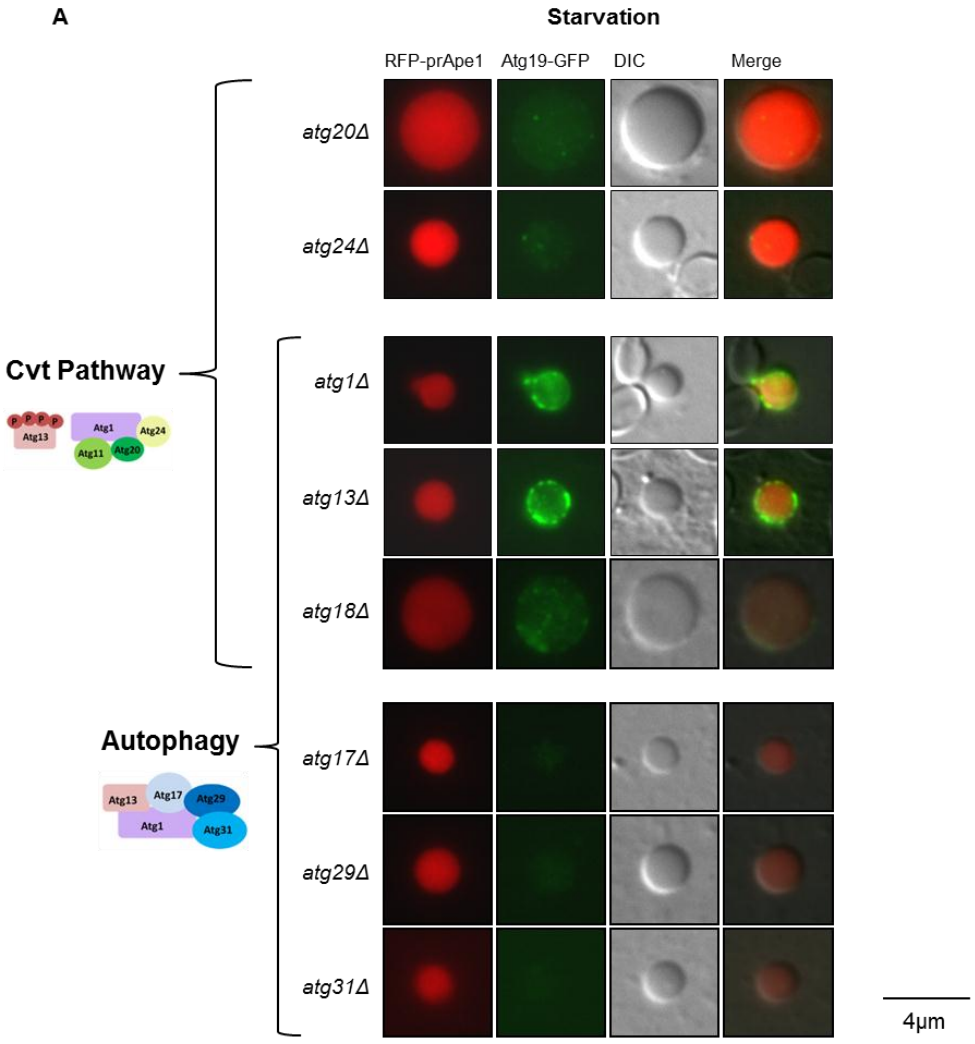
A
Starvation
RFP-prApe1
Atg19-GFP
DIC
Merge
atg20Δ
atg24Δ
Cvt Pathway
atg1Δ
atg13Δ
atg18Δ
Autophagy
atg17Δ
atg29Δ
atg31Δ
4μm
B
N
+
-
atg20Δ
atg24Δ
atg1Δ
atg13Δ
atg18Δ
atg17Δ
atg29Δ
atg31Δ
C
Starvation
RFP-prApe1
Atg19-GFP
DIC
Merge
atg1Δ
atg1Δ20C
atg1ΔK54A/M102A

Figure 5.2. <u>Atg1-Atg13 kinase activity blocks Atg19 localization to prApe1 aggregates *in vitro* after starvation, independently of Atg binding partners.</u> A) Atg1 and Atg13 help block Atg19 localization to prApe1 aggregates *in vitro* after starvation. Lysates from isogenic cells with different autophagy genes knocked out, including the key regulator Atg1 and its modulator Atg13, as well as other autophagic proteins that interact with the Atg1-Atg13 complex for recruitment of autophagic machinery during autophagosome and/or Cvt vesicle formation. Cells also have RFP-prApe1 and Atg19-GFP, and were starved for 4 hours. Hundreds of Ape1 aggregates were examined. Aggregate size varies from about 0.5-4 μm. Only in *atg1*Δ and *atg13*Δ cells did Atg19 continue to frequently localize to Ape1 aggregates *in vitro* after starvation (about 75% of aggregates had green rings around them, similar to the aggregates shown in the figure from *atg1*Δ and *atg13*Δ lysates), suggesting the Atg1-Atg13 complex blocks Atg19 *in vitro* localization to aggregates after starvation. In other strains Atg19-GFP localization was diminished after starvation (about 60% of aggregates had almost no Atg19-GFP visible on their surface and are similar to aggregates from *atg17*Δ and *atg18*Δ cells). **B) The quantity of Atg19 remains similar before and after starvation, except in *atg29*Δ where there is less Atg19 after starvation, while the overall level of Atg19 in *atg31*Δ is low.** Equal amounts of cells were used for preparing protein samples, to measure the levels of Atg19. Cell quantity was estimated by measuring absorbance using a spectrophotometer. Protein samples were analyzed through SDS-PAGE and Western blot using an antibody against Atg19. **C) Atg1 kinase activity is required for regulation of Atg19 localization to prApe1 aggregates, but its C-terminus is not.** After starvation, Atg19 continued to localize to aggregates *in vitro* when Atg1 lacked kinase activity (Atg1ΔK54A M102A) but failed to localize when Atg1 was missing 20 C-terminal amino acids (Atg1ΔC20). The 20 C-terminal amino acids of Atg1 may play a structural role in PAS assembly. Their deletion somewhat disrupts, but not abolishes, the Atg1 interaction with Atg13, and disrupts recruitment of the Atg17-Atg29-Atg31 complex. **A and C**). For lysis, cells were broken mechanically using glass beads in a 50mM potassium phosphate buffer, pH 7.

Atg19 amino acids 300-395 are required for regulating its localization to aggregates

We proceeded to explore which domains of Atg19 determined regulation of localization after starvation (Fig. 5.3.A). Like full-length Atg19-GFP, Atg19Δ395-415-GFP localized poorly to aggregates *in vitro* when cells were starved. However, Atg19Δ300-415-GFP co-localized with aggregates *in vitro* after starvation. This suggests the C-terminus of Atg19, specifically amino acids 300-395, help regulate its localization during starvation.

Wild-type lysate does not disrupt Atg19 or Atg8 localization to aggregates

Atg19 binds Atg11 and Atg8 to prApe1 aggregates for formation of the Cvt vesicle and transport to the vacuole [55, 59]. After starvation, Atg8 only localized effectively to prApe1 aggregates in *atg1Δ* cells, similarly to Atg19 localization (Fig. 5.3.B). This suggests that Atg19 binding to Atg11, and its subsequent recruitment of Atg8, is not affected after starvation in *atg1Δ* cells. This also suggests that Atg19 is functional *in vitro*, still able to recruit Atg8 for tethering membrane to the Cvt complex. Addition of lysate from wild-type cells failed to disrupt Atg19 binding to aggregates *in vitro*, when the prApe1-Atg19 aggregates came from *atg1*Δ cells (Fig. 5.3.B). Therefore, the mechanism that regulates Atg19 binding during starvation is not functional in our present *in vitro* assay, additional cellular components, like ATP, may be required.

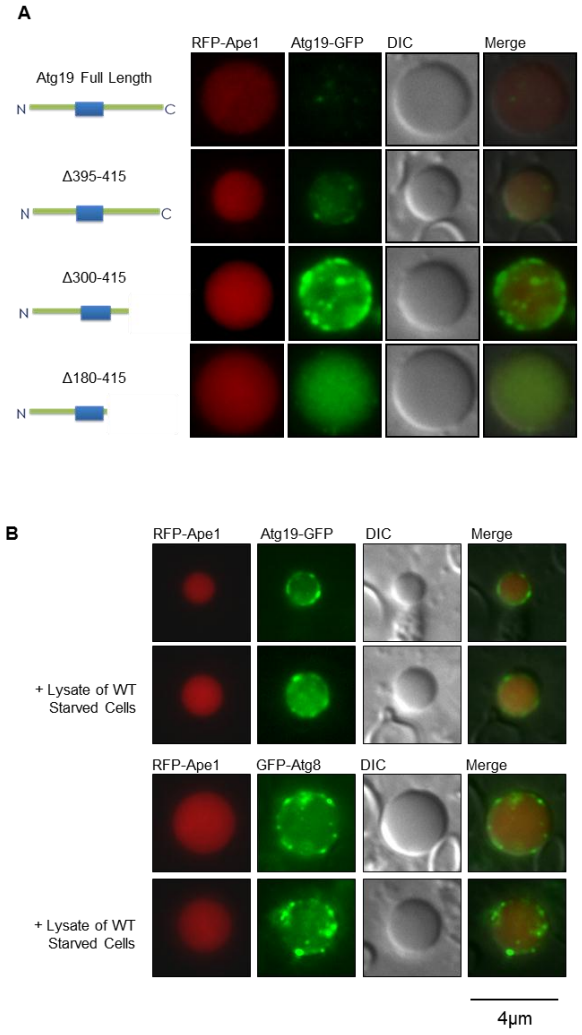

Figure 5.3. <u>The C-terminus of Atg19 is required for blocking Atg19 localization to prApe1 aggregates *in vitro*, and addition of wild-type lysate does not cause Atg19 or Atg8 dissociation</u>. A) The Atg19 internal region 180-395 regulates Atg19 binding *in vitro*. Starved wild-type cells with RFP-prApe1 and Atg19-GFP with C-terminal deletions. Atg19Δ300-415-GFP and AtgΔ180-415-GFP continued to co-localize with aggregates *in vitro* even after cells were starved, while Atg19Δ395-415-GFP co-localization *in vitro* was blocked. **B) Addition of lysate from wild-type cells grown under starvation does not block *in vitro* co-localization by Atg19 or Atg8 from *atg1*Δ starved cells.** Lysates from starved *atg1*Δ cells with RFP-prApe1 and either Atg19-GFP or GFP-Atg8 were mixed with lysates from starved wild-type cells. Both Atg19-GFP and GFP-Atg8 continued to localize to aggregates after wild-type lysate was added. This suggests the mechanism that blocks Atg19 *in vitro* co-localization with aggregates after starvation was inactive after cells were broken apart. **A and B)** Cells were mechanically lysed using glass beads in a 50mM potassium phosphate buffer, pH 7.

Chapter 6

Discussion

The Mechanism of prApe1 Aggregation

Dodecamerization

Ape1 dodecamers are very stable structures that require high proton concentrations for disassembly, suggesting strong protein interactions must be involved. Ape1Δ2-45 dodecamerization would explain how Ape1Δ2-45-GFP can be incorporated into prApe1 aggregates in wild-type cells, hence suggesting that the propeptide is not required for dodecamerization (Fig. 3.5.A). This was confirmed using a glycerol gradient in which prApe1, mApe1 and Ape1Δ2-45 were present in the same fraction as 670 kDa thyroglobulin: prApe1 has a 61 kDa molecular weight, so the dodecamer weighs 732 kDa; meanwhile mApe1 and Ape1Δ2-45 weigh 56 kDa, hence the dodecamer weighs 672 kDa (Fig. 3.5.B).

prApe1 aggregates in cytosol, while mApe1 aggregates disassemble in the vacuole

The propeptide is required for aggregation, both *in vivo* and *in vitro*. Ape1Δ2-45-GFP in *ape1Δ* cells shows no aggregation, with a diffuse GFP cytosolic signal, and Ape1Δ2-45-GFP does not bind RFP-prApe1/prApe1 aggregates *in vitro* (Fig. 3.3 and

3.4.A). Also, after differential centrifugation, prApe1Δ2-45 and mApe1 were present in the supernatant fraction constituted of soluble protein, while prApe1 was in the pellet fraction constituted of aggregates (Fig. 3.4.B). In agreement with the previous study, aggregates disassemble after propeptide cleavage by PrtK, suggesting aggregates disassemble in the vacuole due to cleavage of the propeptide by proteinase B, and that propeptides are accessible for protein interactions and so are localized on the surface of dodecamers (Fig. 3.4.C). The prompt disassembly of aggregates after propeptide cleavage suggests binding between dodecamers is fairly weak and requires a high prApe1 concentration for the aggregation threshold to be reached. A low binding affinity of dodecamers would facilitate aggregate disassembly once in the vacuole which would then permit rapid accessibility to substrate.

Propeptide Dimerization causes Aggregation

The propeptide can independently bind to prApe1 but not to mApe1, since propeptide-6xHis-coated agarose beads bound prApe1 and not mApe1, suggesting propeptides from separate dodecamers interact directly, forming dimers/trimers during aggregation (Fig. 3.6.A). However, prApe1 or propeptide-6xHis coated agarose beads did not bind a construct of the propeptide tagged with HA, while preliminary studies using Nuclear Magnetic Resonance (NMR) suggest that the propeptide aggregates at high concentrations (data not shown). Furthermore, a very high concentration of the propeptide, 2 mg/ml, was required to disassemble aggregates *in vitro* (Fig. 3.6.B). This suggests that the interaction between single propeptides is weak. However, several

propeptides clustering closely together, as would occur on the surface of agarose beads coated with propetide-6xHis, may form a more stable structure. Dodecamerization clusters propeptides together, forming propeptide dimers/trimers on dodecamer surfaces, which may in turn bind with higher affinity to propeptides on separate dodecamers.

The structure of *S. cerevisiae* prApe1 dodecamers, based on the structure of its homologue in *B. burgdorferi*, predicts that in a dodecamer, the way prApe1 proteins are arranged forms clusters of three propeptides on each of the four faces of the tetrameric dodecamer, thus forming propeptide trimers (Fig. 6.1). Consequently, during aggregation the propeptide trimer on one side of the dodecamer could bind to a propeptide trimer of another dodecamer. Hence, aggregation would be caused by two propeptide trimers coming together to form propeptide hexamers. However, aggregates constituted by a mix of prApe1 and Ape1Δ2-45 can form, suggesting not all twelve propeptides of a dodecamer are required for aggregation (Fig. 8A). Binding between some sides of each dodecamer may be sufficient to form stable aggregates. After all, once prApe1 begins to aggregate, dodecamers in the interior of the spherical aggregate would be completely surrounded and bound to other dodecamers, making the aggregate very stable even if the dodecamer-dodecamer interaction is weak. This model of aggregation would explain the presence of a single aggregate per cell, since as aggregates grow they become more and more stable. Small aggregates would more readily disassemble, while those incorporated into a larger, single aggregate would not. This is consistent with prApe1 aggregation *in vitro*, in which shortly after cell lysis numerous small aggregates were visible, but over time a lesser number but much larger aggregates were present (data not shown).

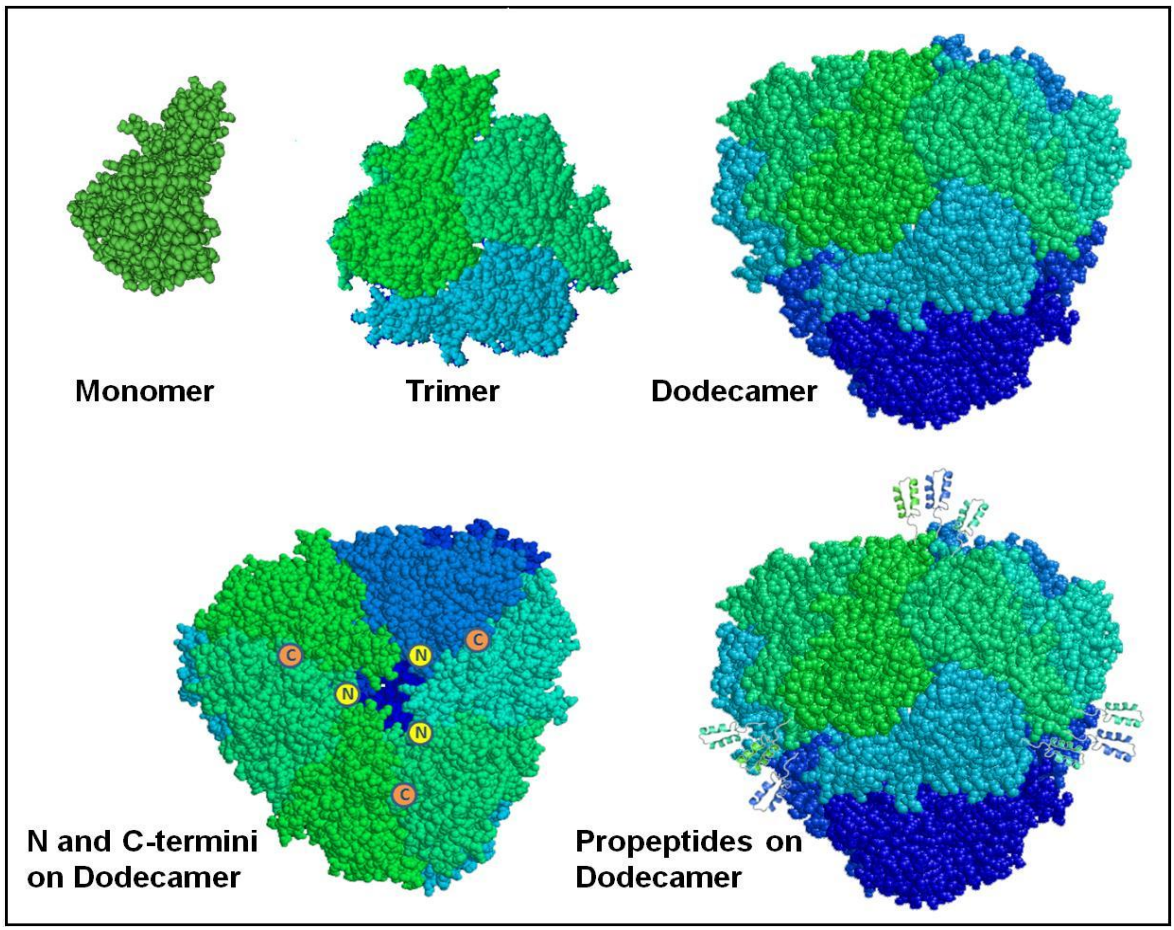

Figure 6.1. <u>Propeptides may be positioned in close proximity to each other on the surface of dodecamers</u>. prApe1 forms dodecamers, which bind together to form aggregates. Based on the molecular structure of *Borrelia burgdorferi* aminopeptidase, prApe1 is thought to assemble into trimers, four of which in turn come together to form a dodecamer. In comparison to the *B. burgdorferi* aminopeptidase, prApe1 has additional amino acids on its N- & C-termini, 45 & 10 respectively. Based on the localization of the N- terminus on the *B. burgdorferi* aminopeptidase, we propose that dodecamerization positions propeptides close together on the surface of dodecamers, forming propeptide trimers.

The four N-terminal amino acids are required for aggregation

Further studies showed that deletion of the four N-terminal amino acids disrupts aggregation, with prApe1Δ2-4-GFP in *ape1Δ* cells forming multiple punctate aggregates instead of a single punctate aggregate like in full length prApe1-GFP, prApe1Δ2-GFP and prApe1Δ2-3-GFP (Fig. 3.3). Furthermore, prApe1Δ2-4 does not bind propeptide-6xHis coated agarose beads while prApe1, prApe1Δ2 and prApe1Δ2-3 do (Fig. 3.6.C). The propeptide is predicted to form a helix-turn-helix, including an N-terminal amphipathic helix [70]. Under this scenario, deletion of the four N-terminal amino acids of the amphipathic helix disrupts aggregation, perhaps by changing the positioning of the N-terminal helix or by disrupting its helical structure.

Spherical aggregates suggest formation of regular polyhedra

Ape1 forms tetrahedral dodecamers, which further bind to form spherical aggregates *in vivo* and *in vitro* (Fig. 3.1). Under the microscope, the punctate or tubular Atg19 structures on the aggregate surface serve as markers, so aggregates can be observed to "roll" on the slide. Furthermore, when moving the stage up and down, observing the different cross-sections of the aggregate, the spherical shape also becomes apparent. The aggregate spherical shape suggests dodecamers might assemble into regular polyhedra, for example, one that is constituted by icosahedral structures, each made up of 20 dodecamers (Fig. 6.2). Alternatively, regular polyhedra are not formed, and defective aggregation perhaps merely represents aggregates that dissociate too

readily for the autophagic machinery to proper assemble on their surface and form the Cvt vesicle.

Computer models show that tetrahedrons optimally pack into icosahedral structures, which are regular polyhedrons with 20 identical, triangular faces [222]. This would enable each dodecamer to contact 4 similar dodecamers, in which each side would bind to another dodecamer, generating a very stable structure. Icosahedrons have a spherical-like shape, and the further addition of dodecamers to the icosahedral surface would continue to generate a regular, optimally packed, spherical structure.

Addition of the propeptide to Ape1 homologues that also form dodecamers was not sufficient for aggregation or binding to the propeptide (Fig. 3.7). This suggests that correct positioning of the propeptide, and an appropriate dodecamer shape and surface polarity, are also important for aggregation. Such a specialized structure is consistent with aggregation forming a very specific polyhedron, rather than dodecamers simply clustering together in a random fashion. Icosahedral structures are common in viral coats and some enzyme complexes [223-228]. It may be that polyhedral enzymatic complexes are more common than we think, but go unnoticed by standard molecular biology techniques [229]. One of the benefits of icosahedral shapes is that they provide a good enclosure, for protecting viral DNA/RNA, or preventing inappropriate substrates from reaching an enzymatic active site [230]. Although clathrin does not form icosahedral structures, nevertheless it is a good example of how spherical polyhedra are used as structural components, in this case forming vesicles for cellular transport [231]. Similarly, prApe1 icosahedral structures could prevent binding to the wrong substrate

while in cytosol, and help form a structural scaffold for Cvt vesicle formation. In agreement with the previous statement, proper aggregation is critical for Cvt vesicle formation (Fig. 3.3). Better understanding of how Ape1 assembles into regular polyhedra could advance the nanoscale compartmentalization of drugs for better delivery [232, 233].

The Mechanism of Atg19 Binding to prApe1 Aggregates

The propeptide is necessary and sufficient for Atg19 binding

The current model for the Cvt pathway is that Atg19 binds prApe1 aggregates in cytosol, and recruits autophagy proteins for Cvt vesicle formation and vacuolar transport [216, 234]. The propeptide is required and sufficient for prApe1 binding to Atg19 (Fig. 4.1, 4.2 and 4.3). While prApe1-GFP was transported to the vacuole in *ape1Δ* cells, prApe1Δ2-45-GFP was not and remained in cytosol (Fig. 3.3). Similarly, while GFP-Atg19 binds RFP-prApe1/prApe1 aggregates *in vitro*, GFP-Atg19 does not bind DSP cross-linked aggregates that have their propeptides cleaved off using PrtK, suggesting aggregation is not sufficient for Atg19 binding (Fig. 4.2.B). Meanwhile, Atg19 binding to propeptide-6xHis-coated agarose beads shows the propeptide is sufficient for Atg19 binding (Fig. 4.3.B). Consistent with this, in two-hybrid assays AD-Atg19 binds BD-prApe1 and BD-propeptide, but not BD-prApe1Δ2-45 (Fig. 4.3.A).

Thus, a propeptide that is only 45 amino acids long causes both aggregation and recruitment of a receptor, while facilitating vesicle formation and very likely inhibiting prApe1 proteolytic activity in cytosol. Although Ape1 has homologues and paralogues with similar dodecameric structures, some lack a propeptide and cannot form aggregates and remain in cytosol. Consequently, the Ape1 propeptide has large repercussions on its quaternary structure, localization and function.

The mechanism of prApe1 aggregation differs from Atg19 recruitment

Although the propeptide is sufficient for prApe1 and Atg19 binding, there are differences in how these proteins interact. Firstly, while propeptide-6xHis binding to prApe1 requires a 0.5 M sodium chloride or 0.2 M potassium phosphate buffer, binding to Atg19 does not (Fig. 3.6.A and 4.3.B). Aggregates were more stable in the presence of ions that, based on the Hofmeister series, potentiate hydrophobicity [193]. Consistent with this, propeptide-6xHis binds prApe1 in a 0.5 M sodium chloride buffer, but not in a low ionic strength buffer. This suggests hydrophobicity is important in prApe1 binding to the propeptide and in aggregation. It is conceivable that propeptides have an N-terminal amphipathic helix and that non-polar regions of propeptides are pushed together by hydrophobicity, forming propeptide trimers or hexamers and causing aggregation. However, propeptide-6xHis binds Atg19 in a 0.5 M sodium chloride buffer, as well as in a low ionic strength buffer, suggesting Atg19 binding is less dependent on hydrophobicity and instead involves electrostatic interactions.

Another difference between aggregation and Atg19 recruitment is illustrated by which amino acids are required for propeptide binding to prApe1 or Atg19. The binding of propeptide-6xHis to prApe1 requires the four N-terminal amino acids while, Atg19 binding does not, since Atg19 still binds prApe1Δ2-4 (Fig. 3.6.C and 4.1.). However, AD-Atg19 does not bind BD-prApe1Δ2-5, nor does GFP-Atg19 effectively bind RFP-prApe1Δ2-5, showing removal of the five N-terminal amino acids disrupts Atg19 binding (Fig. 4.1). Interestingly, although Atg19 can bind to prApe1Δ2-4, prApe1Δ2-4 was not effectively transported to the vacuole: no prApe1Δ2-4-GFP was visible in the vacuole,

and no mApe1 was present (Fig. 3.3, 3.6.C and 4.1). Moreover, Atg11 also localizes to defective RFP-prApe1Δ2-4 aggregates, suggesting Atg19 can bind and recruit Atg11 even if aggregation is defective (Fig. 4.4). Hence, lack of vacuolar transport of prApe1Δ2-4 was likely due to defective aggregation interfering with the assembly of core autophagic proteins or of membrane. For vacuolar transport, it is not sufficient for dodecamers to clump together and bind the receptor Atg19 and the adaptor protein Atg11 (Fig. 4.1. and 4.4.). In addition, they must form a regular structured aggregate, with a specific shape and positioning of dodecamers that may serve as a scaffold for bending the membrane into a Cvt vesicle. However, transport of prApe1Δ2-4 to the vacuole by the autophagic pathway during starvation conditions is most likely unaffected, since autophagosome formation is not dependent on Ape1.

The localization of Atg19 on aggregates further suggests the binding mechanism is different, since Atg19 localizes to the surface of aggregates, instead of being homogenously incorporated. Even though the mechanisms of Atg19 binding differs from that of prApe1 aggregation, nevertheless Atg19 and prApe1 may compete for an overlapping binding site, which prApe1 binds more strongly than Atg19; consequently Atg19 does not block aggregation. Its interaction with the propeptide must be dynamic and hence Atg19 binds and dissociates, enabling additional dodecamers to bind the propeptides and gradually enlarge the aggregate. This would explain why prApe1 continues to aggregate even when Atg19 appears to bind throughout its surface. However, at a very high Atg19 concentration, Atg19 would probably disrupt aggregation

by physically interfering with dodecamer binding to the propeptides and cause aggregates to disassemble, just as a high propeptide concentration disrupts aggregation (Fig. 3.6.B).

Ape1 propeptides bind directly to Atg19 coiled-coils

The coiled-coil domain of Atg19 is necessary and sufficient for binding to prApe1; even more, the coiled-coil also interacts with a construct consisting of just the N-terminal 45amino acid propeptide segment or prApe1 (Fig. 4.5). The propeptide is hypothesized to form a helix-turn-helix structure, hence it follows that prApe1 aggregation, as well as Atg19 binding to the propeptide, involves the dimerization of α-helical structures. In the case of prApe1 hydrophobicity is involved, while Atg19 involves electrostatic interactions (Fig. 3.6.A and 4.3.B). The proximity of the binding sites is consistent with Atg19 competing with prApe1 for binding with the propeptide. Atg19 is effectively displaced by incoming prApe1 proteins to ensure proper aggregation.

Ensuring Atg19 only localizes to aggregate surface for vesicle formation

Competition for propeptide binding between prApe1 and Atg19 is not the only factor that determines Atg19 surface localization. Atg19 fails to localize solely to the surface of aggregates when large portions of the N- and C-terminus were deleted, and instead binds inside prApe1 aggregates (Fig. 4.7.A). This suggests that the N- and C-terminus directly regulate localization of Atg19, perhaps by physically or electrostatically interfering with Atg19 coiled-coil binding to Ape1 propeptides inside aggregates. Alternatively, deletion of these domains may interfere with binding to additional cargo and autophagic proteins

and membrane outside of aggregates. This is plausible for deletions at the C-terminus, where the binding domains for Ape4, Ams1, Atg11 and Atg8 are found (Figure 4.8.A) [220]. However, Atg19 localizes to the surface of aggregates in the absence of Ams1, Atg11 and Atg8, while Ape4 interacts weakly with Atg19; hence we propose that it is the Atg19 N- and C-terminal domains themselves that directly interfere with Atg19 binding inside aggregates, or that Atg19 has additional protein-interactions that have not been identified.

It is critical for Atg19, together with its binding proteins Atg11 and Atg8, to localize to the surface of aggregates. Inside aggregates Atg19 is less accessible, PrtK failed to readily degrade Atg19Δ180-415-GFP embedded within prApe1 aggregates (Figure 4.7.B and C). Atg19, Atg8 and Atg11 surface localization makes them physically accessible to cytosolic proteins, so they can readily recruit the machinery and membrane for vesicle formation. Surface localization would also facilitate Atg19 binding to its additional cargo, such as Ams1, which co-localizes with Atg19 on the aggregate surface (Fig. 4.8.A). By assembling the autophagic machinery on the surface of aggregates, aggregates themselves can serve as a scaffold for bending membrane to facilitate vesicle formation.

Often Atg19 and Atg8 do not assemble uniformly on the aggregate surface, instead forming puncta or tubular structures (Fig. 5.3.B). These structures may represent the assembly of the autophagic machinery, including autophagic membrane containing Atg8-PE. However, even in *ams1*Δ*/atg11*Δ*/atg8*Δ cells, Atg19 still forms some punctate or tubular structures (Fig. 4.8.C). Perhaps Atg19 can multimerize to form some kind of

scaffolding structure. Several autophagic proteins form multimers, including Atg9, Atg11 and Atg16; their purpose for multimerizing is not yet understood. Some mammalian autophagic receptors also form multimers, including NBR1, which oligomerizes, and p62, which is polymeric. NBR1 and p62 bind ubiquitinated, misfolded proteins that are targeted for degradation via autophagy [235, 236]. Receptor multimerization may help to sequester cargo and to correctly position the autophagic machinery, surrounding the cargo and assembling autophagic proteins and membrane around it to facilitate autophagosome formation. Alternatively, Atg19 binding to its additional cargo or to additional unknown proteins may concentrate it at specific locations; after all, Ape4 forms dodecamers just like prApe1 does. Atg19 multimerizing could also be partly responsible for Atg19 localizing only to the surface of aggregates, since multimers would be too large to enter aggregates.

Large aggregates are not transported intact to the vacuole

Atg19 localization at the aggregate surface is consistent with its role as a receptor or adaptor of prApe1 that initiates Cvt vesicle formation. Entire aggregates are not transported intact to the vacuole, since in *atg15Δ* cells, in which the inner membrane of the Cvt vesicles remains intact inside the vacuole, several small prApe1-GFP aggregates moving rapidly by Brownian motion were visible inside the vacuole (data not shown). Perhaps after Atg19 binding a portion of the aggregate is broken off, with the aid of autophagic proteins, during membrane recruitment. The formation of the Cvt vesicle itself may mechanically break or pinch off a portion of aggregates, perhaps in the form of

an icosahedron or a similar polyhedral structure, for vacuolar transport. Alternatively, as prApe1 is incorporated into aggregates, the concentration of soluble prApe1 in cytosol decreases below the aggregation threshold, facilitating Atg19 binding and membrane recruitment. Furthermore, perhaps the Atg19 and Atg8 punctate and tubular structures on aggregates represent regions where the autophagic machinery is assembling and pinching off portions of the Cvt complex for vesicle formation.

prApe1 and Atg19 differ from Ams1 and Atg34

Atg34, the paralogue of Atg19, similarly binds to Ams1, Atg8 and Atg11; it helps transport Ams1 to the vacuole via autophagy during starvation [237]. Since Atg34 recruits Ams1 to autophagosomes instead of initiating Cvt vesicle formation, it does not rely on Ape1 aggregation for Ams1 vacuolar transport. In stark contrast, during nutrient-rich growth Atg19 transport and consequently that of its additional cargo Ams1 and Ape4, is dependent on Ape1 [56, 219]. Although Ams1 oligomerizes and Ape4 forms dodecamers in cytosol similarly to Ape1, they have not been shown to form aggregates, and just as Atg19 and Atg11 binding to defective aggregates is not sufficient for vacuolar transport, Atg19 binding to Ams1 and Ape4 is also not sufficient for Cvt vesicle completion [56, 219, 238]. Consequently, proper prApe1 aggregation is critical for transport of additional Cvt cargo. Furthermore, although Atg19 and its paralogue Atg34 both link cargo to autophagic proteins, Atg19 has an additional role by being part of specialized machinery for the bending of membrane around the Cvt complex for vesicle formation.

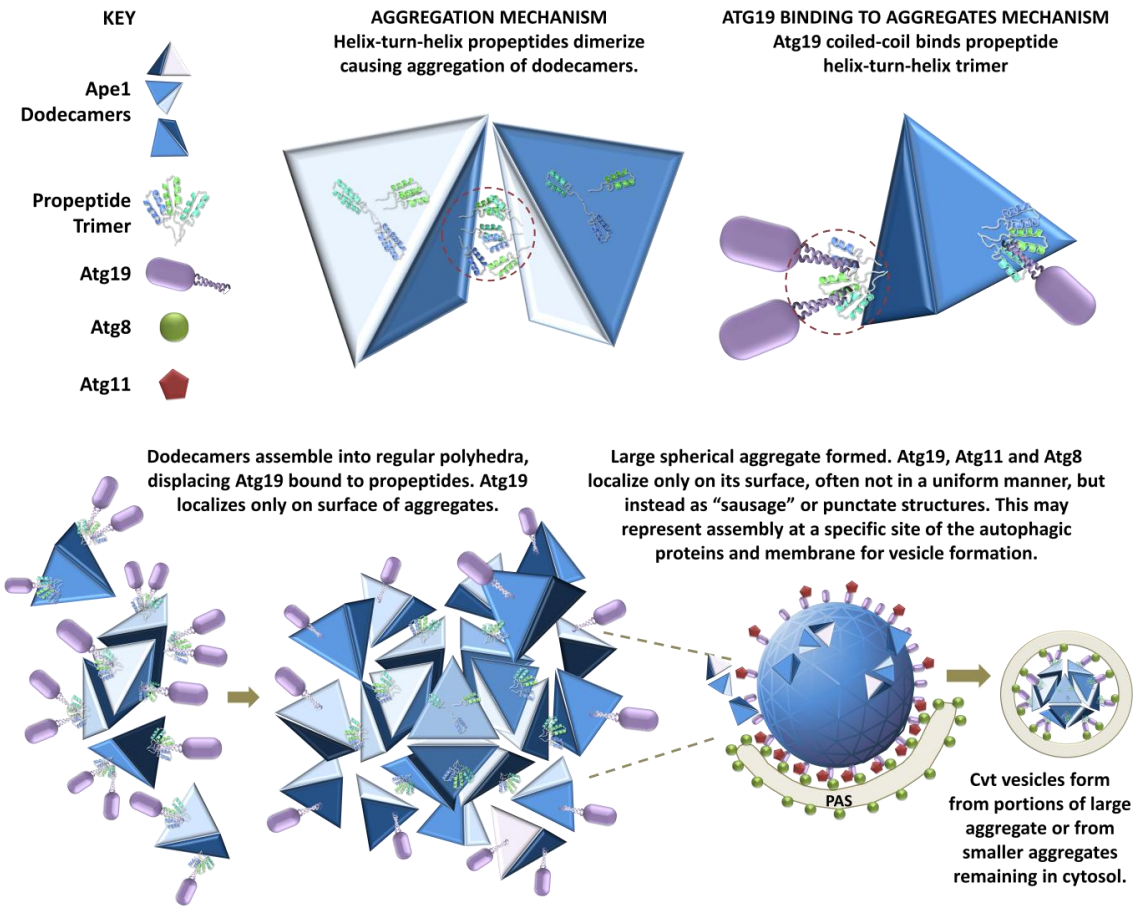

Figure 6.2. A new model for Cvt vesicle formation: Ape1 aggregation and recruitment of autophagic proteins. Binding of propeptide trimers from different dodecamers, forming hexamers, may cause aggregation. Based on the structure of its homologue in *B. burgdorferi*, prApe1 proteins are predicted to be arranged in clusters of three propeptides on each of the four faces of the tetrameric dodecamer. Each dodecamer side could then make contact with a different dodecamer via their propeptides. For optimal packing and formation of a regular polyhedral structure, one possibility is that 20 tetramers are arranged into an icosahedron with 20 triangular faces. Further binding of dodecamers in a similar pattern would ultimately form a large spherical aggregate. Atg19 binds aggregates via its coiled-coil, which directly interacts with Ape1 propeptides. Atg19 would compete with prApe1 for binding to the propeptide, but aggregation takes precedence while, the Atg19 N- and C-terminus interfere with Atg19 binding inside aggregates, causing Atg19 and its binding partners Atg11 and Atg8 to remain on the surface of large aggregates for recruiting the autophagic machinery. Small Cvt vesicles are formed from portions of the large aggregate, or from smaller aggregates remaining in cytosol. Transport of additional Cvt pathway cargo, including Ams1, Ape4 and Lap3, is dependent on prApe1 aggregation and Atg19 surface localization under nutrient-rich conditions.

Atg19 Regulation after Starvation

The mechanism of Atg19 binding changes upon starvation

Atg19 plays a role in both the Cvt pathway and autophagy, directing vacuolar proteases Ape1, Ape4 and Ams1 to the vacuole. If the role of Atg19, as a receptor that targets specific vacuolar protease to the PAS, does not differ between nutrient-rich or starvation conditions, then its mechanism of binding to Ape1 would not change. However, Figure 5.1 and 5.2 show that Atg19 co-localizes poorly with aggregates *in vitro* after starvation, even though it still localizes in *vivo*, suggesting its mechanism of binding must have been modified in such a way that Atg19 no longer localizes to aggregates *in vitro*. In wild-type, *atg29*Δ and *atg31*Δ cells the lack of co-localization could be due to the low level of Atg19, perhaps by degradation via autophagy. However, in the other strains where Atg19 co-localization to prApe1 aggregates *in vitro* was also diminished after starvation the amount of Atg19 did not change significantly (Fig. 5.1.B and 5.2.B). Moreover, in strains where prApe1 transport via the Cvt pathway and autophagy is effectively blocked, as in *atg8*Δ*, atg8*Δ *atg11*Δ and *atg18,* Atg19 co-localization to aggregates *in vitro* after starvation was still diminished. All this indicates that Atg19 has not been significantly degraded by vacuolar transport or some alternative pathway. Since Atg8 and Atg11 are the only autophagic proteins known to bind to Atg19 directly, the difference in Atg19 binding *in vitro* must be due to covalent modifications, to changes in the way its cargo binds to Atg19, or to a protein-protein interaction with an unknown partner.

The Atg1-Atg13 complex regulates Atg19 binding

A yeast screen that focused on proteins involved in formation of the PAS for the Cvt pathway and/or autophagy shows that the Atg1-Atg13 complex is involved in blocking Atg19 co-localization to prApe1 aggregates *in vitro*, since in *atg1*Δ or *atg13*Δ cells Atg19 frequently localizes to aggregates *in vitro* even after starvation (Fig. 5.2.A). Interestingly, none of the other autophagic proteins known to bind the Atg1-Atg13 complex affect Atg19 localization *in vitro*, which diminished after starvation in *atg20*Δ, *atg24*Δ, *atg17*Δ, *atg29*Δ, *atg31*Δ and *atg18*Δ. This suggests that the Atg1-Atg13 complex affects Atg19 localization independently of the other two complexes it forms with these proteins. The Atg1-Atg13 complex also plays a role in retrograde transport, a process involving Atg9, Atg2 and Atg18 [89, 147, 239]. In addition, a global yeast screen suggests Atg18 may be a phosphorylation substrate for Atg1 kinase activity [221]. However, Atg19 did not co-localize with prApe1 frequently *in vitro* in *atg18*Δ cells after starvation, suggesting regulation of Atg19 binding by Atg1-Atg13 is not dependent on Atg18 function or retrograde transport.

Atg1 kinase activity is required for Atg19 regulation

Atg1 kinase activity is required for both the Cvt pathway and autophagy, and to interfere with Atg19 localization to aggregates *in vitro* after starvation (Figure 5.2.C) [85, 105]. The 20 C-terminal amino acids of Atg1, which play a key role in its structural function for PAS assembly, are not required for abolishing Atg19 binding *in vitro*. Although this C-terminal region is important for protein-protein interactions, its deletion

does not completely abolish Atg1 binding to Atg13. Consequently, these results are consistent with the lack of *in vitro* localization to aggregates after starvation in *atg13*Δ cells. We propose that Atg1 kinase activity, which is modulated by Atg13, directly or indirectly regulates Atg19 or an additional protein it interacts with, triggering a change in the mechanism of Atg19 localization to Ape1 aggregates. This process could also be dependent on correct disassembly of the PAS and autophagosome expansion, which are mediated by Atg1 kinase activity.

A mass spectrometry study for the identification of phosphoproteins suggests that Atg19 may be phosphorylated at four different sites, including serines at positions 136, 243 and 246; and a threonine at position 411 (Fig. 4.8.A) [240]. However, the threonine at position 411 is in the Atg8 binding domain, and so perhaps it is unlikely it would have a role with prApe1 binding. The other sites are more promising: two serines are in the prApe1 binding domain (about 153-191 amino acid region), at positions 243 and 246, while the other serine is near the prApe1 binding domain, at position 136. Its paralogue Atg34, which targets Ams1 to autophagosomes during starvation, is phosphorylated upon induction of autophagy [72]. Moreover, kinase activity regulates yet another autophagy receptor, optineurin. Phosphorylation at serine-177 enhances its binding to LC3, an Atg8 homologue, and facilitates clearance of cytosolic *Salmonella enterica* in HeLa cells [241]. Lastly, SDS-PAGE and Western blot analysis with an antibody against Atg19 show a shift in the size of Atg19: Atg19 protein bound to propeptide-6xHis migrates more slowly than Atg19 not bound, and Atg19 protein also migrates more slowly after starvation, suggesting Atg19 has been covalently modified in

some way (Fig. 4.3.B and 5.1). When a protein is phosphorylated, it may migrate a little slower. Hence, it is plausible that Atg19 is a substrate for Atg1 kinase activity, and that a similar mechanism may regulate several autophagy receptors, including optineurin, Atg34 and Atg19. After all, autophagy receptor function and structure is somewhat conserved, as is exemplified by the yeast receptors Atg19 and Atg34, and the mammalian receptors/adaptors p62, NBR1 and Nix, all of which bind to Atg8 or its homologue LC3 via a WXXL motif and by forming an intermolecular parallel β-sheet [37-39, 49].

A Novel Atg19 Binding Regulatory Domain

An internal region of Atg19 plays a role in the regulation of its localization to prApe1 aggregates. While full length Atg19-GFP and Atg19Δ395-415-GFP co-localize with prApe1 *in vitro* under nutrient-rich conditions, neither localizes well when cells were starved (Figure 5.3.A). In contrast, Atg19Δ300-415-GFP and Atg19Δ180-415-GFP continue to localize with aggregates *in vitro* even after starvation (Figure 5C). Both Atg19Δ180-415-GFP and Atg19Δ300-415-GFP lack the Atg11 and Atg8 binding domain (Fig. 4.8.A) [49, 219, 220]. However, lack of binding to Atg11 and/or Atg8 does not explain localization to aggregates *in vitro* after starvation, because localization to prApe1 aggregates was also diminished in *atg8*Δ*, atg11*Δ and *atg8*Δ *atg11*Δ starved cells (Figure 5.1.A). The fact that Atg19Δ395-415-GFP fails to bind *in vitro* after starvation is further evidence that the change in localization to prApe1 aggregates is not due to vacuolar degradation via the Cvt pathway or autophagy, since binding to Atg8 is critical for both these processes. While it is plausible that Atg19Δ180-415-GFP continues to localize with

aggregates *in vitro* after starvation simply because it is trapped inside aggregates, this cannot be the case for Atg19Δ300-415-GFP, which localizes on the surface of aggregates.

In conclusion, Atg19 amino acid positions 300-395 are required for changing its mechanism of localization to prApe1 aggregates. This region overlaps with part of the Ams1 and Atg11 binding domain, but also includes a region that may not be required for binding to either: amino acids 368-387 (Fig. 4.8.A). Although previous studies suggest Atg19 may be phosphorylated (at position 136, 243, 246 and 411) and ubiquitinated (at Lysine 213 and 216), none of these sites lie within the 300-395 region that is determining Atg19 binding *in vitro* (Fig. 4.8.A) [240, 242]. However, that does not necessarily eliminate the possibility that covalent modifications at neighboring amino acids, which could affect the structure of adjacent regions, may be involved. After all, Atg1 kinase activity is important for the Cvt pathway and blocks Atg19 localization to prApe1 aggregates *in vitro* after starvation, while ubiquitination plays a role in selective autophagy by targeting misfolded proteins to autophagosomes for degradation [105, 243].

Atg19 may have additional roles, not simply passively binding to cargo

A key question is what the lack of Atg19 localization to prApe1 aggregates *in vitro* represents. The lack of localization *in vitro* after starvation may indicate that Atg19 binds prApe1 with less affinity, or that it binds another protein more readily, or that an additional protein is interacting with Atg19 and preventing it from strongly binding to prApe1. Atg19 may have multiple roles, not simply binding to cargo by default, and

delivering it to the PAS for vacuolar transport; but also modulating its binding in order to regulate the rate of transport. For example, Atg19 could be preferentially binding to another cargo protein whose transport to the vacuole is of higher priority during starvation. Alternatively, it could bind its cargo with lower affinity or be sequestered by an autophagic protein to divert the autophagic machinery away from the Cvt complex during starvation. Since Atg1-Atg13 play a role in retrieval of Atg9 and Atg23, perhaps upon induction of autophagy they also regulate Atg19 retrieval [89]. Under this scenario, Atg1-Atg13 would help retrieve Atg19 from aggregates during starvation *in vivo*, some Atg19-GFP may return to aggregates and so would continue to localize on their surface, but after cell lysis and after retrieval, Atg19 may be irrecoverable, so there would be no Atg19-GFP localizing on aggregates. Another possibility is that, since the formation of Cvt vesicles is a somewhat different process from autophagosome formation, perhaps Atg19 must modify its mechanism of binding to prApe1 for its correct packaging into autophagosomes instead of Cvt vesicles. For example, during the Cvt pathway, Atg19 multimerization could help pinch off small portions of the large aggregate to sequester them into a vesicle. In contrast, during autophagy phosphorylation of Atg19 could prevent it from multimerizing, enabling large autophagosomes to form instead of small Cvt vesicles, so that large cargo, including entire organelles, can be targeted. This is a highly hypothetical model, since Atg19 multimerization and phosphorylation have not been shown.

Atg19 may have multiple roles that are yet to be elucidated. So far we know it helps transport several vacuolar proteases and that the Cvt pathway also transports the cytosolic

protein Lap3 for selective degradation. It has also been proposed that Atg19 may help eliminate retrotransposons and misfolded ER proteins [244, 245].

All things considered, Atg19 may be targeting a variety of proteins for degradation, implying that it must be tightly regulated in response to environmental conditions. Furthermore, correct cargo recognition is critical, and failure can lead to cellular dysfunction, as illustrated by Huntington's disease [246]. Atg19 regulation is dependent on the Atg1-Atg13 complex, which plays a key role in a variety of cellular processes, including organization of the PAS and membrane retrieval in both the Cvt pathway and autophagy. Meanwhile, Atg1 homologues in *D. melanogaster*, *C. elegans* and mammals are involved in inhibiting cell growth and inducing apoptosis, in neuronal development, and in cytoskeletal organization by regulation of myosin II activity [23, 93-104, 247, 248]. Thus Atg1-Atg13 complex modulation of autophagy and cell growth may also rely on Atg1 kinase activity for regulation of autophagic receptors for targeting specific cargo.

A novel *in vitro* assay to study aggregation and recruitment of Atg proteins

Here we present a novel *in vitro* assay to investigate Cvt complex formation, in which both Atg19 and Atg8 assembly on aggregates is stable. This assay is physiologically relevant, since it utilizes lysates that still contain most cytosolic components: cells are densely lysed, so cellular components are only diluted in buffer by about a 1:3 ratio, and a low centrifugal speed is used for the removal of intact cells (1500 RCF for 1 minute). Furthermore, the choice of a 50mM-200mM potassium phosphate buffer, pH 7, ensures the ionic strength of the buffer is somewhat similar to cytosol: cytosolic concentration of potassium and phosphate has been measured to be 290-340mM and 10-75mM, respectively. Meanwhile, for additional free ions including sulfate, calcium, magnesium, sodium and chloride, when their concentration is added together it totals less than 30mM, which contributes little to the cytosolic ionic strength [201-213].

Already, *in vitro* assays have helped us elucidate the mechanism of Atg8 conjugation and of fusion between immature autophagosomes and endosomes [139, 249]. An *in vitro* assay of autophagic vesicle formation would help us better understand the mechanism of membrane recruitment and membrane fusion during autophagosome maturation. For this the Cvt complex could be used as a scaffold for recruitment of the autophagic machinery and membrane. Atg8 binding and its punctate and tubular localization on aggregates *in vitro* suggests that already autophagic proteins and membrane may be assembled on the Cvt complex in this assay (Fig. 5.3B).

Our understanding of the mechanism of Cvt vesicle formation, as summarized in Figure 6.2, was greatly furthered by this novel *in vitro* assay. The ability to visualize large aggregates *in vitro* helped determine the spherical structure of aggregates, which suggests they form a regular shaped structure that is critical for vacuolar transport, most likely serving as a scaffold for vesicle assembly. Also, the localization of Atg19 on large aggregates shows that Atg19 binds solely to the aggregate surface in order to initiate recruitment of the autophagic machinery. This assay also helped to determine what factors that mediate aggregation and Atg19 binding: the amphipathic helix-turn-helix propeptide of Ape1 and the coiled-coil of Atg19. The lack of Atg19 localization to prApe1 aggregates *in vitro* after starvation also helped identify the Atg1-Atg13 complex as a downregulator of Atg19 localization to aggregates upon induction of autophagy. In the future, determining why Atg19 and Atg8 assemble as punctate or tubular structures on the aggregate surface may be the next step in discovering how autophagic proteins can target a variety of cytoplasmic components, including organelles, protein aggregates, bacteria, and how they package them into a vesicle formed almost from scratch.

REFERENCES

1. Petrovski, G. and D.K. Das, *Does autophagy take a front seat in lifespan extension?* Journal of Cellular and Molecular Medicine, 2010. **14**(11): p. 2543-2551.
2. Di Bartolomeo, S., F. Nazio, and F. Cecconi, *The Role of Autophagy During Development in Higher Eukaryotes.* Traffic, 2010. **11**(10): p. 1280-1289.
3. Heath, R.J. and R.J. Xavier, *Autophagy, immunity and human disease.* Curr Opin Gastroenterol, 2009. **25**(6): p. 512-20.
4. Cecconi, F. and B. Levine, *The Role of Autophagy in Mammalian Development: Cell Makeover Rather than Cell Death.* Developmental Cell, 2008. **15**(3): p. 344-357.
5. Levine, B., N. Mizushima, and H.W. Virgin, *Autophagy in immunity and inflammation.* Nature, 2011. **469**(7330): p. 323-35.
6. Madeo, F., N. Tavernarakis, and G. Kroemer, *Can autophagy promote longevity?* Nat Cell Biol, 2010. **12**(9): p. 842-6.
7. Meijer, W.H., et al., *ATG genes involved in non-selective autophagy are conserved from yeast to man, but the selective Cvt and pexophagy pathways also require organism-specific genes.* Autophagy, 2007. **3**(2): p. 106-16.
8. Deretic, V. and D.J. Klionsky, *How cells clean house.* Sci Am, 2008. **298**(5): p. 74-81.
9. Lunemann, J.D., et al., *Beta-amyloid is a substrate of autophagy in sporadic inclusion body myositis.* Ann Neurol, 2007. **61**(5): p. 476-83.
10. Hayward, A.P., J. Tsao, and S.P. Dinesh-Kumar, *Autophagy and plant innate immunity: Defense through degradation.* Semin Cell Dev Biol, 2009. **20**(9): p. 1041-7.
11. Huang, T.H., et al., *Alternate aggregation pathways of the Alzheimer beta-amyloid peptide. An in vitro model of preamyloid.* The Journal of biological chemistry, 2000. **275**(46): p. 36436-40.
12. Davis-Salinas, J., et al., *Amyloid beta-protein induces its own production in cultured degenerating cerebrovascular smooth muscle cells.* J Neurochem, 1995. **65**(2): p. 931-4.
13. Williams, A., et al., *Aggregate-prone proteins are cleared from the cytosol by autophagy: therapeutic implications.* Curr Top Dev Biol, 2006. **76**: p. 89-101.
14. Ravikumar, B. and D.C. Rubinsztein, *Role of autophagy in the clearance of mutant huntingtin: a step towards therapy?* Mol Aspects Med, 2006. **27**(5-6): p. 520-7.
15. Winslow, A.R. and D.C. Rubinsztein, *Autophagy in neurodegeneration and development.* Biochim Biophys Acta, 2008. **1782**(12): p. 723-9.
16. Bjedov, I. and L. Partridge, *A longer and healthier life with TOR down-regulation: genetics and drugs.* Biochem Soc Trans, 2011. **39**(2): p. 460-5.

17. Katewa, S.D. and P. Kapahi, *Role of TOR signaling in aging and related biological processes in Drosophila melanogaster.* Exp Gerontol, 2011. **46**(5): p. 382-90.
18. Chaturvedi, A. and S.K. Pierce, *Autophagy in immune cell regulation and dysregulation.* Current allergy and asthma reports, 2009. **9**(5): p. 341-6.
19. Chen, Z.F., et al., *The double-edged effect of autophagy in pancreatic beta cells and diabetes.* Autophagy, 2011. **7**(1): p. 12-6.
20. Liu, B., et al., *Autophagic pathways as new targets for cancer drug development.* Acta Pharmacol Sin, 2010. **31**(9): p. 1154-1164.
21. White, E. and R.S. DiPaola, *The double-edged sword of autophagy modulation in cancer.* Clinical cancer research : an official journal of the American Association for Cancer Research, 2009. **15**(17): p. 5308-16.
22. Brech, A., et al., *Autophagy in tumour suppression and promotion.* Molecular oncology, 2009. **3**(4): p. 366-75.
23. Melendez, A., et al., *Autophagy genes are essential for dauer development and life-span extension in C. elegans.* Science, 2003. **301**(5638): p. 1387-91.
24. Mortensen, M., et al., *Loss of autophagy in erythroid cells leads to defective removal of mitochondria and severe anemia in vivo.* Proc Natl Acad Sci U S A, 2010. **107**(2): p. 832-7.
25. Tsukamoto, S., et al., *Autophagy is essential for preimplantation development of mouse embryos.* Science, 2008. **321**(5885): p. 117-20.
26. Suzuki, K., et al., *The pre-autophagosomal structure organized by concerted functions of APG genes is essential for autophagosome formation.* Embo J, 2001. **20**(21): p. 5971-81.
27. Komatsu, M., et al., *Essential role for autophagy protein Atg7 in the maintenance of axonal homeostasis and the prevention of axonal degeneration.* Proc Natl Acad Sci U S A, 2007. **104**(36): p. 14489-94.
28. Komatsu, M., et al., *Loss of autophagy in the central nervous system causes neurodegeneration in mice.* Nature, 2006. **441**(7095): p. 880-4.
29. Ohsumi, Y., *Molecular dissection of autophagy: two ubiquitin-like systems.* Nat Rev Mol Cell Biol, 2001. **2**(3): p. 211-6.
30. Kourtis, N. and N. Tavernarakis, *Autophagy and cell death in model organisms.* Cell death and differentiation, 2009. **16**(1): p. 21-30.
31. Nezis, I.P., et al., *Autophagy as a trigger for cell death: autophagic degradation of inhibitor of apoptosis dBruce controls DNA fragmentation during late oogenesis in Drosophila.* Autophagy, 2010. **6**(8): p. 1214-5.
32. Gao, W., et al., *Upregulation of human autophagy-initiation kinase ULK1 by tumor suppressor p53 contributes to DNA-damage-induced cell death.* Cell death and differentiation, 2011.
33. Xie, Z. and D.J. Klionsky, *Autophagosome formation: core machinery and adaptations.* Nat Cell Biol, 2007. **9**(10): p. 1102-9.
34. Lynch-Day, M.A. and D.J. Klionsky, *The Cvt pathway as a model for selective autophagy.* FEBS Lett, 2010. **584**(7): p. 1359-66.

35. Bjorkoy, G., et al., *p62/SQSTM1 forms protein aggregates degraded by autophagy and has a protective effect on huntingtin-induced cell death.* The Journal of Cell Biology, 2005. **171**(4): p. 603-14.
36. Pankiv, S., et al., *p62/SQSTM1 binds directly to Atg8/LC3 to facilitate degradation of ubiquitinated protein aggregates by autophagy.* J Biol Chem, 2007. **282**(33): p. 24131-45.
37. Kirkin, V., et al., *A role for NBR1 in autophagosomal degradation of ubiquitinated substrates.* Mol Cell, 2009. **33**(4): p. 505-16.
38. Novak, I., et al., *Nix is a selective autophagy receptor for mitochondrial clearance.* EMBO Rep, 2010. **11**(1): p. 45-51.
39. Schweers, R.L., et al., *NIX is required for programmed mitochondrial clearance during reticulocyte maturation.* Proc Natl Acad Sci U S A, 2007. **104**(49): p. 19500-5.
40. Wild, P., et al., *Phosphorylation of the Autophagy Receptor Optineurin Restricts Salmonella Growth.* Science, 2011. **333**(6039): p. 228-233.
41. Zheng, Y.T., et al., *The Adaptor Protein p62/SQSTM1 Targets Invading Bacteria to the Autophagy Pathway.* The Journal of Immunology, 2009. **183**(9): p. 5909-5916.
42. Thurston, T.L.M., et al., *The TBK1 adaptor and autophagy receptor NDP52 restricts the proliferation of ubiquitin-coated bacteria.* Nat Immunol, 2009. **10**(11): p. 1215-1221.
43. Talloczy, Z., H.W.t. Virgin, and B. Levine, *PKR-dependent autophagic degradation of herpes simplex virus type 1.* Autophagy, 2006. **2**(1): p. 24-9.
44. Pyo, J.O., et al., *Essential roles of Atg5 and FADD in autophagic cell death: dissection of autophagic cell death into vacuole formation and cell death.* The Journal of biological chemistry, 2005. **280**(21): p. 20722-9.
45. Huang, J., et al., *Antibacterial autophagy occurs at PI(3)P-enriched domains of the endoplasmic reticulum and requires Rab1 GTPase.* Autophagy, 2011. **7**(1): p. 17-26.
46. Shahnazari, S., et al., *A role for diacylglycerol in antibacterial autophagy.* Autophagy, 2011. **7**(3): p. 20-22.
47. Shahnazari, S., et al., *A diacylglycerol-dependent signaling pathway contributes to regulation of antibacterial autophagy.* Cell Host Microbe, 2010. **8**(2): p. 137-46.
48. Zheng, Y.T., et al., *The adaptor protein p62/SQSTM1 targets invading bacteria to the autophagy pathway.* J Immunol, 2009. **183**(9): p. 5909-16.
49. Noda, N.N., et al., *Structural basis of target recognition by Atg8/LC3 during selective autophagy.* Genes Cells, 2008. **13**(12): p. 1211-8.
50. Rabinowitz, J.D. and E. White, *Autophagy and Metabolism.* Science, 2010. **330**(6009): p. 1344-1348.
51. Farre, J.C., J. Vidal, and S. Subramani, *A cytoplasm to vacuole targeting pathway in P. pastoris.* Autophagy, 2007. **3**(3): p. 230-4.

52. Baba, M., et al., *Two distinct pathways for targeting proteins from the cytoplasm to the vacuole/lysosome.* The Journal of Cell Biology, 1997. **139**(7): p. 1687-95.
53. Hutchins, M.U. and D.J. Klionsky, *Vacuolar localization of oligomeric alpha-mannosidase requires the cytoplasm to vacuole targeting and autophagy pathway components in Saccharomyces cerevisiae.* The Journal of biological chemistry, 2001. **276**(23): p. 20491-8.
54. Scott, S.V., et al., *Aminopeptidase I is targeted to the vacuole by a nonclassical vesicular mechanism.* The Journal of Cell Biology, 1997. **138**(1): p. 37-44.
55. Shintani, T. and D.J. Klionsky, *Cargo proteins facilitate the formation of transport vesicles in the cytoplasm to vacuole targeting pathway.* The Journal of biological chemistry, 2004. **279**(29): p. 29889-94.
56. Yuga, M., et al., *Aspartyl Aminopeptidase Is Imported from the Cytoplasm to the Vacuole by Selective Autophagy in Saccharomyces cerevisiae.* The Journal of biological chemistry, 2011. **286**(15): p. 13704-13.
57. Kageyama, T., K. Suzuki, and Y. Ohsumi, *Lap3 is a selective target of autophagy in yeast, Saccharomyces cerevisiae.* Biochemical and biophysical research communications, 2009. **378**(3): p. 551-557.
58. Adachi, W., et al., *Crystallization of Saccharomyces cerevisiae aminopeptidase 1, the major cargo protein of the Cvt pathway.* Acta Crystallogr Sect F Struct Biol Cryst Commun, 2007. **63**(Pt 3): p. 200-3.
59. Scott, S.V., et al., *Cvt19 Is a Receptor for the Cytoplasm-to-Vacuole Targeting Pathway.* Molecular cell, 2001. **7**(6): p. 1131-1141.
60. Kumeta, H., et al., *The NMR structure of the autophagy-related protein Atg8.* Journal of biomolecular NMR, 2010. **47**(3): p. 237-41.
61. Nakatogawa, H., Y. Ichimura, and Y. Ohsumi, *Atg8, a ubiquitin-like protein required for autophagosome formation, mediates membrane tethering and hemifusion.* Cell, 2007. **130**(1): p. 165-78.
62. Yorimitsu, T. and D.J. Klionsky, *Atg11 links cargo to the vesicle-forming machinery in the cytoplasm to vacuole targeting pathway.* Molecular biology of the cell, 2005. **16**(4): p. 1593-605.
63. Kim, J., et al., *Convergence of multiple autophagy and cytoplasm to vacuole targeting components to a perivacuolar membrane compartment prior to de novo vesicle formation.* The Journal of biological chemistry, 2002. **277**(1): p. 763-73.
64. Kim, J., et al., *Transport of a large oligomeric protein by the cytoplasm to vacuole protein targeting pathway.* The Journal of Cell Biology, 1997. **137**(3): p. 609-18.
65. Metz, G., R. Marx, and K.H. Rohm, *The quaternary structure of yeast aminopeptidase I. 1. Molecular forms and subunit size.* Z Naturforsch C, 1977. **32**(11-12): p. 929-37.
66. Andrei-Selmer, C., et al., *A new class of mutants deficient in dodecamerization of aminopeptidase 1 and vacuolar transport.* The Journal of biological chemistry, 2001. **276**(15): p. 11606-14.

67. Chang, Y.H. and J.A. Smith, *Molecular cloning and sequencing of genomic DNA encoding aminopeptidase I from Saccharomyces cerevisiae.* The Journal of biological chemistry, 1989. **264**(12): p. 6979-83.
68. Cueva, R., N. Garcia-Alvarez, and P. Suarez-Rendueles, *Yeast vacuolar aminopeptidase yscI. Isolation and regulation of the APE1 (LAP4) structural gene.* FEBS Lett, 1989. **259**(1): p. 125-9.
69. Oda, M.N., et al., *Identification of a cytoplasm to vacuole targeting determinant in aminopeptidase I.* The Journal of Cell Biology, 1996. **132**(6): p. 999-1010.
70. Martinez, E., et al., *Folding of the presequence of yeast pAPI into an amphipathic helix determines transport of the protein from the cytosol to the vacuole.* J Mol Biol, 1997. **267**(5): p. 1124-38.
71. Schu, P., *Aminopeptidase I enzymatic activity.* Methods Enzymol, 2008. **451**: p. 67-78.
72. Suzuki, K., et al., *Selective transport of alpha-mannosidase by autophagic pathways: identification of a novel receptor, Atg34p.* The Journal of biological chemistry, 2010. **285**(39): p. 30019-25.
73. Noda, T. and Y. Ohsumi, *Tor, a phosphatidylinositol kinase homologue, controls autophagy in yeast.* The Journal of biological chemistry, 1998. **273**(7): p. 3963-6.
74. Dann, S.G. and G. Thomas, *The amino acid sensitive TOR pathway from yeast to mammals.* FEBS Lett, 2006. **580**(12): p. 2821-9.
75. Neufeld, T.P., *TOR-dependent control of autophagy: biting the hand that feeds.* Current opinion in cell biology, 2010. **22**(2): p. 157-68.
76. Chang, Y.Y. and T.P. Neufeld, *An Atg1/Atg13 complex with multiple roles in TOR-mediated autophagy regulation.* Molecular biology of the cell, 2009. **20**(7): p. 2004-14.
77. Kamada, Y., et al., *Tor-mediated induction of autophagy via an Apg1 protein kinase complex.* The Journal of Cell Biology, 2000. **150**(6): p. 1507-13.
78. Kamada, Y., et al., *Tor directly controls the Atg1 kinase complex to regulate autophagy.* Molecular and cellular biology, 2010. **30**(4): p. 1049-58.
79. Stephan, J.S., et al., *The Tor and PKA signaling pathways independently target the Atg1/Atg13 protein kinase complex to control autophagy.* Proc Natl Acad Sci U S A, 2009. **106**(40): p. 17049-54.
80. Kamada, Y., *Prime-numbered Atg proteins act at the primary step in autophagy: unphosphorylatable Atg13 can induce autophagy without TOR inactivation.* Autophagy, 2010. **6**(3): p. 415-6.
81. Cheong, H., et al., *Atg17 regulates the magnitude of the autophagic response.* Molecular biology of the cell, 2005. **16**(7): p. 3438-53.
82. Kabeya, Y., et al., *Atg17 functions in cooperation with Atg1 and Atg13 in yeast autophagy.* Molecular biology of the cell, 2005. **16**(5): p. 2544-53.
83. Kabeya, Y., et al., *Characterization of the Atg17-Atg29-Atg31 complex specifically required for starvation-induced autophagy in Saccharomyces cerevisiae.* Biochemical and biophysical research communications, 2009. **389**(4): p. 612-5.

84. Sekito, T., et al., *Atg17 recruits Atg9 to organize the pre-autophagosomal structure.* Genes to cells : devoted to molecular & cellular mechanisms, 2009. **14**(5): p. 525-38.
85. Cheong, H., et al., *The Atg1 Kinase Complex Is Involved in the Regulation of Protein Recruitment to Initiate Sequestering Vesicle Formation for Nonspecific Autophagy in Saccharomyces cerevisiae.* Mol. Biol. Cell, 2008. **19**(2): p. 668-681.
86. Kawamata, T., et al., *Characterization of a novel autophagy-specific gene, ATG29.* Biochemical and biophysical research communications, 2005. **338**(4): p. 1884-9.
87. Matsuura, A., et al., *Apg1p, a novel protein kinase required for the autophagic process in Saccharomyces cerevisiae.* Gene, 1997. **192**(2): p. 245-50.
88. Nice, D.C., et al., *Cooperative binding of the cytoplasm to vacuole targeting pathway proteins, Cvt13 and Cvt20, to phosphatidylinositol 3-phosphate at the pre-autophagosomal structure is required for selective autophagy.* The Journal of biological chemistry, 2002. **277**(33): p. 30198-207.
89. Reggiori, F., et al., *The Atg1-Atg13 complex regulates Atg9 and Atg23 retrieval transport from the pre-autophagosomal structure.* Dev Cell, 2004. **6**(1): p. 79-90.
90. Suzuki, K., et al., *Hierarchy of Atg proteins in pre-autophagosomal structure organization.* Genes to cells : devoted to molecular & cellular mechanisms, 2007. **12**(2): p. 209-18.
91. Kawamata, T., et al., *Organization of the pre-autophagosomal structure responsible for autophagosome formation.* Molecular biology of the cell, 2008. **19**(5): p. 2039-50.
92. Scott, S.V., et al., *Apg13p and Vac8p are part of a complex of phosphoproteins that are required for cytoplasm to vacuole targeting.* The Journal of biological chemistry, 2000. **275**(33): p. 25840-9.
93. Ogura, K., et al., *Caenorhabditis elegans unc-51 gene required for axonal elongation encodes a novel serine/threonine kinase.* Genes Dev, 1994. **8**(20): p. 2389-400.
94. Dunlop, E.A., et al., *ULK1 inhibits mTORC1 signaling, promotes multisite Raptor phosphorylation and hinders substrate binding.* Autophagy, 2011. **7**(7).
95. Egan, D., et al., *The autophagy initiating kinase ULK1 is regulated via opposing phosphorylation by AMPK and mTOR.* Autophagy, 2011. **7**(6).
96. Ganley, I.G., et al., *ULK1.ATG13.FIP200 complex mediates mTOR signaling and is essential for autophagy.* The Journal of biological chemistry, 2009. **284**(18): p. 12297-305.
97. Jung, C.H., et al., *ULK-Atg13-FIP200 complexes mediate mTOR signaling to the autophagy machinery.* Molecular biology of the cell, 2009. **20**(7): p. 1992-2003.
98. Kim, J. and K.L. Guan, *Regulation of the autophagy initiating kinase ULK1 by nutrients: Roles of mTORC1 and AMPK.* Cell Cycle, 2011. **10**(9).
99. Loffler, A.S., et al., *Ulk1-mediated phosphorylation of AMPK constitutes a negative regulatory feedback loop.* Autophagy, 2011. **7**(7).

100. Chan, E.Y. and S.A. Tooze, *Evolution of Atg1 function and regulation.* Autophagy, 2009. **5**(6): p. 758-65.
101. Hosokawa, N., et al., *Nutrient-dependent mTORC1 association with the ULK1-Atg13-FIP200 complex required for autophagy.* Molecular biology of the cell, 2009. **20**(7): p. 1981-91.
102. Mao, K. and D.J. Klionsky, *AMPK Activates Autophagy by Phosphorylating ULK1.* Circulation research, 2011. **108**(7): p. 787-8.
103. Mercer, C.A., A. Kaliappan, and P.B. Dennis, *A novel, human Atg13 binding protein, Atg101, interacts with ULK1 and is essential for macroautophagy.* Autophagy, 2009. **5**(5): p. 649-62.
104. Chan, E.Y., et al., *Kinase-inactivated ULK proteins inhibit autophagy via their conserved C-terminal domains using an Atg13-independent mechanism.* Molecular and cellular biology, 2009. **29**(1): p. 157-71.
105. Abeliovich, H., et al., *Chemical genetic analysis of Apg1 reveals a non-kinase role in the induction of autophagy.* Molecular biology of the cell, 2003. **14**(2): p. 477-90.
106. Tooze, S.A. and T. Yoshimori, *The origin of the autophagosomal membrane.* Nature cell biology, 2010. **12**(9): p. 831-5.
107. Juhasz, G. and T.P. Neufeld, *Autophagy: a forty-year search for a missing membrane source.* PLoS Biol, 2006. **4**(2): p. e36.
108. Mari, M., et al., *An Atg9-containing compartment that functions in the early steps of autophagosome biogenesis.* The Journal of Cell Biology, 2010. **190**(6): p. 1005-22.
109. Mari, M. and F. Reggiori, *Atg9 trafficking in the yeast Saccharomyces cerevisiae.* Autophagy, 2007. **3**(2): p. 145-8.
110. Mari, M. and F. Reggiori, *Atg9 reservoirs, a new organelle of the yeast endomembrane system?* Autophagy, 2010. **6**(8): p. 1221-3.
111. Geng, J., et al., *Post-Golgi Sec proteins are required for autophagy in Saccharomyces cerevisiae.* Molecular biology of the cell, 2010. **21**(13): p. 2257-69.
112. van der Vaart, A., J. Griffith, and F. Reggiori, *Exit from the Golgi is required for the expansion of the autophagosomal phagophore in yeast Saccharomyces cerevisiae.* Mol Biol Cell, 2010. **21**(13): p. 2270-84.
113. Yen, W.L., et al., *The conserved oligomeric Golgi complex is involved in double-membrane vesicle formation during autophagy.* The Journal of Cell Biology, 2010. **188**(1): p. 101-14.
114. van der Vaart, A. and F. Reggiori, *The Golgi complex as a source for yeast autophagosomal membranes.* Autophagy, 2010. **6**(6): p. 800-1.
115. Barrowman, J., et al., *TRAPP complexes in membrane traffic: convergence through a common Rab.* Nat Rev Mol Cell Biol, 2010. **11**(11): p. 759-763.
116. Lynch-Day, M.A., et al., *Trs85 directs a Ypt1 GEF, TRAPPIII, to the phagophore to promote autophagy.* Proceedings of the National Academy of Sciences, 2010. **107**(17): p. 7811-7816.

117. Axe, E.L., et al., *Autophagosome formation from membrane compartments enriched in phosphatidylinositol 3-phosphate and dynamically connected to the endoplasmic reticulum.* The Journal of Cell Biology, 2008. **182**(4): p. 685-701.
118. Matsunaga, K., et al., *Autophagy requires endoplasmic reticulum targeting of the PI3-kinase complex via Atg14L.* The Journal of Cell Biology, 2010. **190**(4): p. 511-21.
119. Matsunaga, K., et al., *Two Beclin 1-binding proteins, Atg14L and Rubicon, reciprocally regulate autophagy at different stages.* Nature cell biology, 2009. **11**(4): p. 385-96.
120. Yla-Anttila, P., et al., *3D tomography reveals connections between the phagophore and endoplasmic reticulum.* Autophagy, 2009. **5**(8): p. 1180-5.
121. Hailey, D.W., et al., *Mitochondria supply membranes for autophagosome biogenesis during starvation.* Cell, 2010. **141**(4): p. 656-67.
122. Ravikumar, B., et al., *Plasma membrane contributes to the formation of pre-autophagosomal structures.* Nat Cell Biol, 2010. **12**(8): p. 747-757.
123. Kametaka, S., et al., *Apg14p and Apg6/Vps30p form a protein complex essential for autophagy in the yeast, Saccharomyces cerevisiae.* The Journal of biological chemistry, 1998. **273**(35): p. 22284-91.
124. Kihara, A., et al., *Two distinct Vps34 phosphatidylinositol 3-kinase complexes function in autophagy and carboxypeptidase Y sorting in Saccharomyces cerevisiae.* The Journal of Cell Biology, 2001. **152**(3): p. 519-30.
125. Obara, K., T. Sekito, and Y. Ohsumi, *Assortment of phosphatidylinositol 3-kinase complexes--Atg14p directs association of complex I to the pre-autophagosomal structure in Saccharomyces cerevisiae.* Molecular biology of the cell, 2006. **17**(4): p. 1527-39.
126. Levine, B., S. Sinha, and G. Kroemer, *Bcl-2 family members: dual regulators of apoptosis and autophagy.* Autophagy, 2008. **4**(5): p. 600-6.
127. Furuya, N., et al., *The evolutionarily conserved domain of Beclin 1 is required for Vps34 binding, autophagy and tumor suppressor function.* Autophagy, 2005. **1**(1): p. 46-52.
128. Fimia, G.M., et al., *Ambra1 regulates autophagy and development of the nervous system.* Nature, 2007. **447**(7148): p. 1121-5.
129. Schu, P.V., et al., *Phosphatidylinositol 3-kinase encoded by yeast VPS34 gene essential for protein sorting.* Science, 1993. **260**(5104): p. 88-91.
130. Stack, J.H. and S.D. Emr, *Vps34p required for yeast vacuolar protein sorting is a multiple specificity kinase that exhibits both protein kinase and phosphatidylinositol-specific PI 3-kinase activities.* The Journal of biological chemistry, 1994. **269**(50): p. 31552-62.
131. Stack, J.H., et al., *Vesicle-mediated protein transport: regulatory interactions between the Vps15 protein kinase and the Vps34 PtdIns 3-kinase essential for protein sorting to the vacuole in yeast.* The Journal of Cell Biology, 1995. **129**(2): p. 321-34.

132. Herman, P.K., J.H. Stack, and S.D. Emr, *A genetic and structural analysis of the yeast Vps15 protein kinase: evidence for a direct role of Vps15p in vacuolar protein delivery.* Embo J, 1991. **10**(13): p. 4049-60.
133. Obara, K. and Y. Ohsumi, *PtdIns 3-Kinase Orchestrates Autophagosome Formation in Yeast.* Journal of lipids, 2011. **2011**: p. 498768.
134. Harding, T.M., et al., *Isolation and characterization of yeast mutants in the cytoplasm to vacuole protein targeting pathway.* The Journal of Cell Biology, 1995. **131**(3): p. 591-602.
135. Stromhaug, P.E., et al., *Atg21 is a phosphoinositide binding protein required for efficient lipidation and localization of Atg8 during uptake of aminopeptidase I by selective autophagy.* Molecular biology of the cell, 2004. **15**(8): p. 3553-66.
136. Krick, R., et al., *The relevance of the phosphatidylinositolphosphat-binding motif FRRGT of Atg18 and Atg21 for the Cvt pathway and autophagy.* FEBS Lett, 2006. **580**(19): p. 4632-8.
137. Efe, J.A., R.J. Botelho, and S.D. Emr, *Atg18 regulates organelle morphology and Fab1 kinase activity independent of its membrane recruitment by phosphatidylinositol 3,5-bisphosphate.* Molecular biology of the cell, 2007. **18**(11): p. 4232-44.
138. Obara, K., et al., *The Atg18-Atg2 complex is recruited to autophagic membranes via phosphatidylinositol 3-phosphate and exerts an essential function.* The Journal of biological chemistry, 2008. **283**(35): p. 23972-80.
139. Ichimura, Y., et al., *In vivo and in vitro reconstitution of Atg8 conjugation essential for autophagy.* The Journal of biological chemistry, 2004. **279**(39): p. 40584-92.
140. Noda, N.N., Y. Ohsumi, and F. Inagaki, *Atg8-family interacting motif crucial for selective autophagy.* FEBS Letters, 2010. **584**(7): p. 1379-85.
141. Xie, Z., U. Nair, and D.J. Klionsky, *Atg8 controls phagophore expansion during autophagosome formation.* Molecular biology of the cell, 2008. **19**(8): p. 3290-8.
142. Hanada, T., et al., *The Atg12-Atg5 conjugate has a novel E3-like activity for protein lipidation in autophagy.* The Journal of biological chemistry, 2007. **282**(52): p. 37298-302.
143. Reggiori, F., et al., *Atg9 cycles between mitochondria and the pre-autophagosomal structure in yeasts.* Autophagy, 2005. **1**(2): p. 101-9.
144. He, C., et al., *Recruitment of Atg9 to the preautophagosomal structure by Atg11 is essential for selective autophagy in budding yeast.* The Journal of Cell Biology, 2006. **175**(6): p. 925-35.
145. Munakata, N. and D.J. Klionsky, *"Autophagy suite": Atg9 cycling in the cytoplasm to vacuole targeting pathway.* Autophagy, 2010. **6**(6): p. 679-85.
146. Reggiori, F., et al., *The actin cytoskeleton is required for selective types of autophagy, but not nonspecific autophagy, in the yeast Saccharomyces cerevisiae.* Mol Biol Cell, 2005. **16**(12): p. 5843-56.
147. Krick, R., et al., *Dissecting the localization and function of Atg18, Atg21 and Ygr223c.* Autophagy, 2008. **4**(7): p. 896-910.

148. He, C., M. Baba, and D.J. Klionsky, *Double duty of Atg9 self-association in autophagosome biogenesis.* Autophagy, 2009. **5**(3): p. 385-7.
149. Meiling-Wesse, K., F. Bratsika, and M. Thumm, *ATG23, a novel gene required for maturation of proaminopeptidase I, but not for autophagy.* FEMS Yeast Res, 2004. **4**(4-5): p. 459-65.
150. Tucker, K.A., et al., *Atg23 is essential for the cytoplasm to vacuole targeting pathway and efficient autophagy but not pexophagy.* The Journal of biological chemistry, 2003. **278**(48): p. 48445-52.
151. Yen, W.L. and D.J. Klionsky, *Atg27 is a second transmembrane cycling protein.* Autophagy, 2007. **3**(3): p. 254-6.
152. Yen, W.L., et al., *Atg27 is required for autophagy-dependent cycling of Atg9.* Molecular biology of the cell, 2007. **18**(2): p. 581-93.
153. Ichimura, Y., et al., *A ubiquitin-like system mediates protein lipidation.* Nature, 2000. **408**(6811): p. 488-92.
154. Kim, J., W.P. Huang, and D.J. Klionsky, *Membrane recruitment of Aut7p in the autophagy and cytoplasm to vacuole targeting pathways requires Aut1p, Aut2p, and the autophagy conjugation complex.* The Journal of Cell Biology, 2001. **152**(1): p. 51-64.
155. Noda, N.N., et al., *Crystallization of the Atg12-Atg5 conjugate bound to Atg16 by the free-interface diffusion method.* J Synchrotron Radiat, 2008. **15**(Pt 3): p. 266-8.
156. Kim, J., et al., *Apg7p/Cvt2p is required for the cytoplasm-to-vacuole targeting, macroautophagy, and peroxisome degradation pathways.* Molecular biology of the cell, 1999. **10**(5): p. 1337-51.
157. Tanida, I., et al., *Apg7p/Cvt2p: A novel protein-activating enzyme essential for autophagy.* Molecular biology of the cell, 1999. **10**(5): p. 1367-79.
158. Yuan, W., P.E. Stromhaug, and W.A. Dunn, Jr., *Glucose-induced autophagy of peroxisomes in Pichia pastoris requires a unique E1-like protein.* Molecular biology of the cell, 1999. **10**(5): p. 1353-66.
159. Hanada, T., et al., *The amino-terminal region of Atg3 is essential for association with phosphatidylethanolamine in Atg8 lipidation.* FEBS Letters, 2009. **583**(7): p. 1078-1083.
160. Yamaguchi, M., et al., *Autophagy-related protein 8 (Atg8) family interacting motif in Atg3 mediates the Atg3-Atg8 interaction and is crucial for the cytoplasm-to-vacuole targeting pathway.* The Journal of biological chemistry, 2010. **285**(38): p. 29599-607.
161. Shintani, T., et al., *Apg10p, a novel protein-conjugating enzyme essential for autophagy in yeast.* EMBO J, 1999. **18**(19): p. 5234-41.
162. Kuma, A., et al., *Formation of the approximately 350-kDa Apg12-Apg5.Apg16 multimeric complex, mediated by Apg16 oligomerization, is essential for autophagy in yeast.* The Journal of biological chemistry, 2002. **277**(21): p. 18619-25.

163. Mizushima, N., T. Noda, and Y. Ohsumi, *Apg16p is required for the function of the Apg12p-Apg5p conjugate in the yeast autophagy pathway.* EMBO J, 1999. **18**(14): p. 3888-96.
164. He, C. and D.J. Klionsky, *Atg9 trafficking in autophagy-related pathways.* Autophagy, 2007. **3**(3): p. 271-4.
165. Yen, W.L., et al., *Atg27 is required for autophagy-dependent cycling of Atg9.* Mol Biol Cell, 2007. **18**(2): p. 581-93.
166. Sato, T.K., et al., *Class C Vps protein complex regulates vacuolar SNARE pairing and is required for vesicle docking/fusion.* Mol Cell, 2000. **6**(3): p. 661-71.
167. Darsow, T., S.E. Rieder, and S.D. Emr, *A multispecificity syntaxin homologue, Vam3p, essential for autophagic and biosynthetic protein transport to the vacuole.* The Journal of Cell Biology, 1997. **138**(3): p. 517-29.
168. Fischer von Mollard, G. and T.H. Stevens, *The Saccharomyces cerevisiae v-SNARE Vti1p is required for multiple membrane transport pathways to the vacuole.* Mol Biol Cell, 1999. **10**(6): p. 1719-32.
169. Sato, T.K., T. Darsow, and S.D. Emr, *Vam7p, a SNAP-25-like molecule, and Vam3p, a syntaxin homolog, function together in yeast vacuolar protein trafficking.* Molecular and cellular biology, 1998. **18**(9): p. 5308-19.
170. Polupanov, A.S., V.Y. Nazarko, and A.A. Sibirny, *CCZ1, MON1 and YPT7 genes are involved in pexophagy, the Cvt pathway and non-specific macroautophagy in the methylotrophic yeast Pichia pastoris.* Cell biology international, 2011. **35**(4): p. 311-9.
171. Wang, C.W., et al., *Yeast homotypic vacuole fusion requires the Ccz1-Mon1 complex during the tethering/docking stage.* The Journal of Cell Biology, 2003. **163**(5): p. 973-85.
172. Wang, C.W., et al., *The Ccz1-Mon1 protein complex is required for the late step of multiple vacuole delivery pathways.* The Journal of biological chemistry, 2002. **277**(49): p. 47917-27.
173. Nordmann, M., et al., *The Mon1-Ccz1 complex is the GEF of the late endosomal Rab7 homolog Ypt7.* Curr Biol, 2010. **20**(18): p. 1654-9.
174. Ishihara, N., et al., *Autophagosome requires specific early Sec proteins for its formation and NSF/SNARE for vacuolar fusion.* Mol Biol Cell, 2001. **12**(11): p. 3690-702.
175. Teter, S.A., et al., *Degradation of lipid vesicles in the yeast vacuole requires function of Cvt17, a putative lipase.* The Journal of biological chemistry, 2001. **276**(3): p. 2083-7.
176. Epple, U.D., E.L. Eskelinen, and M. Thumm, *Intravacuolar membrane lysis in Saccharomyces cerevisiae. Does vacuolar targeting of Cvt17/Aut5p affect its function?* The Journal of biological chemistry, 2003. **278**(10): p. 7810-21.
177. Epple, U.D., et al., *Aut5/Cvt17p, a putative lipase essential for disintegration of autophagic bodies inside the vacuole.* J Bacteriol, 2001. **183**(20): p. 5942-55.
178. Yang, Z., et al., *Atg22 recycles amino acids to link the degradative and recycling functions of autophagy.* Mol Biol Cell, 2006. **17**(12): p. 5094-104.

179. King, J.S. and R.H. Insall, *Autophagy and cellular adaptation to mechanical stress in Dictyostelium and mammalian cells.* Autophagy Keystone Symposia, 2011.
180. Bernales, S., S. Schuck, and P. Walter, *ER-phagy: selective autophagy of the endoplasmic reticulum.* Autophagy, 2007. **3**(3): p. 285-7.
181. Jimenez, A., et al., *Selective recruitment of autophagic machineries upon targeted damage of trafficking organelles.* Autophagy Keystone Symposia, 2011.
182. Hutchins, M.U., M. Veenhuis, and D.J. Klionsky, *Peroxisome degradation in Saccharomyces cerevisiae is dependent on machinery of macroautophagy and the Cvt pathway.* Journal of cell science, 1999. **112 (Pt 22)**: p. 4079-87.
183. Dunn, W.A., Jr., et al., *Pexophagy: the selective autophagy of peroxisomes.* Autophagy, 2005. **1**(2): p. 75-83.
184. Monastyrska, I., et al., *The Hansenula polymorpha ATG25 gene encodes a novel coiled-coil protein that is required for macropexophagy.* Autophagy, 2005. **1**(2): p. 92-100.
185. Massey, A., R. Kiffin, and A.M. Cuervo, *Pathophysiology of chaperone-mediated autophagy.* Int J Biochem Cell Biol, 2004. **36**(12): p. 2420-34.
186. Santambrogio, L. and A.M. Cuervo, *Chasing the elusive mammalian microautophagy.* Autophagy, 2011. **7**(6).
187. Cemma, M., P.K. Kim, and J.H. Brumell, *The ubiquitin-binding adaptor proteins p62/SQSTM1 and NDP52 are recruited independently to bacteria-associated microdomains to target Salmonella to the autophagy pathway.* Autophagy, 2011. **7**(3): p. 22-26.
188. Codogno, P. and A.J. Meijer, *Atg5: more than an autophagy factor.* Nat Cell Biol, 2006. **8**(10): p. 1045-1047.
189. Banta, L.M., et al., *Organelle assembly in yeast: characterization of yeast mutants defective in vacuolar biogenesis and protein sorting.* J. Cell Biol, 1988. **107**(4): p. 1369-83.
190. Wang, H., et al., *The purification of human urinary kallikrein with ion-exchange radial flow membrane chromatography.* Biomed Chromatogr, 1996. **10**(3): p. 139-43.
191. Sans, N., et al., *Synapse-associated protein 97 selectively associates with a subset of AMPA receptors early in their biosynthetic pathway.* J Neurosci, 2001. **21**(19): p. 7506-16.
192. James, P., J. Halladay, and E.A. Craig, *Genomic libraries and a host strain designed for highly efficient two-hybrid selection in yeast.* Genetics, 1996. **144**(4): p. 1425-36.
193. Hofmeister, F., *Zur Lehre von der Wirkung der Salze [Title translation: About the science of the effect of salts.]*. Arch Exp Pathol Pharmakol, 1888. **24**: p. 247–260.
194. Moelbert, S., B. Normand, and P. De Los Rios, *Kosmotropes and chaotropes: modelling preferential exclusion, binding and aggregate stability.* Biophys Chem, 2004. **112**(1): p. 45-57.

195. Perez-Jimenez, R., et al., *The efficiency of different salts to screen charge interactions in proteins: a Hofmeister effect?* Biophys J, 2004. **86**(4): p. 2414-29.
196. Zhou, H.X., *Interactions of macromolecules with salt ions: an electrostatic theory for the Hofmeister effect.* Proteins, 2005. **61**(1): p. 69-78.
197. Vrbka, L., et al., *Specific ion effects at protein surfaces: a molecular dynamics study of bovine pancreatic trypsin inhibitor and horseradish peroxidase in selected salt solutions.* J Phys Chem B, 2006. **110**(13): p. 7036-43.
198. Broering, J.M. and A.S. Bommarius, *Evaluation of Hofmeister effects on the kinetic stability of proteins.* J Phys Chem B, 2005. **109**(43): p. 20612-9.
199. Collins, K.D., *Ions from the Hofmeister series and osmolytes: effects on proteins in solution and in the crystallization process.* Methods, 2004. **34**(3): p. 300-11.
200. Lang, F., *Mechanisms and significance of cell volume regulation.* J Am Coll Nutr, 2007. **26**(5 Suppl): p. 613S-623S.
201. van Eunen, K., et al., *Measuring enzyme activities under standardized in vivo-like conditions for systems biology.* FEBS Journal, 2010. **277**(3): p. 749-760.
202. Olz, R., et al., *Energy flux and osmoregulation of Saccharomyces cerevisiae grown in chemostats under NaCl stress.* J Bacteriol, 1993. **175**(8): p. 2205-13.
203. Roomans, G.M. and L.A. Seveus, *Subcellular localization of diffusible ions in the yeast Saccharomyces cerevisiae: quantitative microprobe analysis of thin freeze-dried sections.* J Cell Sci, 1976. **21**(1): p. 119-27.
204. Sunder, S., et al., *Regulation of intracellular level of Na+, K+ and glycerol in Saccharomyces cerevisiae under osmotic stress.* Mol Cell Biochem, 1996. **158**(2): p. 121-4.
205. Gonzalez, B., et al., *Dynamic in vivo (31)P nuclear magnetic resonance study of Saccharomyces cerevisiae in glucose-limited chemostat culture during the aerobic-anaerobic shift.* Yeast, 2000. **16**(6): p. 483-97.
206. Greenfield, N.J., M. Hussain, and J. Lenard, *Effects of growth state and amines on cytoplasmic and vacuolar pH, phosphate and polyphosphate levels in Saccharomyces cerevisiae: a 31P-nuclear magnetic resonance study.* Biochim Biophys Acta, 1987. **926**(3): p. 205-14.
207. Theobald, U., J. Mohns, and M. Rizzi, *Determination of in-vivo cytoplasmic orthophosphate concentration in yeast.* Biotechnology Techniques, 1996. **10**(5): p. 297-302.
208. Beeler, T., K. Bruce, and T. Dunn, *Regulation of cellular Mg2+ by Saccharomyces cerevisiae.* Biochim Biophys Acta, 1997. **1323**(2): p. 310-8.
209. Tunnicliffe, H.E., *Glutathione: The Occurrence and Quantitative Estimation of Glutathione in Tissues.* Biochem J, 1925. **19**(2): p. 194-8.
210. Elskens, M.T., C.J. Jaspers, and M.J. Penninckx, *Glutathione as an endogenous sulphur source in the yeast Saccharomyces cerevisiae.* Journal of General Microbiology, 1991. **137**(3): p. 637-644.
211. Okorokov, L.A., et al., *Ca(2+)-transporting ATPase(s) of the reticulum type in intracellular membranes of Saccharomyces cerevisiae: biochemical identification.* FEMS Microbiol Lett, 1997. **146**(1): p. 39-46.

212. Eilam, Y., *Studies on calcium efflux in the yeast Saccharomyces cerevisiae.* Microbios, 1982. **35**(140): p. 99-110.
213. Coury, L.A., et al., *The yeast Saccharomyces cerevisiae does not sequester chloride but can express a functional mammalian chloride channel.* FEMS Microbiol Lett, 1999. **179**(2): p. 327-332.
214. Chang, Y.H. and J.A. Smith, *Molecular cloning and sequencing of genomic DNA encoding aminopeptidase I from Saccharomyces cerevisiae.* J Biol Chem, 1989. **264**(12): p. 6979-83.
215. Andrei-Selmer, C., et al., *A new class of mutants deficient in dodecamerization of aminopeptidase 1 and vacuolar transport.* J Biol Chem, 2001. **276**(15): p. 11606-14.
216. Kim, J., et al., *Transport of a large oligomeric protein by the cytoplasm to vacuole protein targeting pathway.* J Cell Biol, 1997. **137**(3): p. 609-18.
217. Min, T., Gorman, J., Shapiro, L., *The crystal structure of aminopeptidase I (yscI) from Borrelia burgdorferi.* PDB ID 1y7e.
218. Oda, M.N., et al., *Identification of a cytoplasm to vacuole targeting determinant in aminopeptidase I.* J Cell Biol, 1996. **132**(6): p. 999-1010.
219. Shintani, T., et al., *Mechanism of cargo selection in the cytoplasm to vacuole targeting pathway.* Dev Cell, 2002. **3**(6): p. 825-37.
220. Watanabe, Y., et al., *Selective transport of alpha-mannosidase by autophagic pathways: structural basis for cargo recognition by Atg19 and Atg34.* The Journal of biological chemistry, 2010. **285**(39): p. 30026-33.
221. Ptacek, J., et al., *Global analysis of protein phosphorylation in yeast.* Nature, 2005. **438**(7068): p. 679-84.
222. Haji-Akbari, A., et al., *Disordered, quasicrystalline and crystalline phases of densely packed tetrahedra.* Nature, 2009. **462**(7274): p. 773-7.
223. Kuhn, R.J. and M.G. Rossmann, *Structure and assembly of icosahedral enveloped RNA viruses.* Adv Virus Res, 2005. **64**: p. 263-84.
224. Newcomb, W.W., et al., *Assembly of the herpes simplex virus capsid: characterization of intermediates observed during cell-free capsid formation.* J Mol Biol, 1996. **263**(3): p. 432-46.
225. Fornasari, M.S., et al., *Sequence determinants of quaternary structure in lumazine synthase.* Mol Biol Evol, 2004. **21**(1): p. 97-107.
226. Milne, J.L., et al., *Molecular architecture and mechanism of an icosahedral pyruvate dehydrogenase complex: a multifunctional catalytic machine.* EMBO J, 2002. **21**(21): p. 5587-98.
227. Walz, J., et al., *Tricorn protease exists as an icosahedral supermolecule in vivo.* Mol Cell, 1997. **1**(1): p. 59-65.
228. Hino, T., et al., *An icosahedral assembly of the light-harvesting chlorophyll a/b protein complex from pea chloroplast thylakoid membranes.* Acta Crystallogr D Biol Crystallogr, 2004. **60**(Pt 5): p. 803-9.
229. Baumeister, W. and A.C. Steven, *Macromolecular electron microscopy in the era of structural genomics.* Trends Biochem Sci, 2000. **25**(12): p. 624-31.

230. Kentsis, A. and K.L. Borden, *Physical mechanisms and biological significance of supramolecular protein self-assembly.* Curr Protein Pept Sci, 2004. **5**(2): p. 125-34.
231. Crowther, R.A. and B.M. Pearse, *Assembly and packing of clathrin into coats.* J Cell Biol, 1981. **91**(3 Pt 1): p. 790-7.
232. Raman, S., et al., *Structure-based design of peptides that self-assemble into regular polyhedral nanoparticles.* Nanomedicine, 2006. **2**(2): p. 95-102.
233. Bhatia, D., et al., *Icosahedral DNA nanocapsules by modular assembly.* Angew Chem Int Ed Engl, 2009. **48**(23): p. 4134-7.
234. Shintani, T. and D.J. Klionsky, *Cargo proteins facilitate the formation of transport vesicles in the cytoplasm to vacuole targeting pathway.* J Biol Chem, 2004. **279**(29): p. 29889-94.
235. Itakura, E. and N. Mizushima, *p62 Targeting to the autophagosome formation site requires self-oligomerization but not LC3 binding.* J Cell Biol, 2011. **192**(1): p. 17-27.
236. Lamark, T., et al., *NBR1 and p62 as cargo receptors for selective autophagy of ubiquitinated targets.* Cell Cycle, 2009. **8**(13): p. 1986-90.
237. Watanabe, Y., et al., *Selective transport of alpha-mannosidase by autophagic pathways: structural basis for cargo recognition by Atg19 and Atg34.* J Biol Chem, 2010. **285**(39): p. 30026-33.
238. Scott, S.V., et al., *Cvt19 is a receptor for the cytoplasm-to-vacuole targeting pathway.* Mol Cell, 2001. **7**(6): p. 1131-41.
239. Nair, U., et al., *Roles of the lipid-binding motifs of Atg18 and Atg21 in the cytoplasm to vacuole targeting pathway and autophagy.* The Journal of biological chemistry, 2010. **285**(15): p. 11476-88.
240. Chi, A., et al., *Analysis of phosphorylation sites on proteins from Saccharomyces cerevisiae by electron transfer dissociation (ETD) mass spectrometry.* Proc Natl Acad Sci U S A, 2007. **104**(7): p. 2193-8.
241. Wild, P., et al., *Phosphorylation of the autophagy receptor optineurin restricts Salmonella growth.* Science, 2011. **333**(6039): p. 228-33.
242. Baxter, B.K., et al., *Atg19p ubiquitination and the cytoplasm to vacuole trafficking pathway in yeast.* The Journal of biological chemistry, 2005. **280**(47): p. 39067-76.
243. Kraft, C., M. Peter, and K. Hofmann, *Selective autophagy: ubiquitin-mediated recognition and beyond.* Nat Cell Biol, 2010. **12**(9): p. 836-41.
244. Suzuki, K., et al., *Selective autophagy regulates insertional mutagenesis by the Ty1 retrotransposon in Saccharomyces cerevisiae.* Dev Cell, 2011. **21**(2): p. 358-65.
245. Mazon, M.J., P. Eraso, and F. Portillo, *Efficient degradation of misfolded mutant Pma1 by endoplasmic reticulum-associated degradation requires Atg19 and the Cvt/autophagy pathway.* Mol Microbiol, 2007. **63**(4): p. 1069-77.

246. Martinez-Vicente, M., et al., *Cargo recognition failure is responsible for inefficient autophagy in Huntington's disease.* Nature neuroscience, 2010. **13**(5): p. 567-76.
247. Scott, R.C., G. Juhasz, and T.P. Neufeld, *Direct induction of autophagy by Atg1 inhibits cell growth and induces apoptotic cell death.* Current biology : CB, 2007. **17**(1): p. 1-11.
248. Tang, H.-W., et al., *Atg1-mediated myosin II activation regulates autophagosome formation during starvation-induced autophagy.* EMBO J, 2011. **30**(4): p. 636-651.
249. Morvan, J., et al., *In vitro reconstitution of fusion between immature autophagosomes and endosomes.* Autophagy, 2009. **5**(5): p. 676-89.

VITA

Mariana Morales Quiñones was born in 1983, January 24th, two days after her mother's birthday. Her sister was born 6 years and 1 day afterwards, and was the best belated birthday present anyone could have. She grew up in busy Mexico City, surrounded by mountains, spicy food, and loving friends and family. When still a child, a witchdoctor predicted that she would become a biologist or a doctor.

She then went to graduate school in Columbia, Missouri, to pursue her PhD, while enjoying the unpredictable mid-western weather, freaking out about ticks, biking the Katy Trail, climbing at Capen park, swimming at Stephen's lake, listening to KOPN-Columbia public radio, and eating great Chinese food at New Jingo's. She knocked at her soul mate's door one day, while looking for an apartment to rent, fell in love and 'finally' married him in August of 2010.

She is an almost-vegetarian-cook, a peace activist, a clumsy salsa dancer, a caring teacher, a 10k runner, a chocaholic, a bookworm, a "bike to work" aficionado no-matter-the-weather, an amateur painter, a scuba diver, a messy housemate, a temporary permanent resident in the US, a fluent Spanish speaker, a fun camper, and a curious scientist who talks to her yeast cells during experiments.

Now that she is leaving graduate school behind, she hopes to get more involved with community work, pursue a career in research and teaching, give her friends and family more free hugs and kisses, grow a garden and build a dream home with her husband, get lost in the woods and then sit by a campfire with her loved ones to share s'mores and stories.